AD

USAAVLABS TECHNICAL REPORT 69-2

WIND TUNNEL INVESTIGATION OF SEMIRIGID FULL-SCALE ROTORS OPERATING AT HIGH ADVANCE RATIOS

By

Bruce D. Charles
Watson H. Tanner

January 1969

U. S. ARMY AVIATION MATERIEL LABORATORIES
FORT EUSTIS, VIRGINIA

CONTRACT DAAJ02-67-C-0061
BELL HELICOPTER COMPANY
A DIVISION OF BELL AEROSPACE COMPANY
FORT WORTH, TEXAS

Disclaimers

The findings in this report are not to be construed as an official Department of the Army position unless so designated by other authorized documents.

When Government drawings, specifications, or other data are used for any purpose other than in connection with a definitely related Government procurement operation, the United States Government thereby incurs no responsibility nor any obligation whatsoever; and the fact that the Government may have formulated, furnished, or in way supplied the said drawings, specifications, or other data is not to be regarded by implication or otherwise as in any manner licensing the holder or any other person or corporation, or conveying any rights or permission, to manufacture, use, or sell any patented invention that may in any way be related thereto.

Disposition Instructions

Destroy this report when no longer needed. Do not return it to the originator.

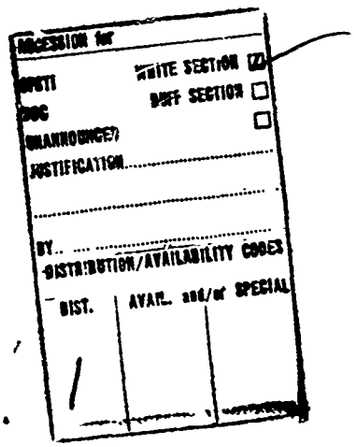

DEPARTMENT OF THE ARMY
U. S. ARMY AVIATION MATERIEL LABORATORIES
FORT EUSTIS, VIRGINIA 23604

This report has been reviewed by the U. S. Army Aviation Materiel Laboratories and is considered to be technically sound. The report is published for the exchange of information and the stimulation of ideas.

Task 1F162204A13903
Contract DAAJ02-67-C-0061
USSAVLABS Technical Report 69-2
January 1969

WIND TUNNEL INVESTIGATION OF SEMIRIGID FULL-SCALE ROTORS OPERATING AT HIGH ADVANCE RATIOS

Bell Helicopter Report 576-099-010

By

B. Charles
W. Tanner

Prepared by

Bell Helicopter Company
A Division of Bell Aerospace Corporation
Fort Worth, Texas

for

U. S. ARMY AVIATION MATERIEL LABORATORIES
FORT EUSTIS, VIRGINIA

SUMMARY

A joint U.S. Army Aviation Materiel Laboratories/NASA-Ames/Bell Helicopter Company experimental investigation of full-scale rotor blades was conducted in the NASA-Ames Large Scale Wind Tunnel. Specifically, a UH-1B 44-foot-diameter rotor having reduced-thickness tips was evaluated in a range of Mach numbers up to 0.94 and advance ratios of up to 0.52. Additionally, UH-1D rotor blades reduced in diameter to 34 feet were tested at advance ratios up to 1.1. Calculated performance is compared with the experimental results obtained to establish the validity of the theoretical technique at high advance ratios. In general, it was found that quasi-static, two-dimensional techniques were adequate up to an advance ratio of about 0.5. Above this advance ratio, theoretical techniques break down, especially with respect to calculating rotor propulsive force or drag.

Theory-experiment comparison with the 44-foot-diameter rotor, operated at high Mach numbers, showed that Mach number effects are predictable to an advance ratio of at least 0.45.

The 34-foot-diameter rotor became increasingly sensitive to control input with advance ratio. At an advance ratio of 1.1, this rotor system displayed a long transient response to a control input before obtaining its steady-state orientation, and at the largest values of collective pitch, the flapping would not completely stabilize.

FOREWORD

The results from the full-scale rotor performance tests of a two-bladed semirigid rotor system are contained in this report. The tests were conducted in the Large Scale Wind Tunnel at NASA-Ames Research Center. The project was performed under Contract DAAJ02-67-C-0061 (Task 1F162204A13903) under the technical cognizance of Patrick Cancro, Project Engineer, U.S. Army Aviation Materiel Laboratories.

The Bell Helicopter Company program was conducted under the technical direction of J. F. Van Wyckhouse, Project Engineer, with the assistance of B. Charles, Research Aerodynamics; W. Wilson, Dynamics; A. Gravely, Dynamic Structures; and N. T. Williams, Administration. The assistance, cooperation, and active participation of John McCloud, III, and James Biggers of the NASA-Ames Research Center, in organizing and conducting the tests, are gratefully acknowledged.

TABLE OF CONTENTS

LIST OF ILLUSTRATIONS

LIST OF SYMBOLS

a	Speed of sound, ft/sec
$a_{1_s}, a_{2_s} \ldots a_{n_s}$	Components of longitudinal flapping with respect to the shaft. Constant coefficients of the cosine terms in the Fourier series expressing flapping with respect to a plane normal to the shaft axis, deg
A_{1_s}	Lateral cyclic pitch with respect to the shaft axis, deg
b	Number of blades
$b_{1_s}, b_{2_s} \ldots b_{n_s}$	Component of lateral flapping with respect to the shaft axis. Constant coefficients of the sine terms of the Fourier series expressing flapping with respect to a plane normal to the shaft axis, deg
B_{1_s}	Longitudinal cyclic pitch with respect to the shaft axis, deg
c	Blade chord, ft
C_D/σ	Rotor drag coefficient, $C_D/\sigma = D/\rho bcR(\Omega R)^2$
$\Delta C_D/\sigma$	Drag coefficient difference, $\Delta C_D/\sigma = C_D/\sigma_{test} - C_D/\sigma_{theory}$
C_L/σ	Rotor lift coefficient, $C_L/\sigma = L/\rho bcR(\Omega R)^2$
C_Q/σ	Rotor torque coefficient, $C_Q/\sigma = Q/\rho bcR^2(\Omega R)^2$
$\Delta C_Q/\sigma$	Torque coefficient difference, $\Delta C_Q/\sigma = C_Q/\sigma_{test} - C_Q/\sigma_{theory}$
D	Drag, the component of the resultant force parallel to the relative wind direction, positive in the downwind direction, lb
f	Equivalent flat plate area, D/q, ft^2
L	Lift, the component of rotor resultant force perpendicular to the relative wind direction in the plane of the relative wind and the shaft, positive up, lb

$\mathscr{L}$	Rolling moment, the moment about the x axis, positive clockwise looking upstream, ft-lb
M	Mach number, $M = V/a$
$M_{(1.0,\ 90.)}$	Advancing tip Mach number, $M_{(1.0,\ 90.)} = (V + \Omega R)/a$
$\mathscr{M}$	Pitching moment, the moment about the y axis, positive nose up, ft-lb
$\mathscr{N}$	Yawing moment, the moment about the z axis, positive clockwise from above, ft-lb
q	Dynamic pressure, lb/sq ft
Q	Shaft torque, the moment about the shaft z axis, positive when torque tends to accelerate the rotor, ft-lb
R	Rotor radius, ft
V	Forward speed, ft/sec
Y	Force perpendicular to L and D forces, positive to the right when viewed from downstream, lb
α_s	Shaft angle of attack, the angle between the relative wind and a plane normal to the shaft axis, positive in nose-up direction, deg
α_c	Control axis angle of attack, the angle between the relative wind, the shaft axis, and the projection of the control axis on the plane of the relative wind axis, positive in nose-up direction, deg
$\theta_{.75R}$	Blade collective pitch angle measured at 0.75R, deg
μ	Advance ratio, $\mu = \frac{V}{\Omega R}$
ρ	Density of air, slugs/ft^3
σ	Rotor solidity, $\sigma = \frac{bc}{\pi R}$
Ω	Rotor shaft angular velocity, rad/sec

Systems of Axes

1. Wind axis system:

x_w Longitudinal Wind Axis. Axis lying along the airstream or relative wind direction.

z_w Normal Wind Axis. Axis perpendicular to the longitudinal wind axis in the plane of the wind axis and the shaft centerline.

y_w Lateral Wind Axis. Axis perpendicular to the x_w and z_w axes.

2. Shaft axis system:

z_s Shaft Axis. Axis coincident with the shaft centerline.

x_s Longitudinal Shaft Axis. Axis perpendicular to the shaft axis, in the plane of the shaft axis and relative wind direction.

y_s Lateral Shaft Axis. Axis perpendicular to the x_s and z_s axes. This axis is coincident with the lateral y_w wind axis.

3. Control axis system:

z_c Control Axis. Axis of no feathering. Axis with reference to which there is no first harmonic pitch change with azimuth angle. This axis may be tilted with respect to the shaft longitudinally (with $B1_s$) and laterally (with $A1_s$), separately or in combination.

x_c Longitudinal Axis. Axis perpendicular to the control axis in the plane of the control axis and the relative wind direction.

y_c Lateral Axis. Axis perpendicular to the x_c and z_c axes.

4. Virtual axis system:

z_v Virtual axis. Axis of no flapping. Axis with respect to which there is no first harmonic blade flapping. This axis is perpendicular to the "tip path plane" for zero flapping hinge offset.

x_v Longitudinal Axis. Axis perpendicular to the vertical axis in the plane of the virtual axis and the relative wind direction.

y_v Lateral Axis. Axis perpendicular to the x_v and z_v axes.

INTRODUCTION

As the state of the art of rotary-wing aircraft advances, it becomes increasingly evident that high advance ratios and high Mach numbers will become standard operating conditions of future rotorcraft. In fact, several compound research aircraft, capable of exploring these regions, have been or are being flown. Presently, existing experimental research consists mainly of scale model rotor tests, such as described in Reference 1, and the limited full-scale wind tunnel high advance ratio tests, as described in Reference 2. It has been well established that scale model data obtained in air cannot be extrapolated to full-scale results because of the Reynolds number effects. Scale results where Reynolds number is maintained by using mediums other than air, such as freon, are not yet available. The limited full-scale semirigid rotor results of Reference 2 were not sufficient for adequate performance correlation and evaluation of theoretical techniques at high advance ratios. References 3 and 4 are representative of the existing state of the art of performance calculations, and both are widely accepted.

Clearly, more full-scale data at high advance ratios must be acquired under controlled conditions. The NASA-Ames Large Scale Wind Tunnel is the only facility where these data can be obtained. Flight test results are not sufficiently accurate to evaluate these regions of flight or to correlate with theoretical techniques in detail. In free flight, conditions cannot be carefully controlled; and as yet, instrumentation techniques have not been evolved to measure rotor forces accurately. Thus, this program was undertaken to provide:

1. Full-scale semirigid rotor performance results at high advance ratios

2. Exploration of the flight test envelope of the U.S. Army Aviation Materiel Laboratories-Bell Helicopter High Performance Helicopter (HPH)

Specifically, a 34-foot-diameter, low-twist rotor was tested up to advance ratios of 1.1; and a 44-foot-diameter, low-twist, thin-tip rotor designed for the HPH was tested in an HPH flight regime up to Mach numbers of 0.94 and advance ratios of 0.52. Additionally, state-of-the-art performance calculations were compared with the test results obtained.

TEST EQUIPMENT

ROTOR TEST MODULE

Figure 1 shows the rotor test module in the NASA-Ames 40- x 80-foot Wind Tunnel. The mounting frame, pylon, and drive system are enclosed by an aerodynamic fairing of tear-drop shape. The maximum diameter of the fairing is 6.66 feet, and the length is 22 feet. Further description of the test module, power distribution panel, control module, and associated instrumentation may be found in Appendix II of Reference 5.

ROTOR SYSTEM AND BLADES

Two 2-bladed, semirigid rotor systems using a UH-1D underslung feathering axis hub were tested. The 44-foot-diameter rotor system had modified UH-1B blades incorporating reduced-thickness tips and low aerodynamic twist. The 34-foot-diameter rotor system had modified low-twist UH-1B blades of reduced diameter. The purpose of the reduced-diameter rotor was to lower the rotational velocity (ΩR) without requiring changes in the standard UH-1D transmission so that high advance ratios ($V/\Omega R$) could be obtained. Basic data for these rotors are given below:

34-Foot Rotor

Airfoil Designation (Root to Tip)	NACA 0012
Chord	1.75 ft
Diameter	34 ft
Twist	-1.42 deg
Disc Area	908 ft^2
Solidity	.0656
Effective Root Cutout	11.8 pct
Lock Number	3.62

44-Foot Tapered Tip Rotor

Airfoil Designation	
Root to .78R	NACA 0012
.78R to Tip	Uniform Thickness Change
Tip	NACA 0006 Mod (See Table I)
Chord	1.75 ft
Diameter	44 ft
Twist	-1.83 deg
Disc Area	1520 ft^2
Solidity	.0506
Effective Root Cutout	9.1 pct
Lock Number	7.05

TABLE I. AIRFOIL CONTOURS,* STATION 264.0
(in percent of airfoil chord)

Station	Upper Surface Ordinate	Lower Surface Ordinate
0	-.647	-.647
.5	.004	-1.219
1.0	.290	-1.419
2.0	.709	-1.661
3.0	1.028	-1.819
4.0	1.300	-1.938
5.0	1.528	-2.033
10.0	2.304	-2.380
12.0	2.485	-2.500
14.0	2.619	-2.619
20.0	2.866	-2.866
25.0	2.971	-2.971
30.0	3.000	-3.000
40.0	2.900	-2.900
50.0	2.647	-2.647
60.0	2.281	-2.281
70.0	1.833	-1.833
78.0	1.419	-1.419
86.0	1.047	-1.047
98.7	.276	-.276
100.0	.128	-.128

*NOTE. NACA Airfoil Conventions Observed

INSTRUMENTATION

Instrumentation was installed to provide rotor and control position data and for monitoring structural loads during the tests. The loads data were monitored by digital readout and oscilloscope and were recorded on magnetic tape using a contractor supplied data acquisition system. Control position data were displayed in digital form on a test control console and were recorded by hand entry in the test log.

Loads data were obtained from foil type (350 ohm) strain gages wired into four active arm bridges and excited by a common DC voltage. The strain gage sensitivities were determined by direct calibration through the expected operating range. The load equivalent electrical output was obtained using a precision resistor shunt on one leg of the bridge. Position data were obtained from potentiometers used as voltage dividers. Positions were calibrated by moving the hardware incrementally through the full operating ranges and plotting electrical output versus mechanical position.

TEST RESULTS

GENERAL DISCUSSION

The advance ratio and Mach number combinations tested with the 44-foot and 34-foot-diameter rotors are shown in Table II and Table III, respectively.

TABLE II. 44-FOOT-DIAMETER ROTOR

ADVANCE RATIO μ	TIP MACH NUMBER $M_{(1.0,\ 90.)}$
0.31	0.88
0.36	0.80
0.36	0.90
0.40	0.85
0.41	0.94
0.45	0.77
0.45	0.90
0.46	0.86
0.51	0.80
0.52	0.81

TABLE III. 34-FOOT-DIAMETER ROTOR

ADVANCE RATIO μ	TIP MACH NUMBER $M_{(1.0,\ 90.)}$
0.51	0.64
0.65	0.54
0.76	0.50
0.86	0.47
0.94	0.49
1.1	0.51

A graphical presentation of the 44-foot-diameter rotor data and the complete NASA-Ames balance data reduction tabulation are presented in Appendixes I and II, respectively. In addition to the performance data, rotor system loads and moments were recorded. The principal purpose of monitoring these data was to assure that maximum acceptable structural loadings were not exceeded and to detect the onset of possible dynamic or aeroelastic problems.

TESTING PROCEDURE

For the 44-foot-diameter rotor at each particular test condition, the rotor rotational speed and the tunnel speed were adjusted to maintain constant values of rotor advance ratio and advancing tip Mach number. The rotor shaft angle (test module pitch) and rotor collective pitch were then varied in even increments to map the test envelope. The rotor cyclic pitch was adjusted to minimize the first harmonic flapping with respect to the rotor shaft, and data were recorded at each incremental combination of shaft angle and collective pitch.

The method used for the 34-foot-diameter rotor was slightly different. Since the 40- x 80-foot Large Scale Wind Tunnel is speed limited ($V_{max} \cong 190$ knots), the procedure used was to fix the tunnel speed and adjust the rotor rotational speed to obtain high advance ratios. The Mach number thus obtained varied with advance ratio but is believed to be small enough in magnitude to be discounted as a prime variable ($M_{(\psi=0,\ 90)} = 0.47$ to 0.64). Once the test conditions were fixed, the rotor shaft angle (test module pitch) and rotor collective pitch were then varied in even increments to map the test envelope. The rotor cyclic pitch was adjusted to minimize the first harmonic flapping with respect to the rotor shaft, and data were recorded at each incremental combination of shaft angle and collective pitch.

The wind tunnel balance data were recorded by NASA-Ames. These data, which appear in Appendix II, were resolved such that all forces were in the relative wind axis system, and all moments were transferred from balance resolving center to the center of rotation of the rotor hub and referenced to the shaft axis system.

DISCUSSION OF RESULTS AND COMPARISON WITH THEORY

Description of the Theory

Since Reference 3 is a widely accepted method for calculating rotorcraft performance, it was desirable to correlate the experimental results of this test with the charts of Reference 3. However, direct comparison was not possible for two reasons: (1) the test Mach numbers were significantly lower, and (2) the test blade solidity was near the lower limit recommended in Reference 3. Therefore, a rotor performance calculating technique based upon Reference 6 was modified to duplicate the charts of Reference 3. The theoretical program also included the simplifying assumptions of that reference, which are:

1. Two-dimensional, steady-state flow is assumed at each blade element.
2. Radial velocity effects are neglected.

3. The blade is considered to be rigid.
4. Rotor inflow is assumed to be constant over the disc.

Furthermore, the technique used the airfoil data of Reference 3 and was checked out against the tables of Reference 7.

Reference 3's assumption of constant rotational speed about the shaft axis is not applicable to the semirigid rotor. The assumption of uniform inflow is believed to be valid for these comparisons, especially for the 34-foot rotor, where the advance ratio is high and the induced velocity is small compared to the forward velocity. Aerodynamically, then, assumptions 1 and 2 are of prime interest; however, it is beyond the scope of this report to isolate the various aerodynamic effects or to offer an improved calculating technique. References 8 and 9 give some insight into radial flow and unsteady effects.

Reference 5 presents theory-experiment comparison using the aforementioned assumptions and shows good correlation at low advance ratios and high advancing tip Mach numbers.

44-Foot-Diameter Rotor

Previous correlations, Reference 5, have shown good agreement at low advance ratio and high advancing tip Mach number for both standard and thin-tipped UH-1D rotors. In this section, theory is compared with full-scale test data obtained with a UH-1B 44-foot-diameter, low-twist, thin-tipped rotor. The regime of operating conditions tested (advance ratio and advancing tip Mach number) partially overlaps that of the earlier test (Reference 5) but extends to higher advance ratios.

The experimental data, Figure 2, are presented in the carpet plot format of Reference 3 for three lift coefficient-solidity ratios. Each graph contains the rotor performance for a given Mach number and advance ratio. The validity of theoretically determined rotor performance at the same operating conditions is illustrated by comparing the experimental data with the dashed-line theory curves. In Figure 2(a-c), these test-theory correlations are shown for advance ratios of 0.36, 0.45 and 0.51, while the Mach number is held approximately constant: $M(1.0, 90.) = 0.8$. The calculated performance shows acceptable agreement with test results for $\mu = 0.36$; but as the advance ratio is increased to $\mu = 0.45$, the agreement begins to deteriorate, particularly at high lift coefficients. Finally, at $\mu = 0.51$, the test data exhibit sizably larger torque coefficients than theory would predict for any given rotor resultant force shown (resultant force coefficient = $\sqrt{C_L^2 + C_D^2}$).

Confirmation of this trend is also found at higher Mach numbers. Figures 2d and 2e present the performance correlation at $\mu = 0.36$ and $\mu = 0.45$ for an advancing tip Mach number $M(1.0, 90.) = 0.9$. The test-theory differences at 0.8 Mach number are nearly identical with the 0.9 Mach number case for 0.45 advance ratio. This not only supports the above statements, but indicates that the observed differences are nearly independent of the advancing tip Mach number.

To summarize these trends graphically, the test-theory differences of Figure 2 are shown cross-plotted (for $C_L/\sigma = 0.04$ and $C_D/\sigma = 0$) as functions of advance ratio and Mach number in Figure 3. The important feature, shown in Figure 3a, is the rapid divergence of test theory agreement with advance ratio in the $\mu = 0.4$ to 0.5 range. In dimensional form, the 0.8 Mach number curve would indicate that theory underestimates the power required by 43 HP at $\mu = 0.4$, whereas for $\mu = 0.51$ the discrepancy is equal to 137 HP. Further, in Figure 3b, the $\mu = 0.45$ curve would show that at $M(1.0, 90.) = 0.8$ the power difference is 63 HP, while at $M(1.0, 90.) = 0.9$ it is 55 HP, indicating the weak influence of advancing tip Mach number on the advance ratio trend.

34-Foot-Diameter Rotor

Correlation with the 44-foot-diameter rotor data has uncovered the inability of theory to predict rotor performance at moderately high advance ratios. In this section, the test-theory comparisons are extended to advance ratios greater than unity, and they show that agreement continues to grow worse as the advance ratio is increased beyond $\mu = 0.5$. These results are not entirely unexpected, however, as quasi-static, rigid blade theory does not account for the nonlinearities associated with high advance ratio operation or radial flow and unsteady effects.

The major drawback of the theory is its failure to yield the correct rotor propulsive force (or C_D/σ) for advance ratios much above $\mu = 0.5$. This is illustrated in Figure 4, which presents drag coefficient/solidity versus angle of attack at constant collective pitches for an advance ratio of 0.86. On this figure, the dashed axis corresponds to the theory axis, which has been shifted 0.005 along the C_D/σ ordinate and 1 degree along the control angle of attack abscissa in order to make the experimental and calculated results agree. To show the order of magnitude of this error, the following numerical example is used. For $\mu = 0.86$ at $M(1.0, 90.) = 0.90$, the forward speed is 255 knots, a normal compound helicopter operating condition. For the UH-1B 44-foot-diameter rotor, $C_D/\sigma = 0.005$ (the error in minimum drag coefficient/solidity on Figure 4 between theory and test) corresponds to an

equivalent flat plate drag area (f) of 1.7 square feet. A well designed compound helicopter cruising at this speed at minimum drag coefficient would have a total f of about 10 square feet. Therefore, if the thrusting power plants were scaled to the theoretical minimum rotor drag, the aircraft would be underpowered by from 15% to 20% at 255 knots.

The vertical axis shift (C_D/σ) required to make the state-of-the-art calculated results agree with experiment is defined as the drag coefficient difference, $\Delta C_D/\sigma$ ($\Delta C_D/\sigma = C_D/\sigma_{test} - C_D/\sigma_{theory}$). This drag coefficient difference versus advance ratio is graphed on Figure 5 (note that the Mach number also varies from 0.47 to 0.64). The values of the circular symbol points in Figure 5 have been obtained from the test-theory correlations presented in Figures 6b through 11b and represent the magnitude of the theory-ordinate shift necessary to give good agreement between the theoretical and experimental drag curves. Therefore, when viewing these drag curves, it is important to realize that the theoretical values (dashed lines) are graphed with respect to an axis which is shifted relative to the axis containing the experimental values. The same technique has been applied to previous high advance ratio results (Reference 2). These results, denoted by triangular symbols, indicate the same trend with advance ratio and confirm the magnitude of test-theory drag differences. The variation is linear with advance ratio, indicating that this error cannot be attributed to a test inaccuracy such as a tare force (probably the most common testing error), since an error in a drag tare would result in a parabolic variation, not a straight line as shown on the figure.

An obvious second error would be that the two-dimensional drag coefficients used in the calculation were optimistic. This can be discounted for two reasons: (1) in the previous section, good performance correlation was obtained at low advance ratio with the same airfoil data, and (2) reasonable power correlation was obtained throughout the advance ratio range, and if the airfoil drag coefficients were increased sufficiently to get C_D/σ agreement, large overestimations of the power required would result.

The previous paragraphs have pointed out one serious shortcoming of the present state-of-the-art performance calculating technique which can create serious problems for all high advance ratio machines. The calculated propulsion force required to overcome the rotor drag is optimistic.

For the lift and torque curves of Figures 6 through 11, no shift was made in the axes. Theory and test are graphed with respect to the same ordinate and abscissa. If a shift in the control axis angle of attack had been made, the lift and torque correlations below rotor stall would be improved

for the lower collective pitches. At the higher collectives, however, this shift would produce an over-correction.

A second test-theory discrepancy which may also be a problem for all compounds and stopped-rotor vehicles is that the theory predicts the wrong trends in autorotation at high advance ratios. This is shown in Figure 12, which gives the lift variation in autorotation at several advance ratios with control axis angle of attack. First, examine the calculated performance (dashed lines). The theory shows a rotation of the autorotation line with advance ratio for all advance ratios. At $\alpha_c = 0$, the autorotating lift increases with advance ratio; at negative angles of attack greater than 2 degrees, the lift decreases with advance ratio. The same trend, with a displacement of the curves to the right is shown for the experimental results (solid lines) up to an advance ratio of 0.94. However, at $\mu = 1.1$, the next test advance ratio, the autorotative lift remains constant at a high value with angle of attack.

To illustrate the practical importance of the difference between the test and the calculated results, consider the following situation. A compound helicopter has a total power failure at $\mu = 1.1$ (V = 300 kts, ΩR = 460 ft/sec), and the machine is configured to enter autorotation at $\alpha = -2°$. The theory shows that the rotor lift is about 2000 pounds for the UH-1 rotor, but the test results give a 4000-pound rotor lift, twice that expected. This compounds the designer's classic problem of the compound helicopter, which is to "dump" the wing lift in high-speed autorotation, since the rotor is producing more lift than expected. Therefore, to maintain a reasonable rate of descent compatible with building up rotor rpm, more wing lift must be "dumped" than anticipated. This is a serious matter in practical design, and the data of Figure 12 indicate that the problem will remain even at an advance ratio of 0.5.

A third possible problem for all high advance ratio machines is shown in Figure 13, which is a graph of mean lift curve slope versus advance ratio. Both the theory and test results show negative slopes in the area of $\mu = 0.9$, a possible instability. In addition to the possible problem area, this figure also shows that the calculated lift curve slopes are good, and the theory also gives the points of inflection and the possible instability.

For the first time, sufficient data have been recorded with this rotor to expose another phenomenon apparently caused by autorotation at high advance ratios. Figures 7 and 8 show that as the rotor enters autorotation at low collective pitches (most notably at $\theta_{.75R} = 0°$), the lift, drag, and torque curves exhibit irregular values. No explanation for the phenomenon has been found. However, it cannot be

attributed to scatter in the test data, since it was repeatable by entering autorotation from both the positive and the negative torque side.

In addition to the phenomenon described above, the rotor system also had a relatively long transient response to a control input at the highest test advance ratio (μ = 1.1). With a control input from a steady-state condition, the rotor would "wander" before it reached a new steady-state orientation. The transient response motion was small in magnitude and could not be detected by eye, but it was detectable on the rotor flapping monitoring instrumentation, which was designed to measure flapping motion of less than 0.1 degree.

At 1.1 advance ratio, rotor sensitivity increased with increased collective pitch and became the limiting factor in the test. At the highest collective pitch for each shaft angle tested, the rotor flapping would no longer stabilize; and although the magnitudes of the transient flapping excursions were small, it was considered unsafe to test beyond the highest collective pitches given in Figure 10 with this particular 34-foot-diameter rotor system.

CONCLUSIONS

Full-scale rotor performance data up to an advance ratio of 1.1 and an advancing tip Mach number of 0.94 have been analyzed and compared with theoretical techniques of Reference 3 to yield the following conclusions:

- Comparison of the 44-foot-diameter rotor data with theory shows that agreement deteriorates rapidly with advance ratio above $\mu \equiv 0.4$ and that Mach number has little effect on this trend.

- Theoretical correlations with the high advance ratio data ($\mu = 0.5$ to 1.1) show that theory predicts optimistic values of rotor propulsive force.

- Based upon quasi-static, two-dimensional techniques, theoretical predictions of advance ratio effects break down in the range $\mu = 0.4$ to 0.5 and should be used with extreme caution to obtain magnitude above $\mu \equiv 0.5$.

- In general, the theory shows the proper trends with advance ratio even when the magnitude of the drag does not correlate well. An exception to this is at the advance ratio of 1.1, where the theory did not properly predict the autorotation trends.

- No stability limits were encountered in the 0.5 Mach number range for advance ratios up to 1.0; however, both test and theory show the existence of a possible instability near $\mu = 0.9$.

- At an advance ratio of 1.1, the rotor system displayed a long transient response to a control input before the steady-state orientation was achieved for all test conditions. At the highest test collective pitch, the flapping would not completely stabilize.

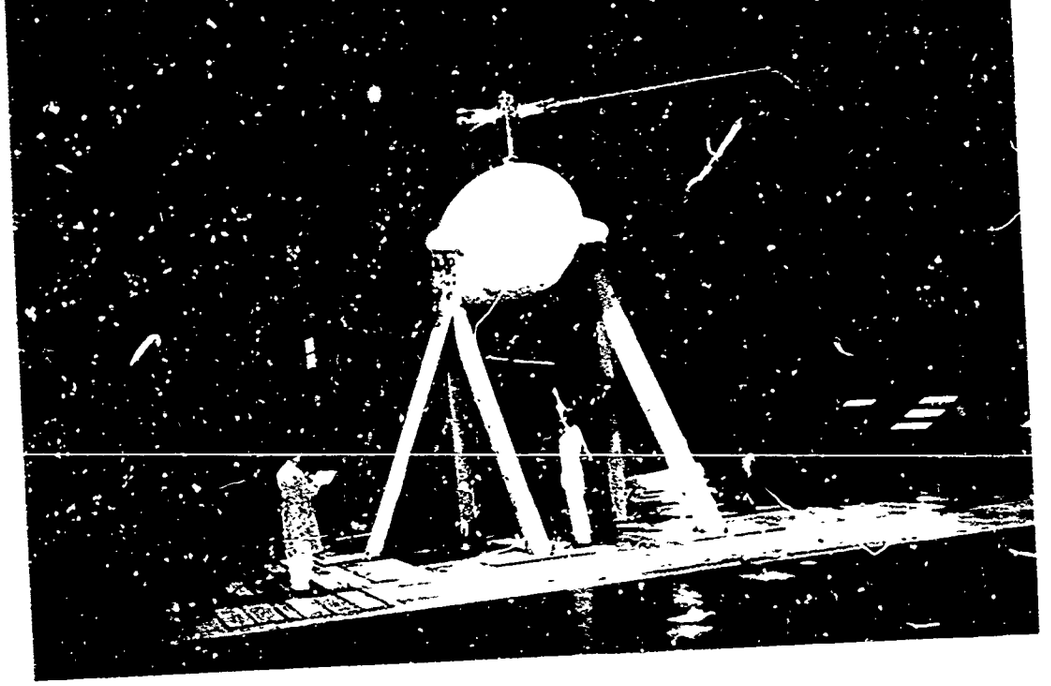

Figure 1. Full-Scale Rotor Wind Tunnel Test Module in the NASA-Ames 40- x 80-Foot Wind Tunnel.

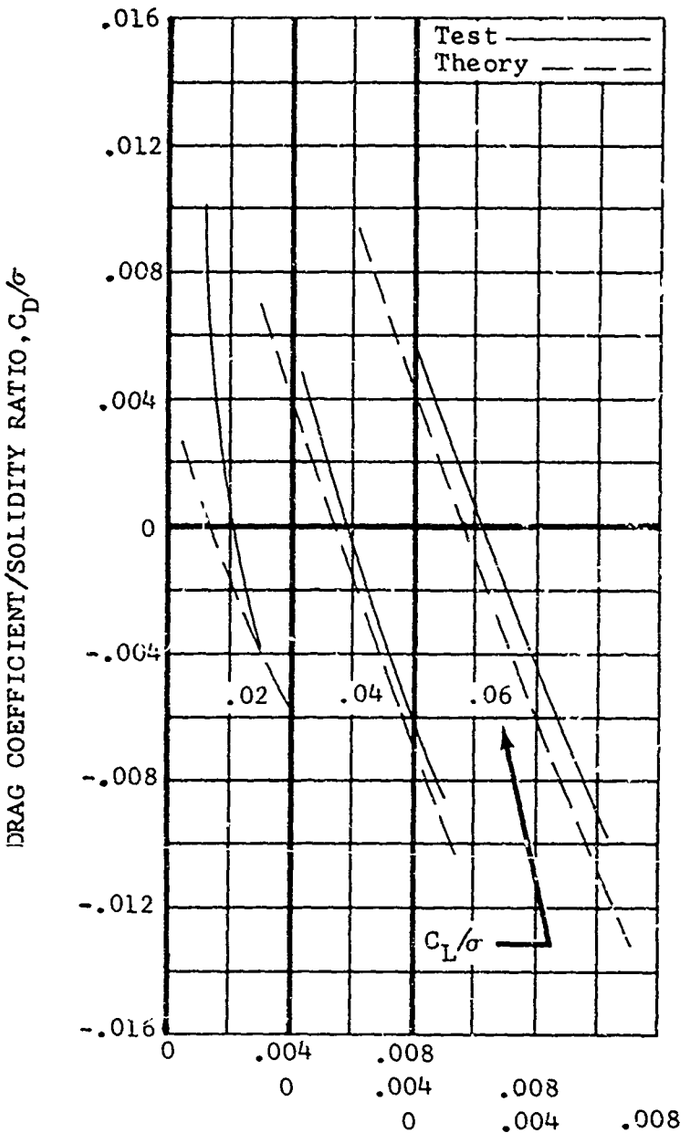

a) $\mu = 0.36$; $M_{(1.0,\ 90.)} = 0.80$

Figure 2. Test-Theory Comparison, Nondimensional Performance of 44-Foot-Diameter Rotor at Various Combinations of Advance Ratio and Advancing Tip Mach Number.

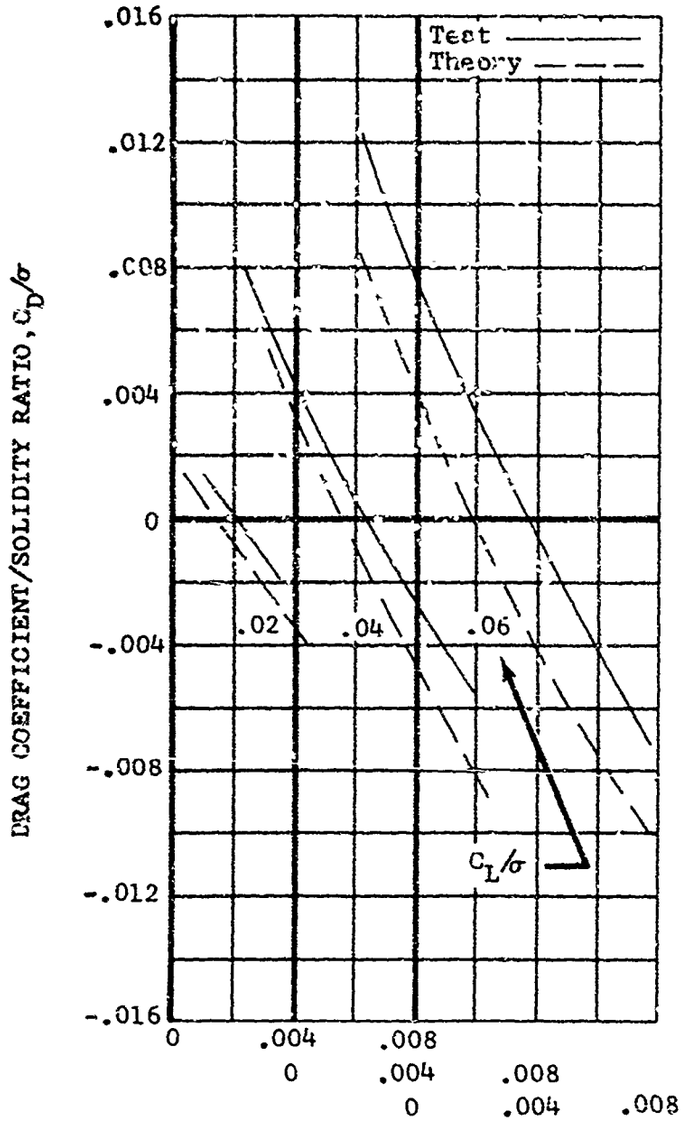

b) μ = 0.45; $M_{(1.0,\ 90.)}$ = 0.77

Figure 2. Continued.

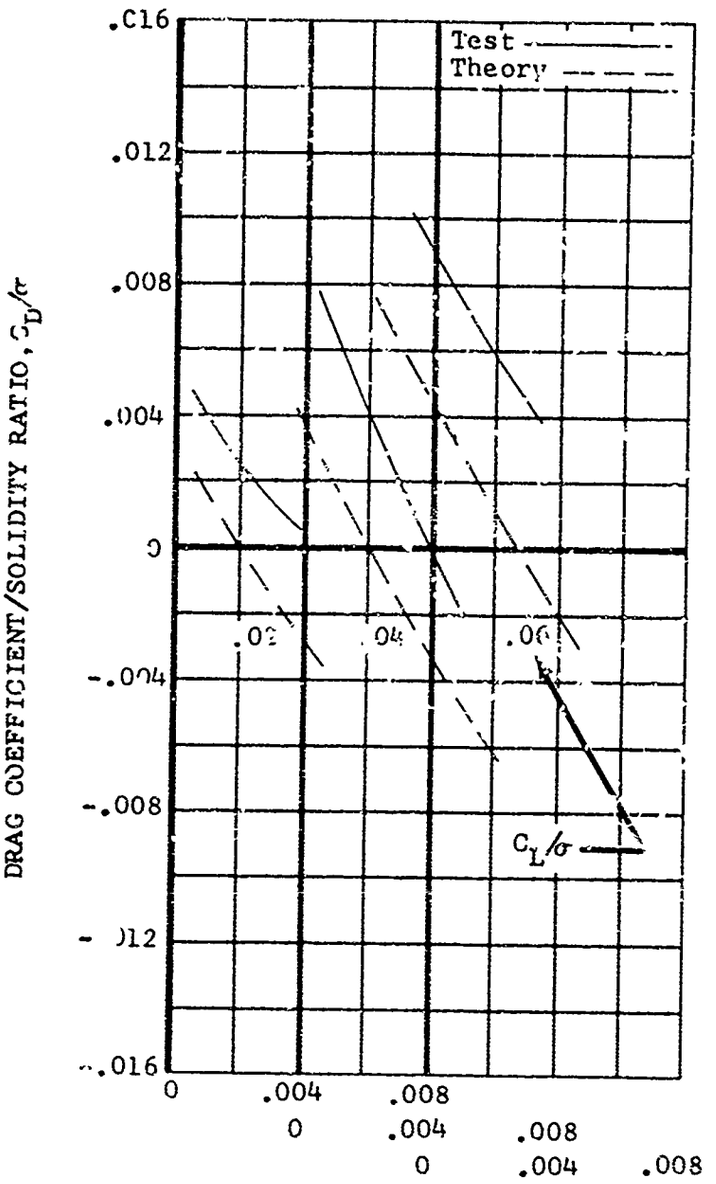

c) μ = 0.51; $M_{(1.0,\ 90.)}$ = 0.80

Figure 2. Continued.

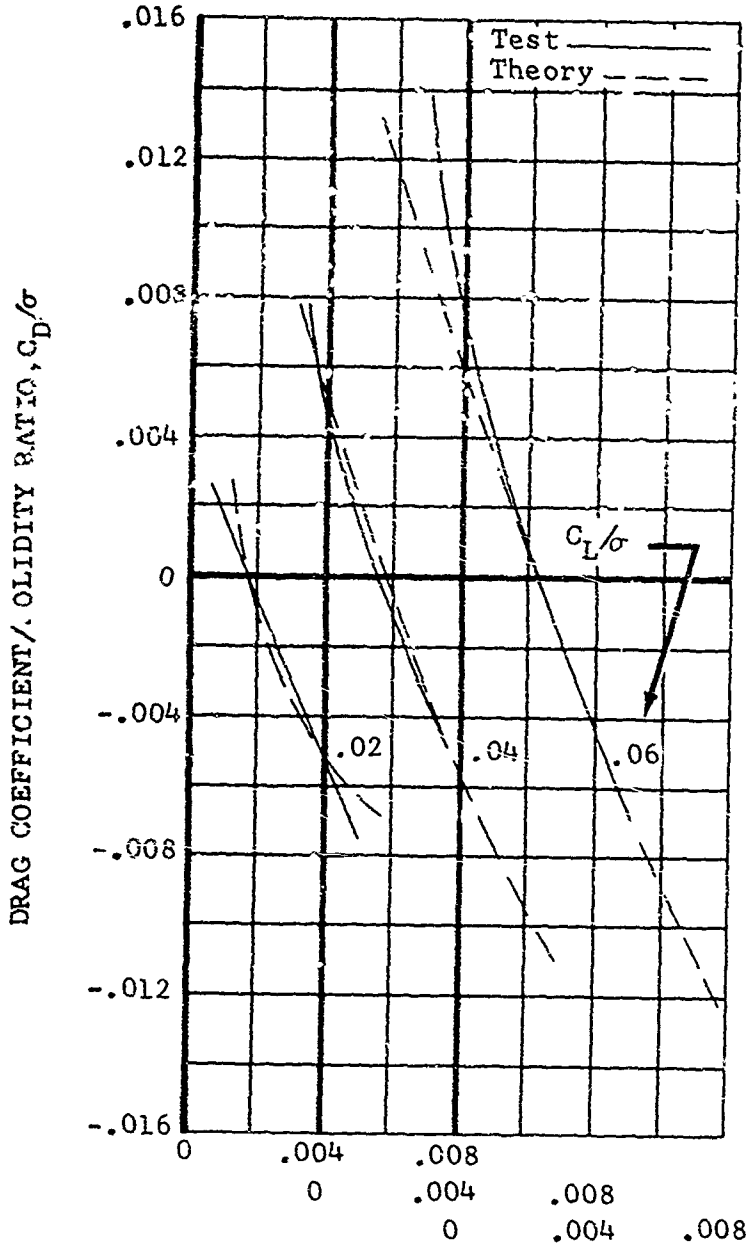

d) μ = 0.36; $M_{(1.0,\ 90.)}$ = 0.90

Figure 2. Continued.

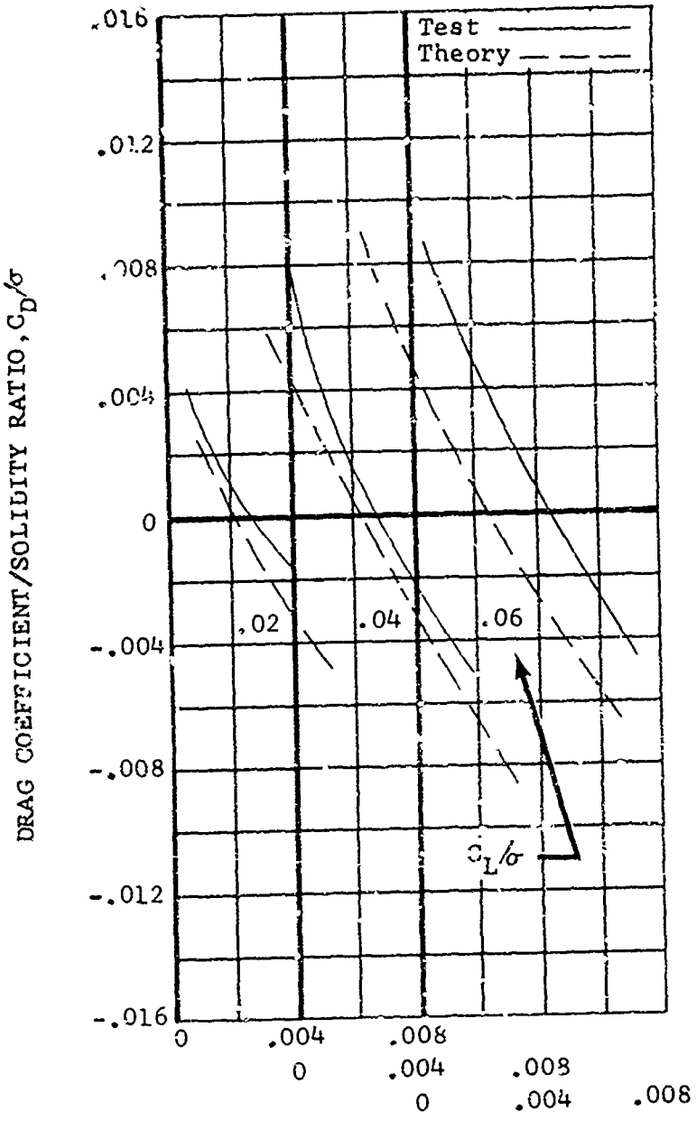

e) $\mu = 0.45$; $M_{(1.0,\ 90.)} = 0.90$

Figure 2. Concluded.

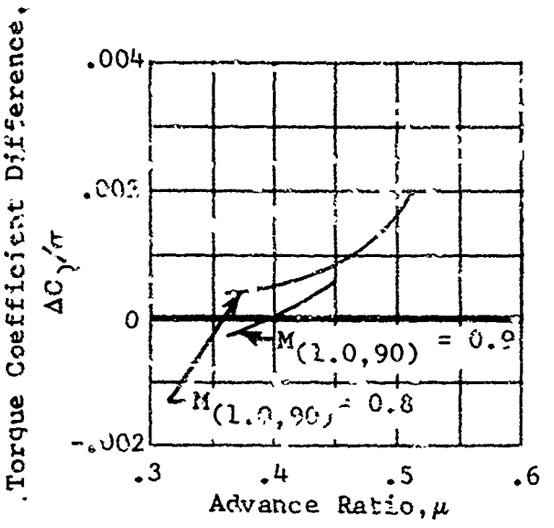

a) C_Q/σ vs μ

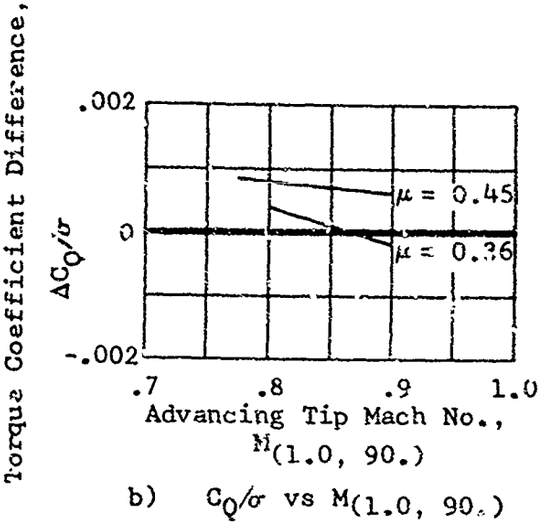

b) C_Q/σ vs $M_{(1.0, 90.)}$

Figure 3. 44-Foot-Diameter Rotor Test-Theory Comparison. Torque Coefficient Difference vs. Advance Ratio and Advancing Tip Mach Number, $C_L/\sigma = 0.04$; $C_D/\sigma = 0$.

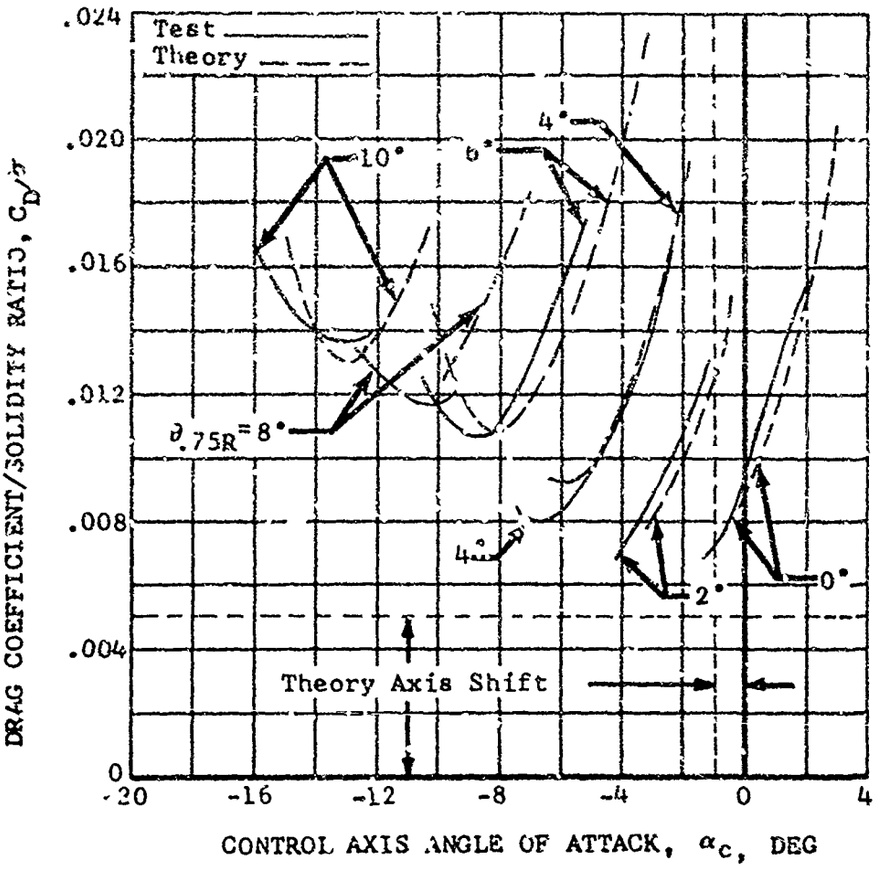

Figure 4. A Comparison of the Test-Theory Drag Coefficient/Solidity Ratio Versus Control Axis Angle of Attack for the 34-Foot-Diameter Rotor at μ = 0.86 and M(1.0, 90,) = 0.47 Illustrating the Required Theory Axis Shift.

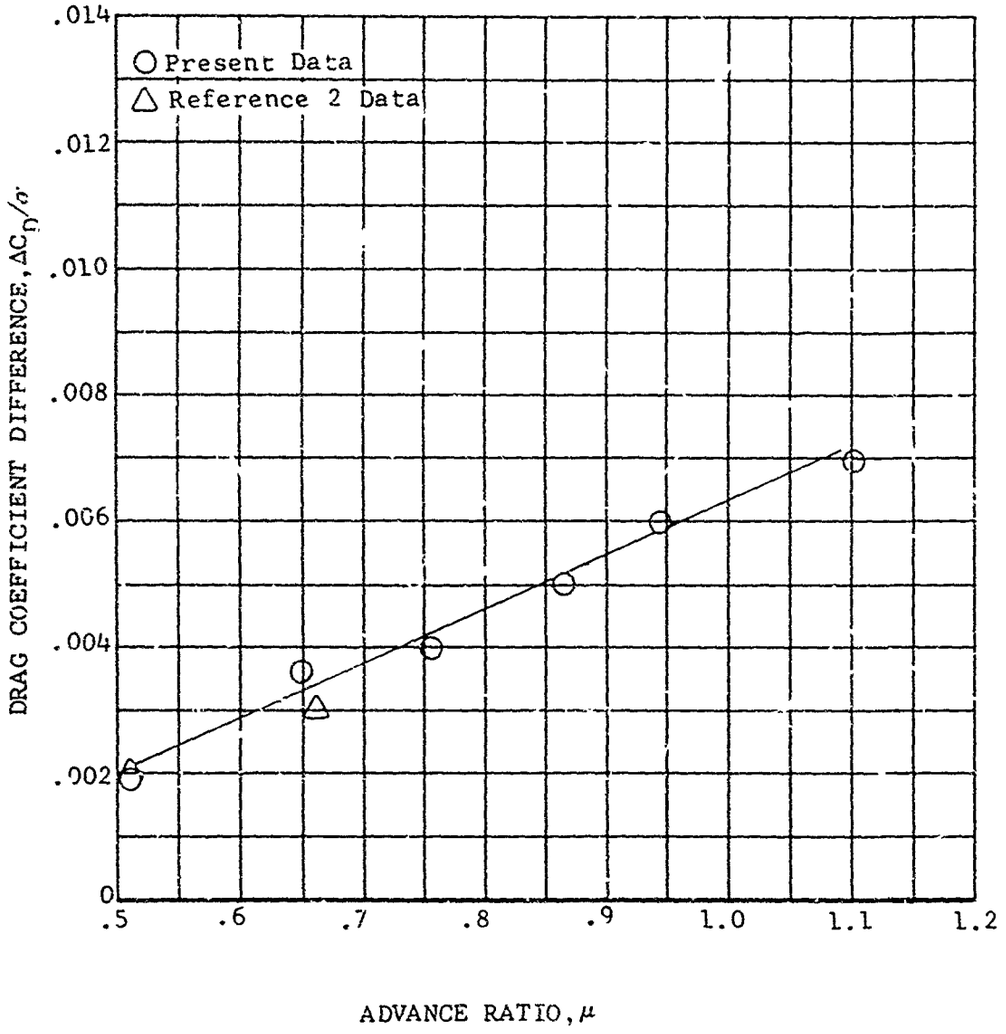

Figure 5. 34-Foot-Diameter Rotor Test-Theory Comparison. Test-Theory Drag Coefficient Difference vs. Advance Ratio for M(1.0, 90.) Varying From 0.47 to 0.64.

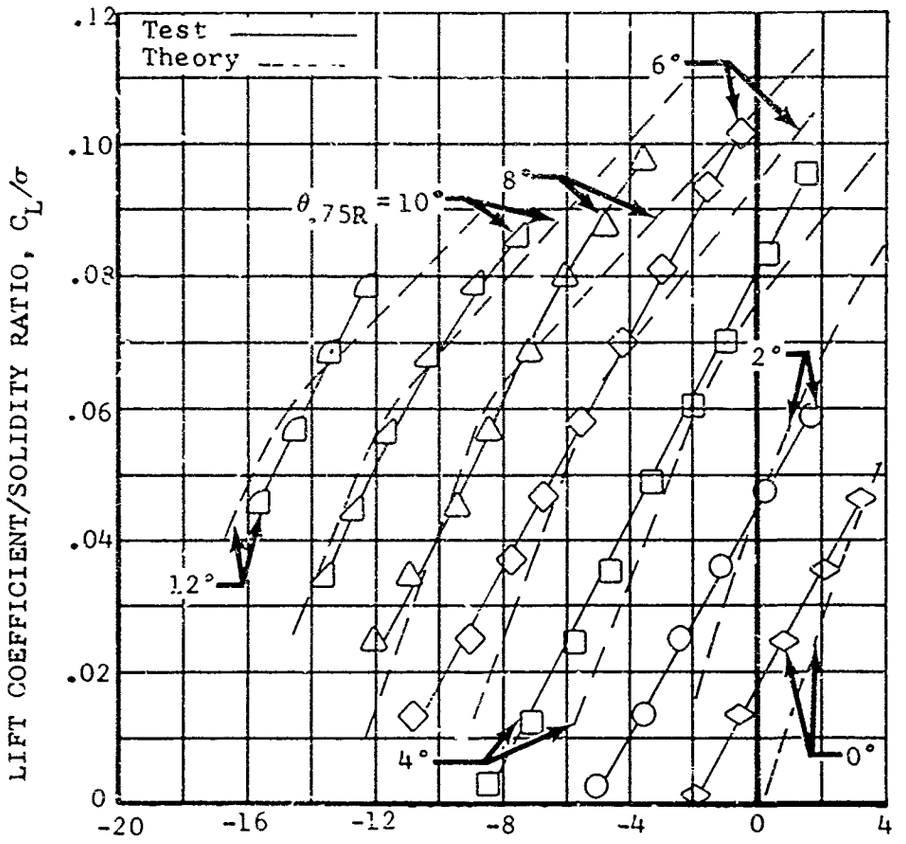

a) C_L/σ vs α_c

Figure 6. Test-Theory Comparison, Nondimensional Performance of the 34-Foot-Diameter Rotor for Various Collective Pitch Angles at $\mu = 0.51$; $M_{(1.0,\ 90.)} = 0.64$.

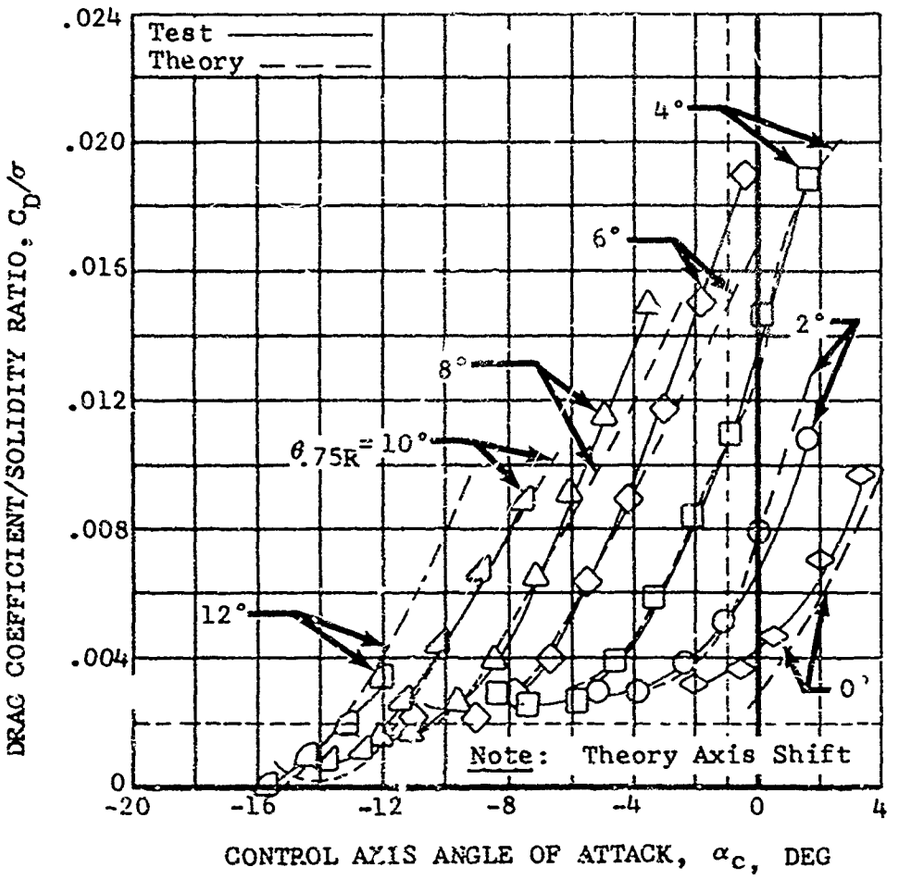

b) C_D/σ vs α_c

Figure 6. Continued.

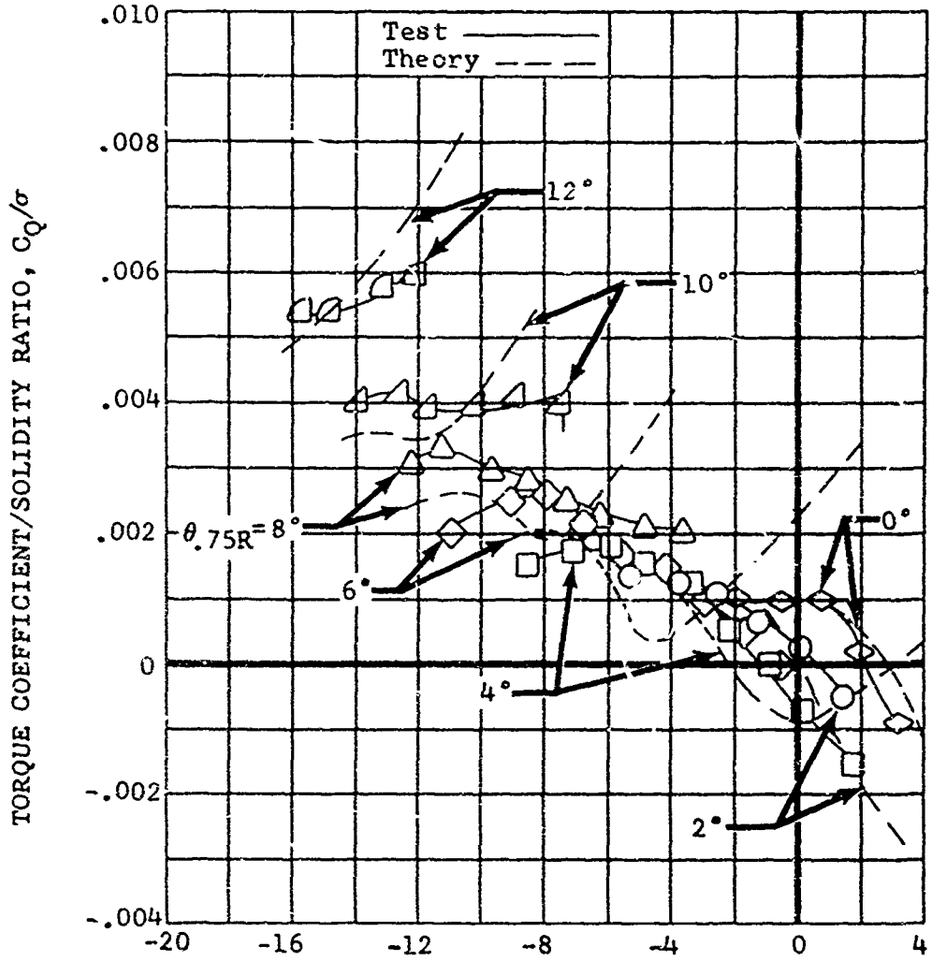

c) C_Q/σ vs α_c

Figure 6. Concluded.

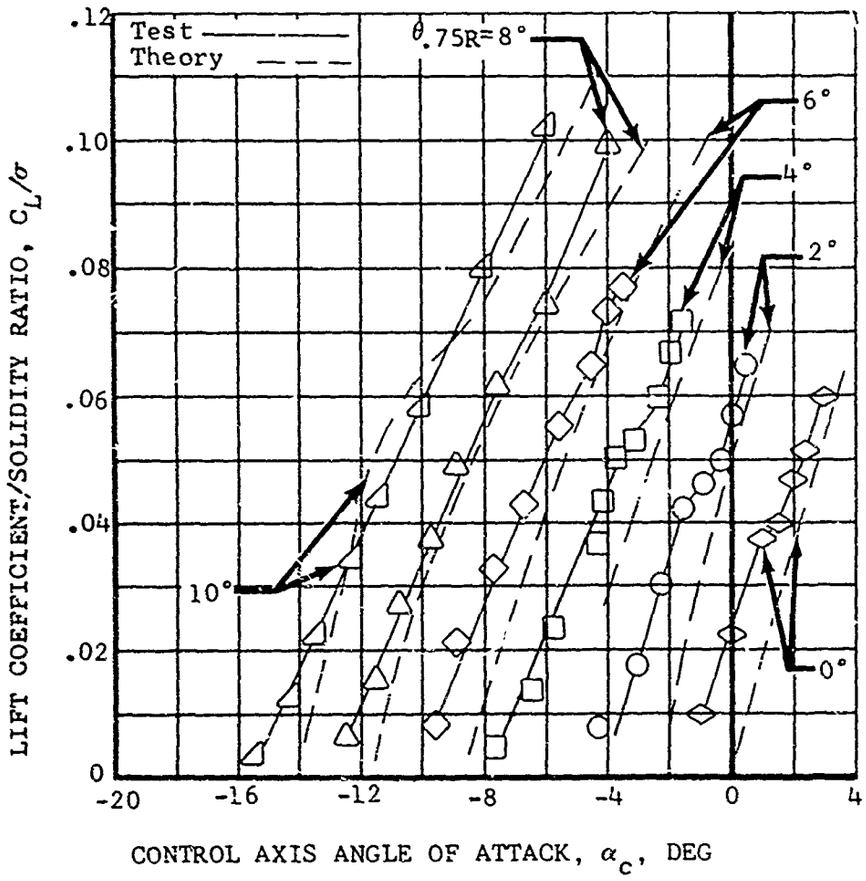

a) C_L/σ vs α_c

Figure 7. Test-Theory Comparison, Nondimensional Performance of the 34-Foot-Diameter Rotor for Various Collective Pitch Angles at μ = 0.65; $M_{(1.0,\ 90.)}$ = 0.54.

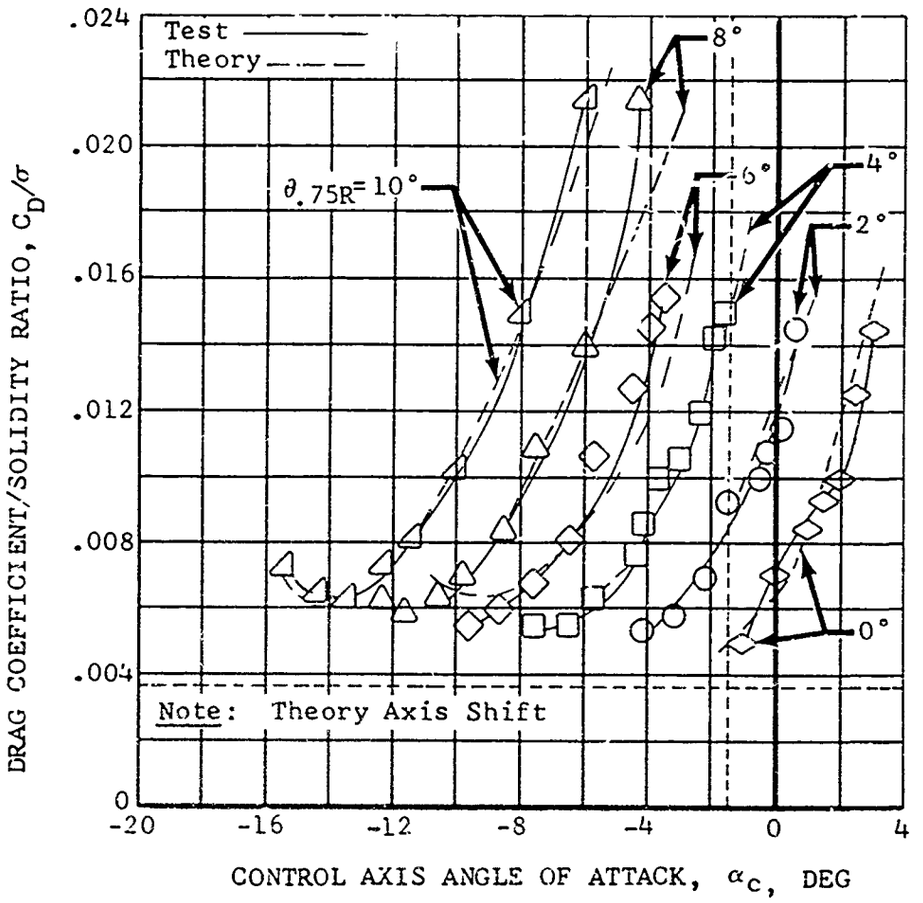

b) C_D/σ vs α_c

Figure 7. Continued.

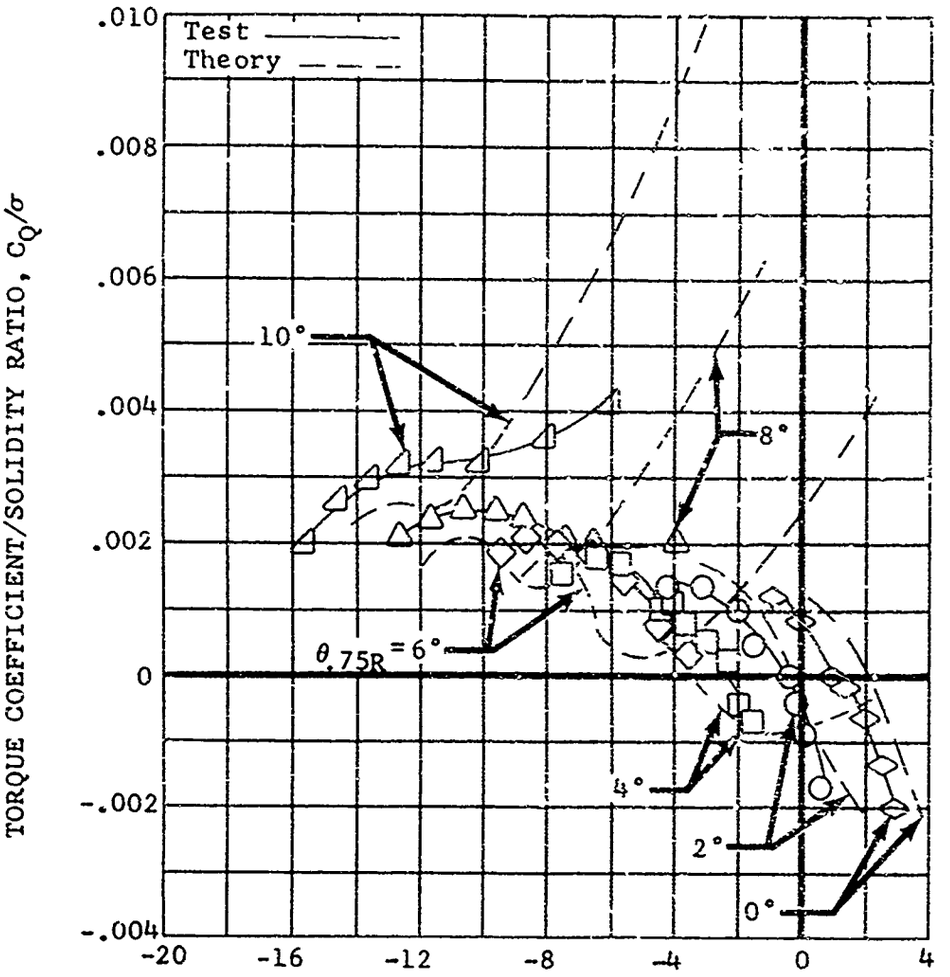

c) C_Q/σ vs α_c

Figure 7. Concluded.

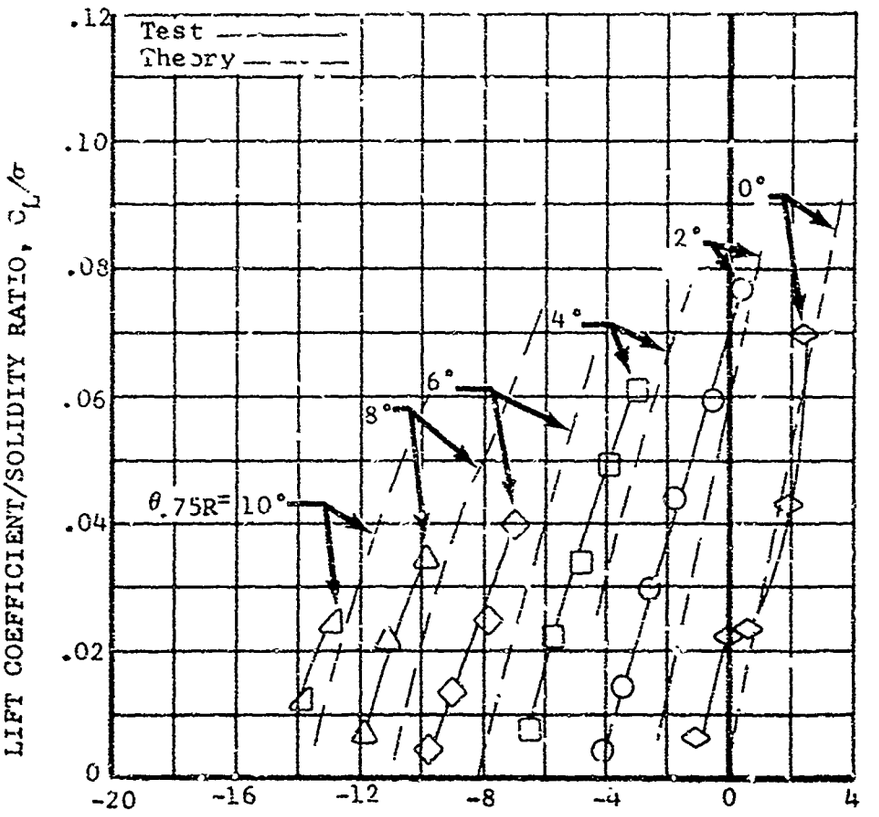

a) C_L/σ vs α_c

Figure 8. Test-Theory Comparison, Nondimensional Performance of the 34-Foot-Diameter Rotor for Various Collective Pitch Angles at μ = 0.76; $M_{(1.0,90.)}$ = 0.50.

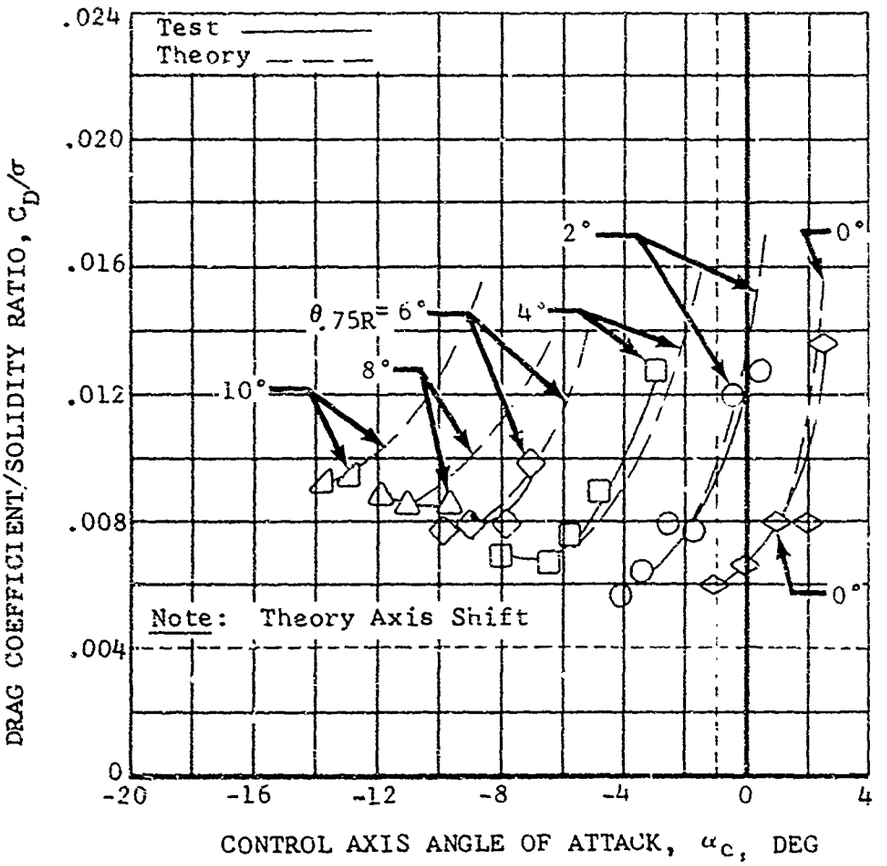

b) C_D/σ vs α_c

Figure 8. Continued.

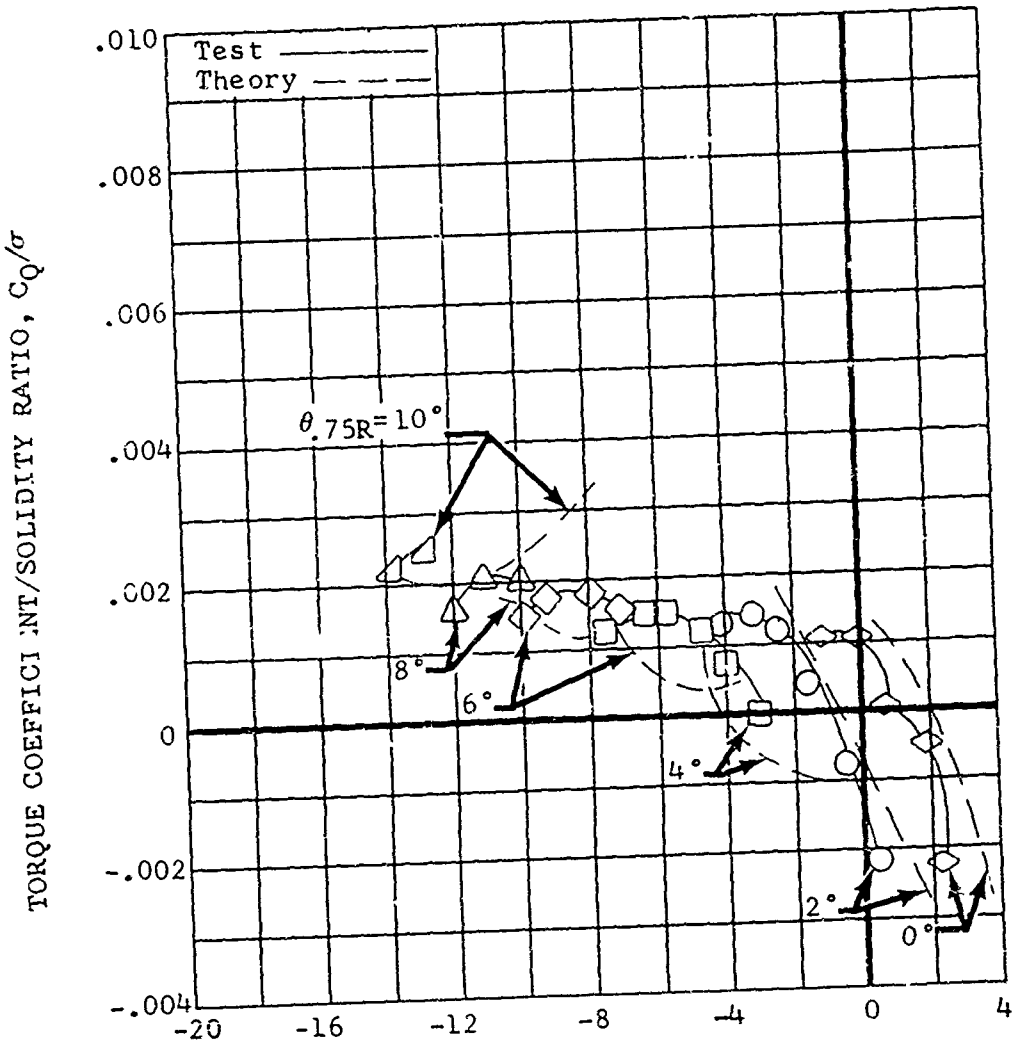

c) C_Q/σ vs α_c

Figure 8. Concluded.

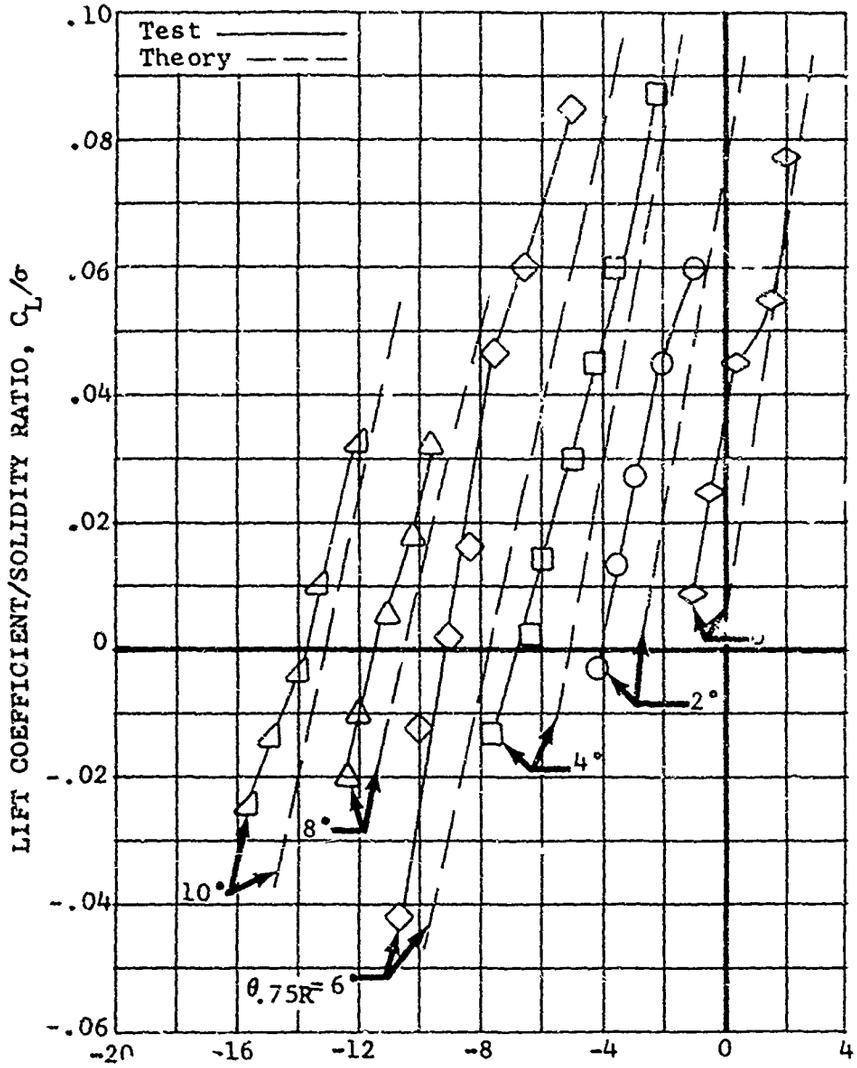

a) C_L/σ vs α_c

Figure 9. Test-Theory Comparison, Nondimensional Performance of the 34-Foot-Diameter Rotor for Various Collective Pitch Angles at μ = 0.86; $M_{(1.0,\ 90.)}$ = 0.47.

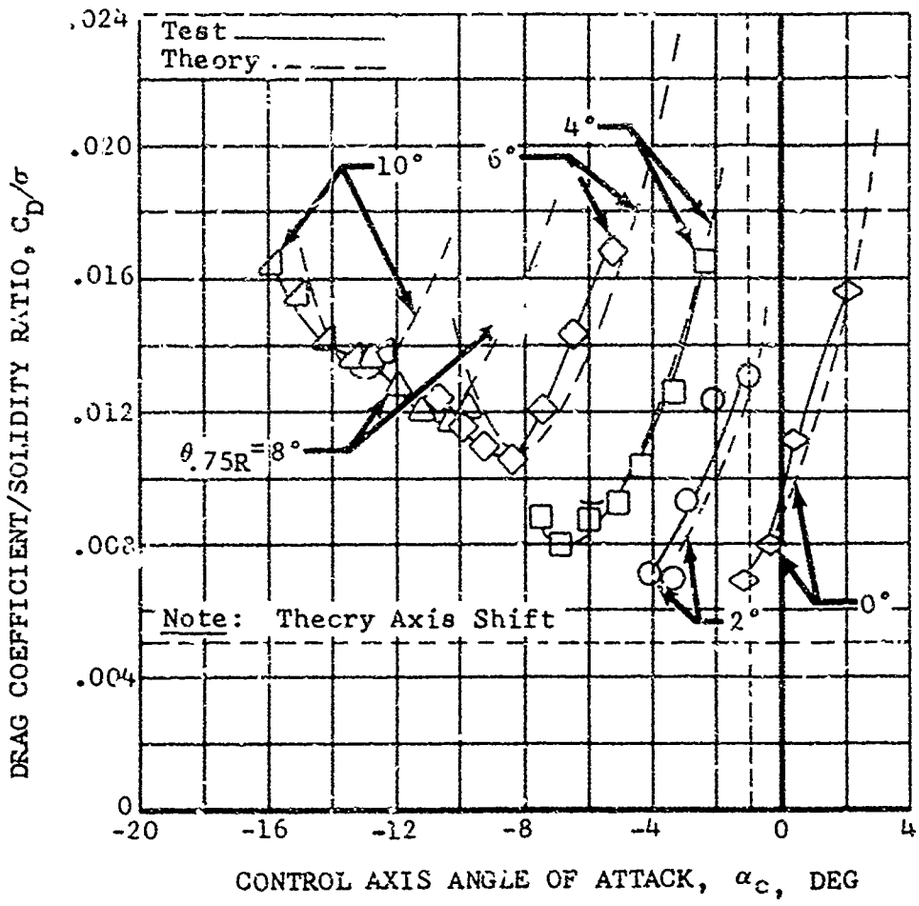

b) C_D/σ vs α_c

Figure 9. Continued.

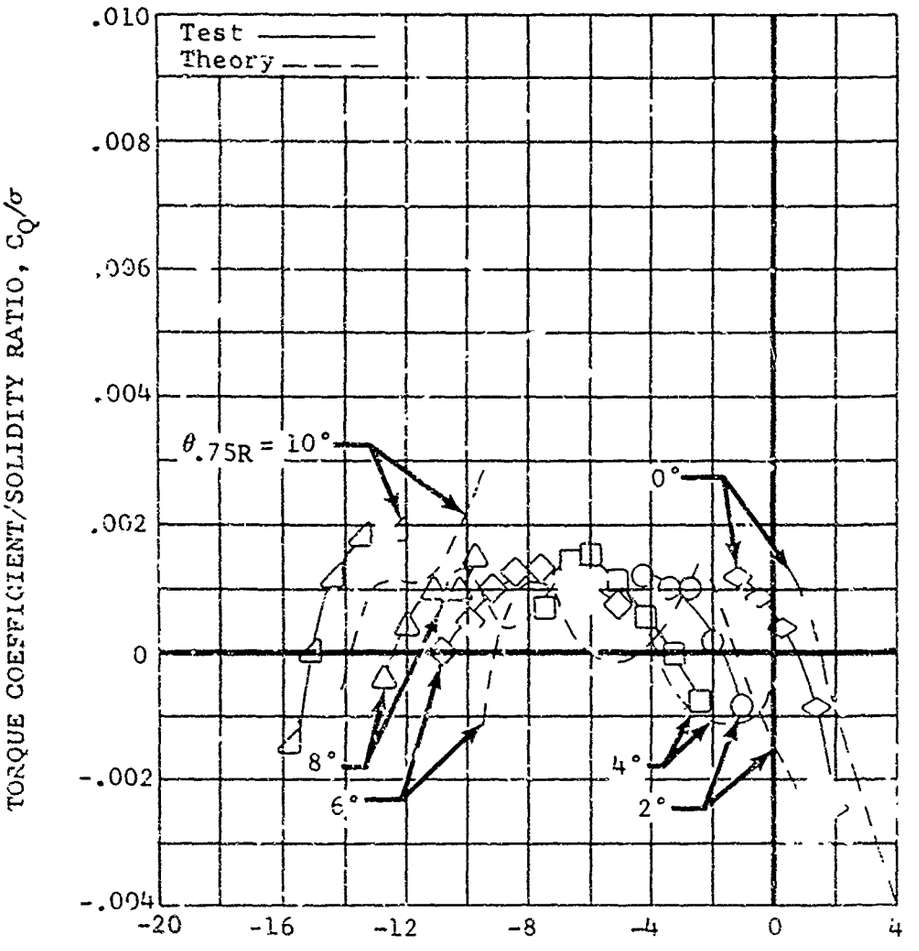

c) C_Q/σ vs α_c

Figure 9. Concluded.

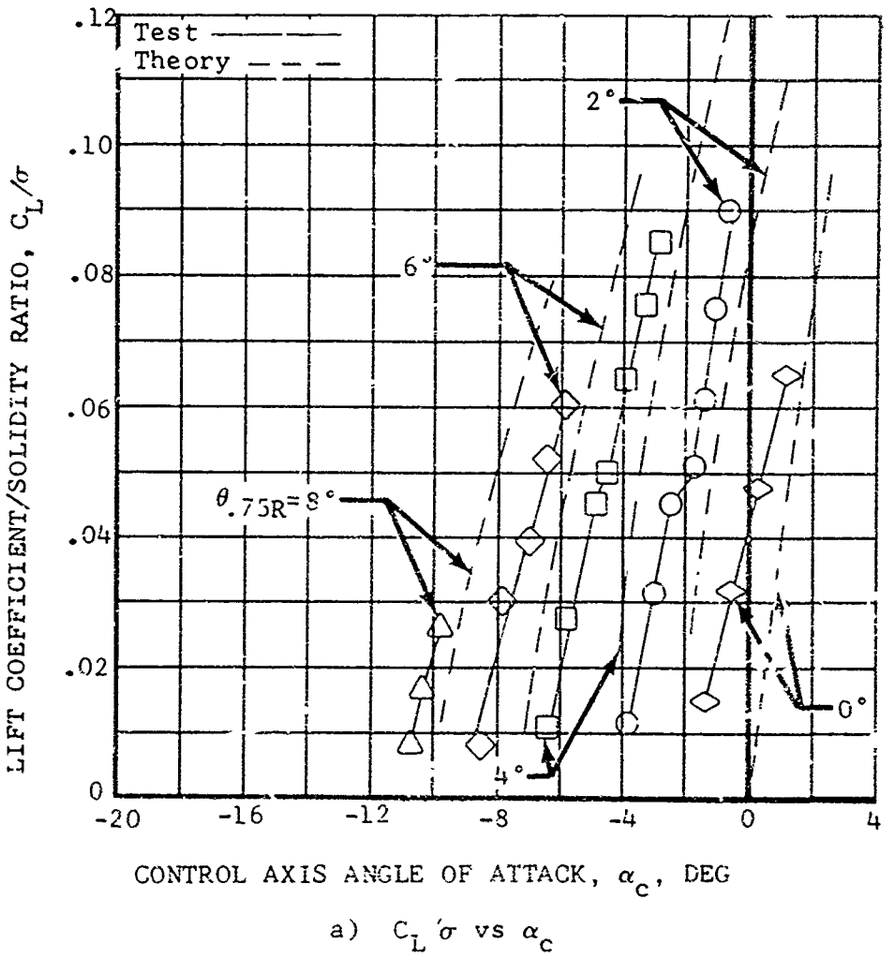

a) C_L/σ vs α_c

Figure 10. Test-Theory Comparison, Nondimensional Performance of the 34-Foot-Diameter Rotor for Various Collective Pitch Angles at μ = 0.94; $M_{(1.0,\ 90.)}$ = 0.49.

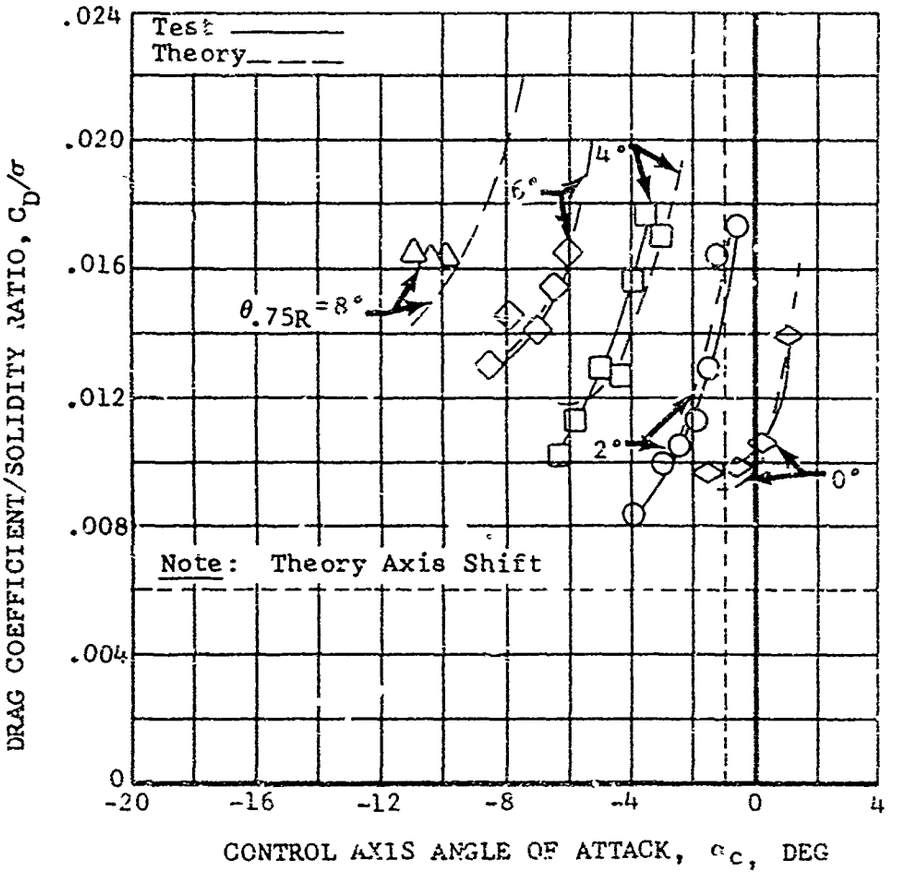

b) C_D/σ vs α_c

Figure 10. Continued.

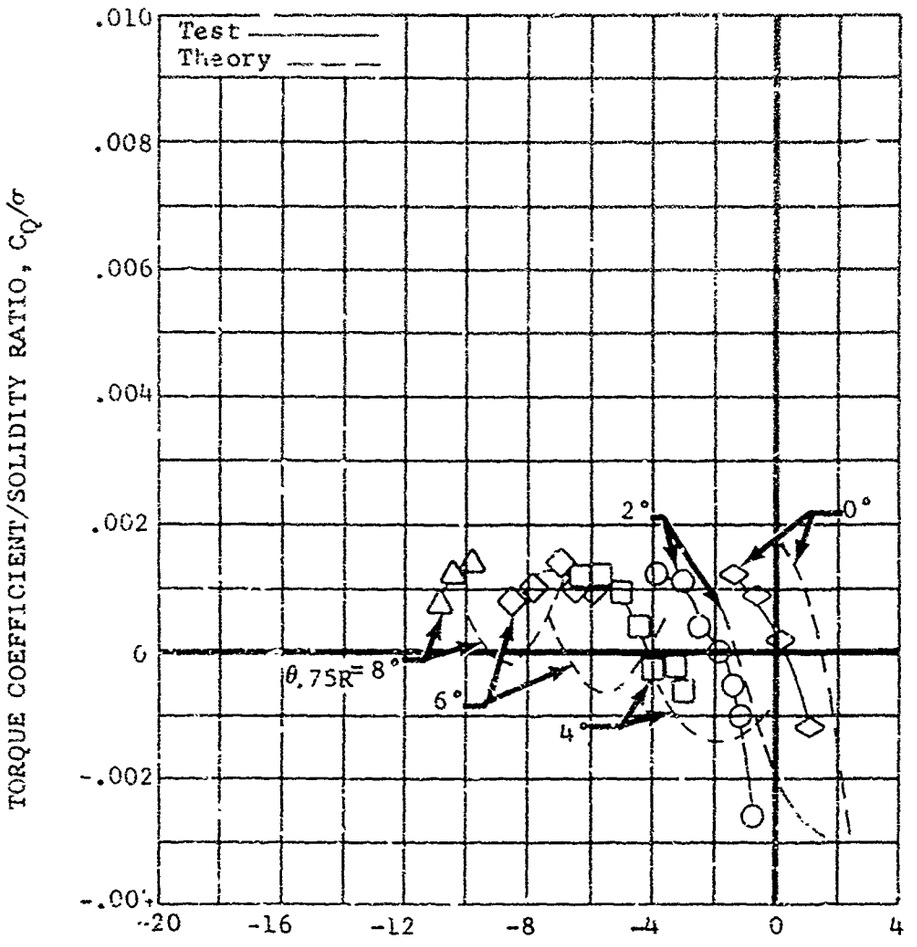

c) C_Q/σ vs α_c

Figure 10. Concluded.

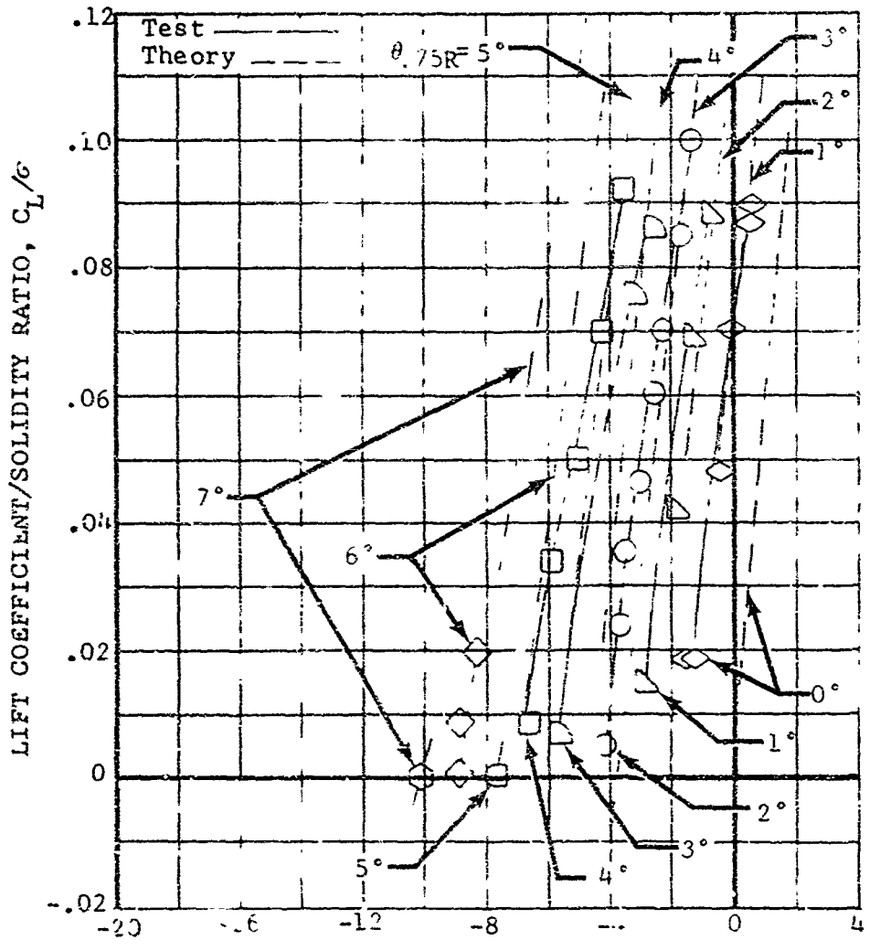

a) C_L/σ vs α_c

Figure 11. Test-Theory Comparison, Nondimensional Performance of the 3/4-Foot-Diameter Rotor for Various Collective Pitch Angles at μ = 1.10; $M_{(1.0,\ 90.)}$ = 0.51.

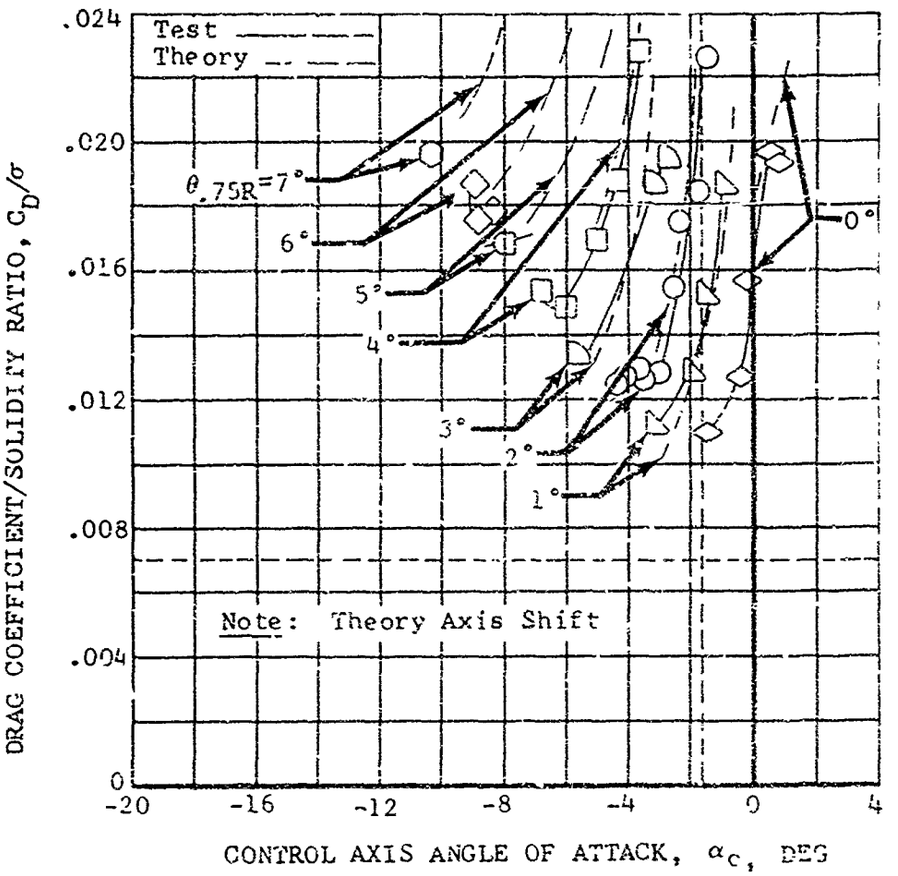

b) C_D/σ vs α_c

Figure 11. Continued.

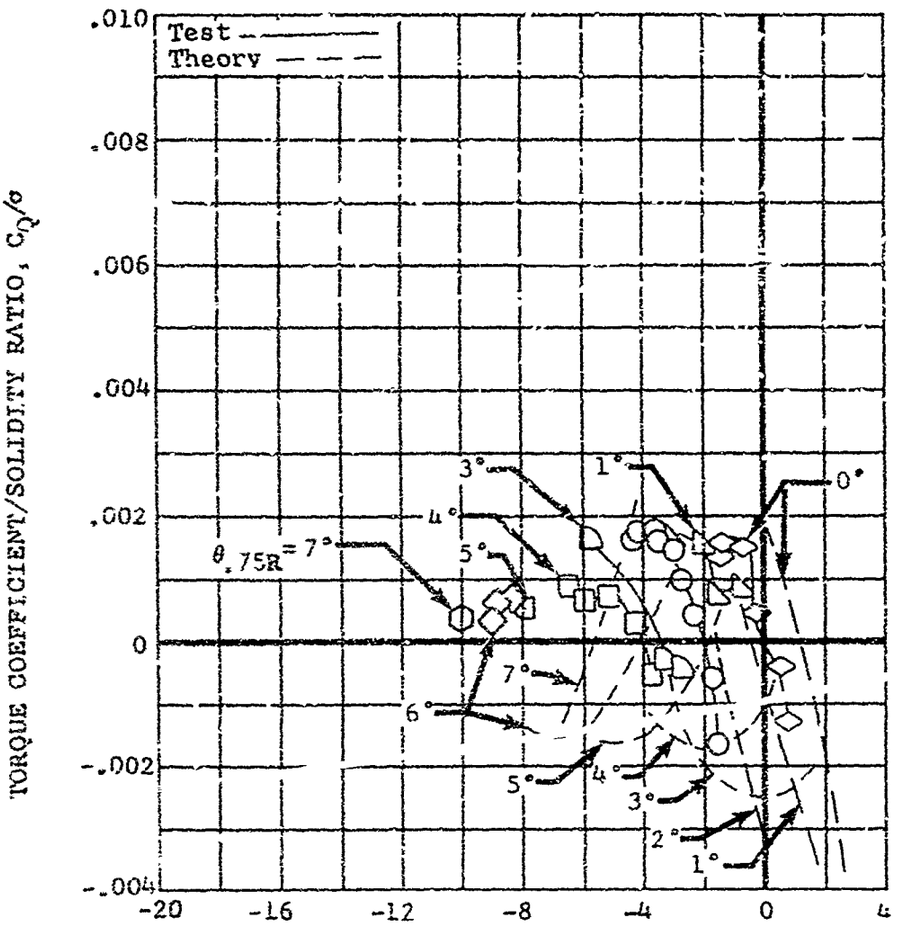

c) C_Q/σ vs α_c

Figure 11. Concluded.

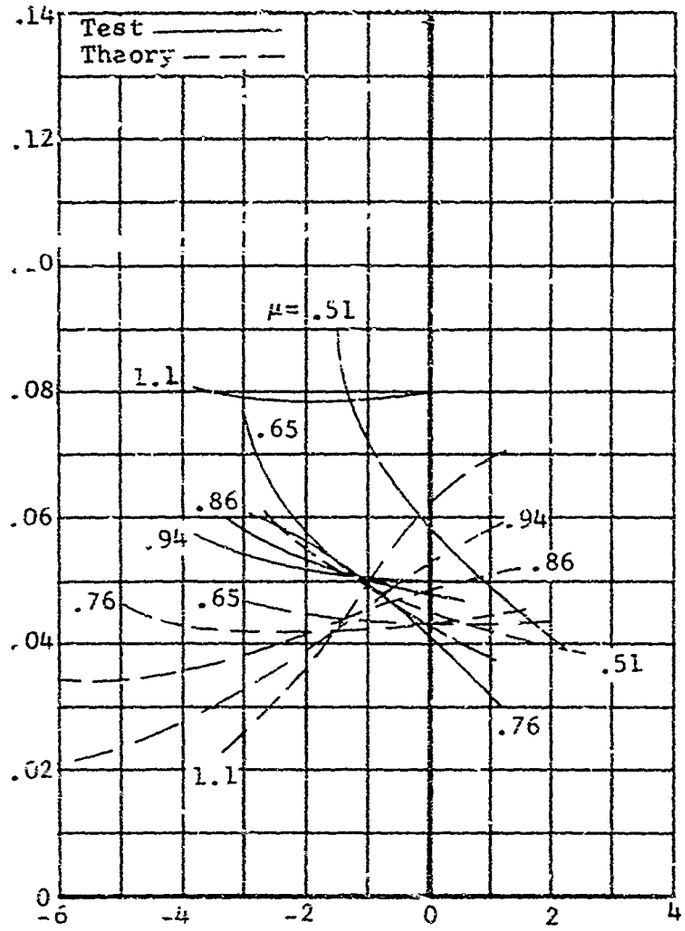

Figure 12. 34-Foot-Diameter Rotor Test-Theory Comparison of the Lift Variation with Control Axis Angle of Attack in Autorotation at Various Advance Ratios.

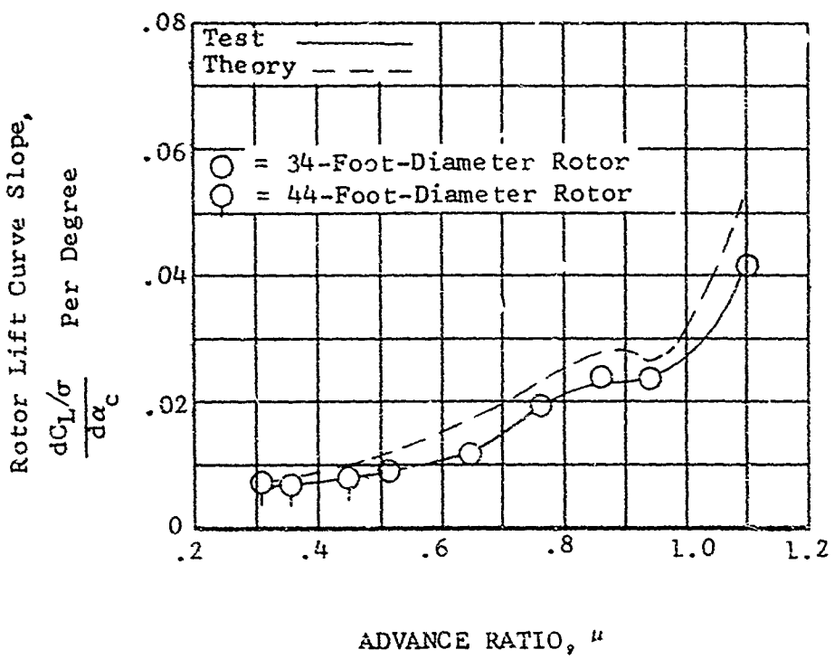

Figure 13. Test-Theory Comparison, Rotor Lift Curve Slope vs. Advance Ratio for Both Rotors.

REFERENCES CITED

1. Bain, Lawrence J., and Landgrebe, Anton J., INVESTIGATION OF COMPOUND HELICOPTER AERODYNAMIC INTERFERENCE EFFECTS, Sikorsky Aircraft Division of United Aircraft Corporation, Stratford, Connecticut; USAAVLABS Technical Report 67-44, U. S. Army Aviation Materiel Laboratories, Fort Eustis, Virginia, November 1967, AD665427.

2. McCloud, John L. III, Biggers, James C., and Stroub, Robert H., AN INVESTIGATION OF FULL-SCALE HELICOPTER ROTORS AT HIGH ADVANCE RATIOS AND ADVANCING TIP MACH NUMBERS, NASA TN D-4632, National Aeronautics and Space Administration, Washington D. C., July 1968.

3. Tanner, W. H., CHARTS FOR ESTIMATING ROTARY WING PERFORMANCE IN HOVER AND AT HIGH FORWARD SPEEDS, Sikorsky Aircraft Division of United Aircraft Corporation, Stratford, Connecticut; NASA CR-114, National Aeronautics and Space Administration, Washington D. C., November 1964.

4. Kisielowski, E., et al., GENERALIZED ROTOR PERFORMANCE, Vertol Division, The Boeing Company, Morton, Pennsylvania; USAAVLABS Technical Report 66-83, U. S. Army Aviation Materiel Laboratories, Fort Eustis, Virginia, February 1967, AD648874.

5. Tanner, W. H., and Van Wyckhouse, J. F., WIND TUNNEL TESTS OF FULL-SCALE ROTORS OPERATING AT HIGH ADVANCING TIP MACH NUMBERS AND ADVANCE RATIOS, Bell Helicopter Company, Fort Worth, Texas; USAAVLABS Technical Report 68-44, U. S. Army Aviation Materiel Laboratories, Fort Eustis, Virginia, July 1968, AD674188.

6. Gessow, Alfred, and Crim, Almer D., A METHOD OF STUDYING THE TRANSIENT BLADE-FLAPPING BEHAVIOR OF LIFTING ROTORS AT EXTREME OPERATING CONDITIONS, NACA TN 3366, Langley Aeronautical Laboratory, Langley Field, Virginia, January 1955.

7. Tanner, W. H., TABLES FOR ESTIMATING ROTARY WING PERFORMANCE AT HIGH FORWARD SPEEDS, Sikorsky Aircraft Division of United Aircraft Corporation, Stratford, Connecticut; NASA CR-114, National Aeronautics and Space Administration, Washington D. C., November 1964.

8. Tanner, W. H., ROTARY WING BOUNDARY LAYER AND RELATED RESEARCHES, Paper presented at Advisory Group for Aerospace Research & Development (AGARD), NATO, Specialists' Meeting on "Fluid Dynamics of Rotor and Fan Supported Aircraft at Subsonic Speeds," Göttingen, Germany, 11-13 September 1967.

9. Carta, F. O., THE UNSTEADY NORMAL FORCE RESPONSE OF AN AIRFOIL IN A PERIODICALLY DISTORTED INLET FLOW INCLUDING STALLING EFFECTS, AIAA Journal of Aircraft, Vol. 4, pp. 416-421, 1967.

10. Paglino, Vincent M., and Logan, Andrew H., AN EXPERIMENTAL STUDY OF THE PERFORMANCE AND STRUCTURAL LOADS OF A FULL-SCALE ROTOR AT EXTREME OPERATING CONDITIONS, Sikorsky Aircraft Division of United Aircraft Corporation, Stratford, Connecticut; USAAVLABS Technical Report 68-3, U. S. Army Aviation Materiel Laboratories, Fort Eustis, Virginia, July 1968, AD674187.

APPENDIX I
GRAPHED DATA

The data presented in this appendix (Figures 14 through 23) are from the wind tunnel balance and model instrumentation as tabulated in Appendix IV. The symbols are actual test points and show lift, drag, and torque coefficients as a function of collective pitch ($\theta_{.75R}$). These data illustrate the consistency of the experimental results.

Rotor rotational speed and tunnel speed were adjusted to obtain the desired advance ratio and advancing tip Mach number. The cyclic pitch was adjusted to minimize first harmonic rotor flapping; and at each combination of shaft angle and collective pitch, the data were recorded. Collective pitch or shaft angle was then changed, and the above procedure was repeated until the envelope was explored.

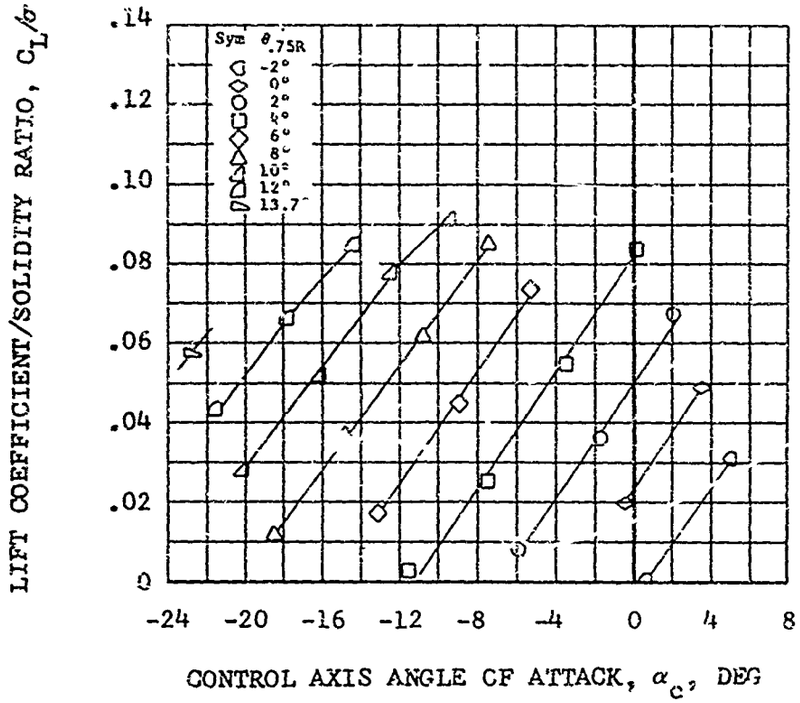

Figure 14. Nondimensional Performance Data for the 44-Foot-Diameter Rotor for Various Blade Collective Pitch Angles, μ = 0.31; $M_{(1.0,\ 90.)}$ = 0.88.

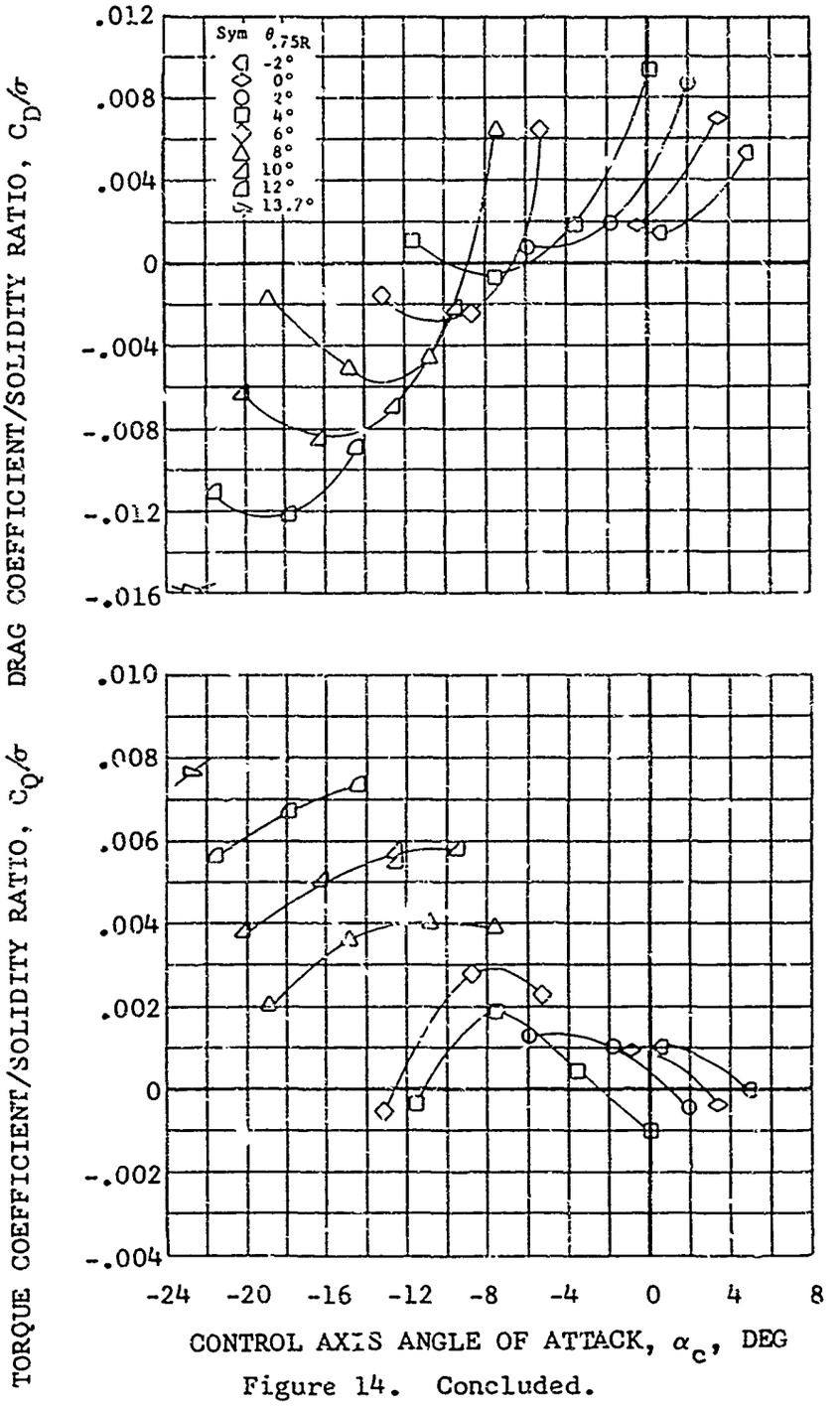

Figure 14. Concluded.

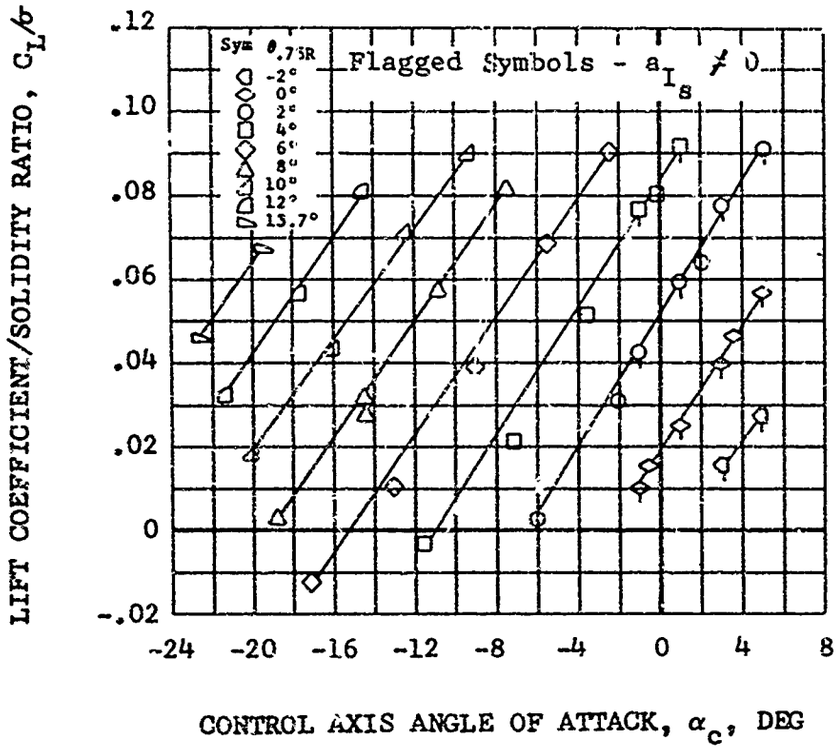

Figure 15. Nondimensional Performance Data for the 44-Foot-Diameter Rotor for Various Blade Collective Pitch Angles, $\mu = 0.36$; $M_{(1.0,\ 90.)} = 0.80$.

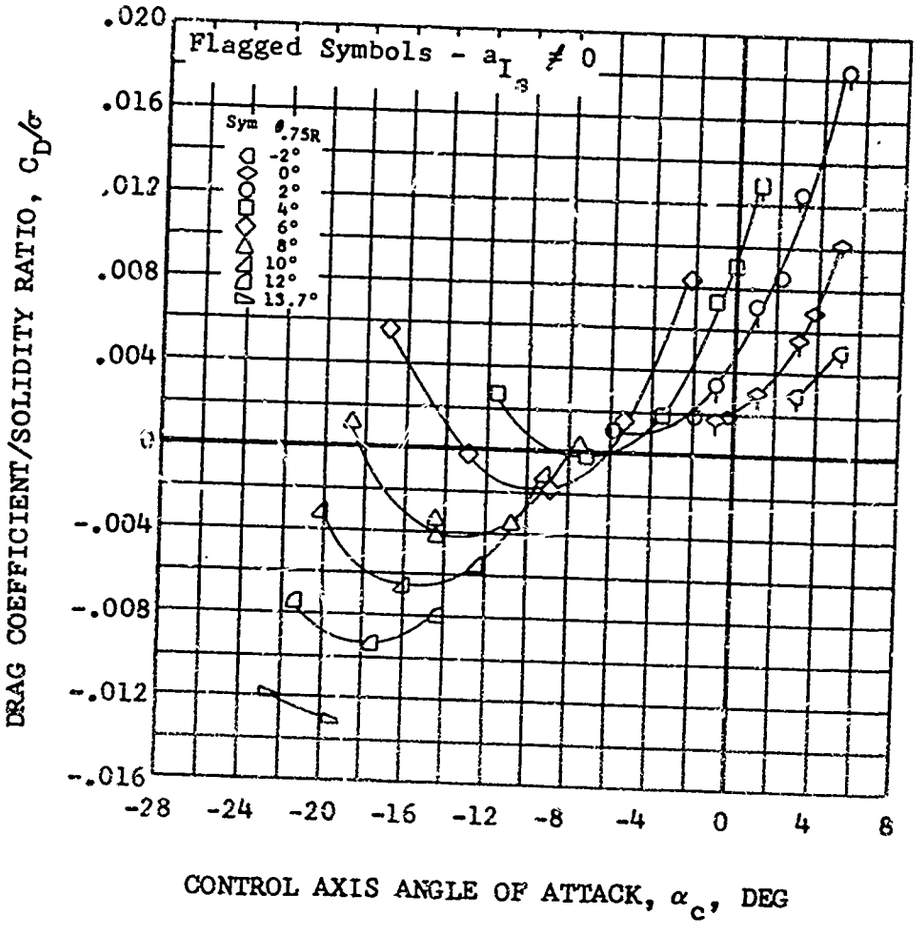

Figure 15. Continued.

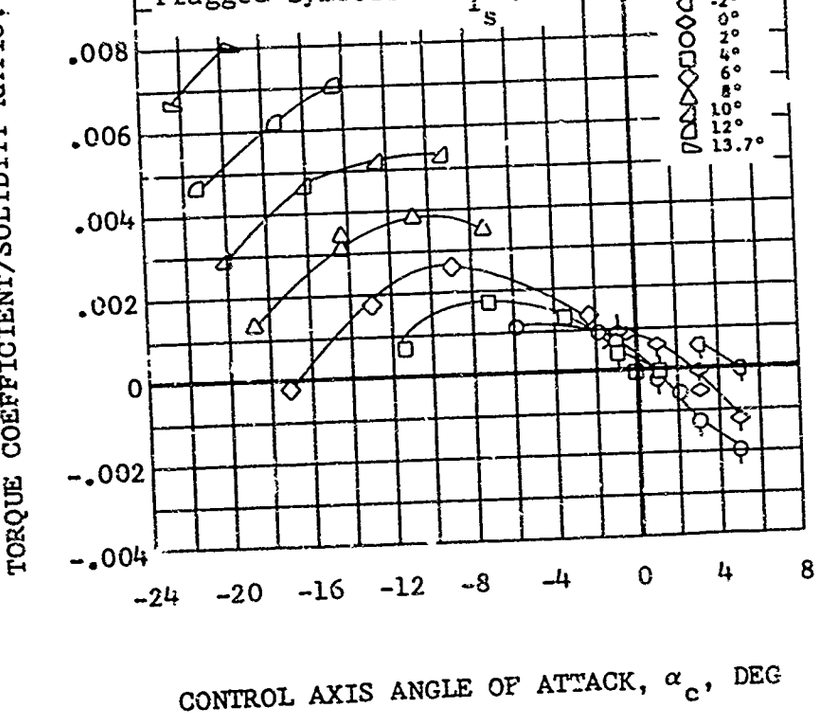

Figure 15. Concluded.

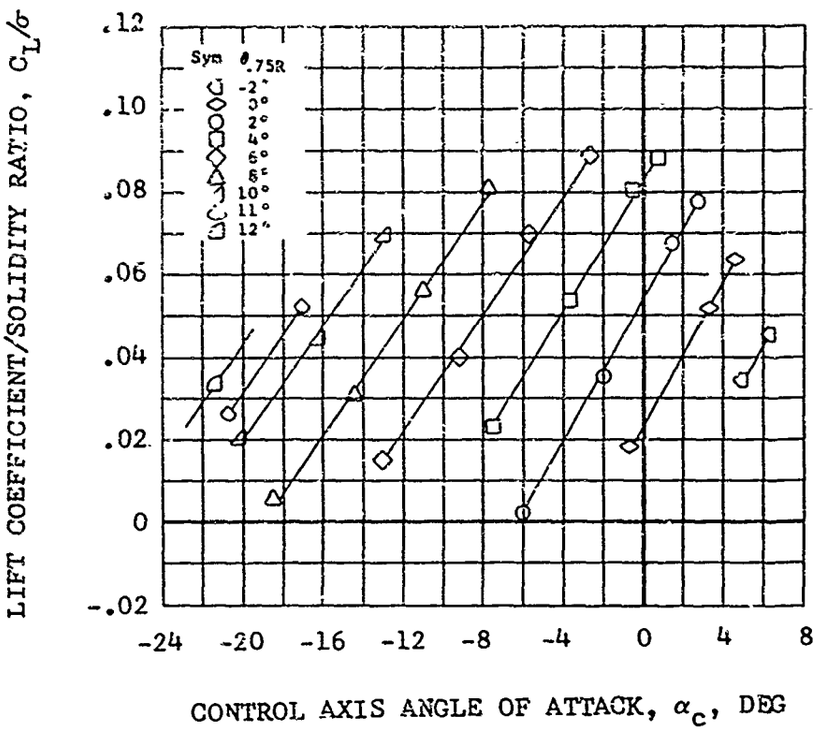

Figure 16. Nondimensional Performance Data for the 44-Foot-Diameter Rotor for Various Blade Collective Pitch Angles, $\mu = 0.36$; $M_{(1.0,\ 90.)} = 0.90$.

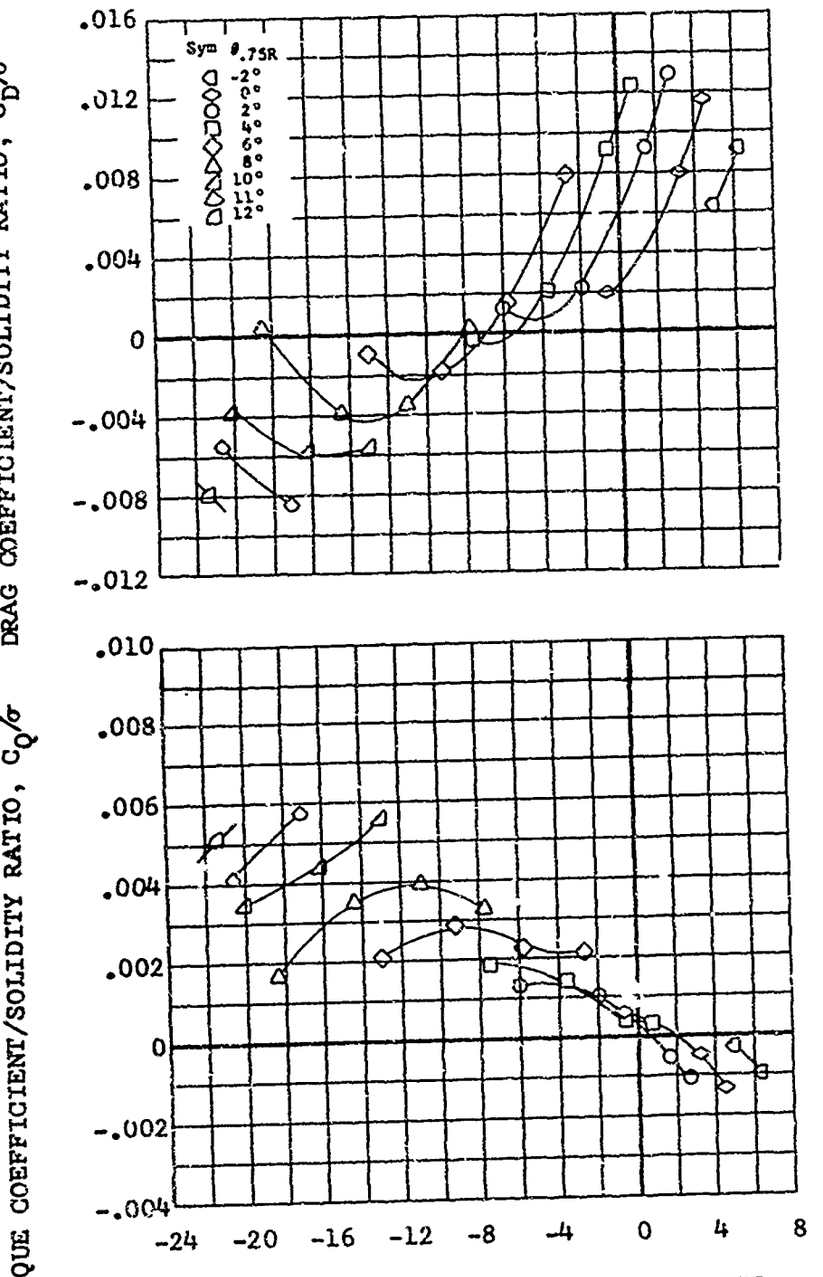

Figure 16. Concluded.

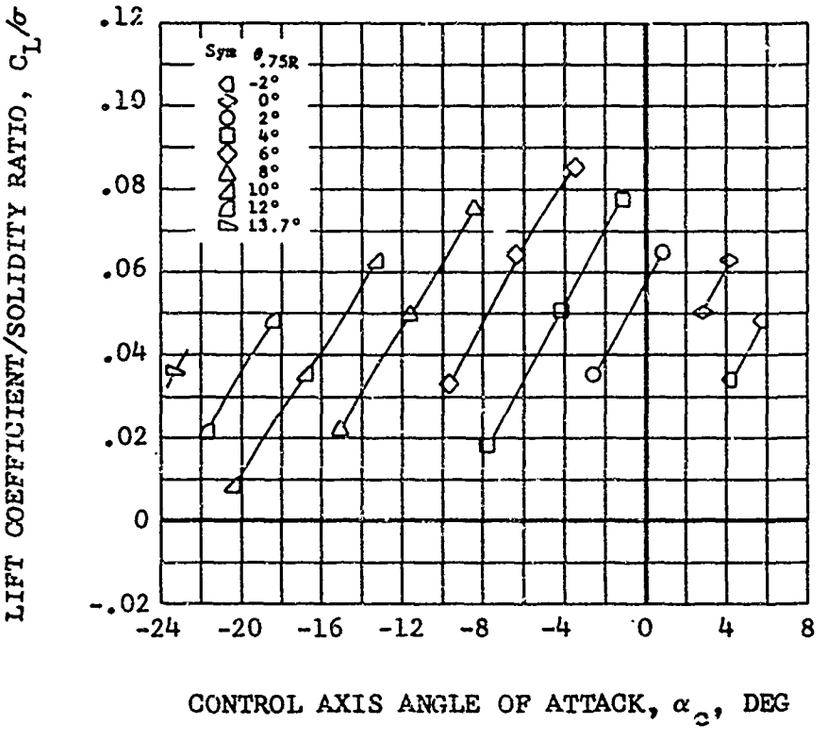

Figure 17. Nondimensional Performance Data for the 44-Foot-Diameter Rotor for Various Blade Collective Pitch Angles, $\mu = 0.40$; $M_{(1.0,\ 90.)} = 0.83$.

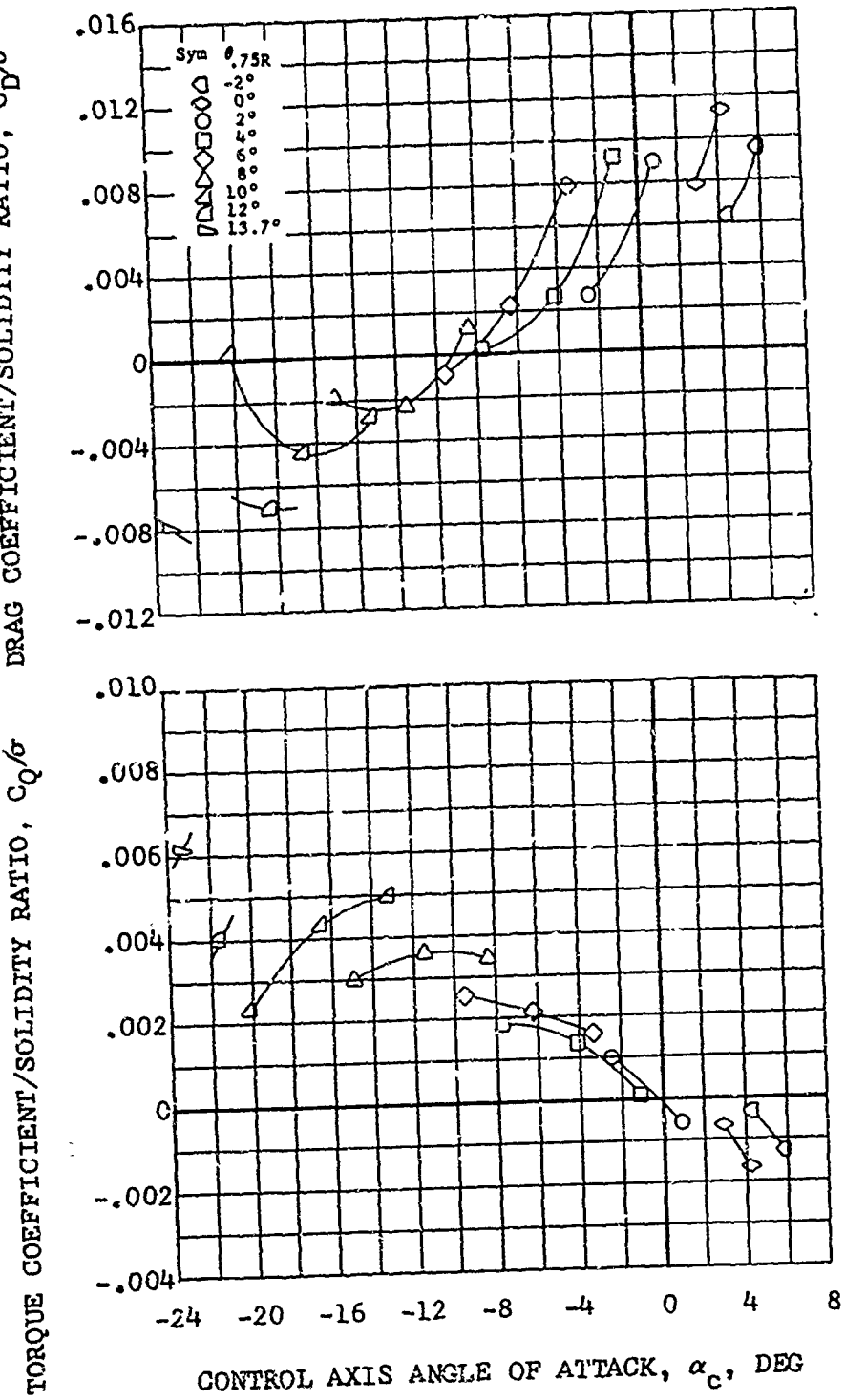

Figure 17. Concluded.

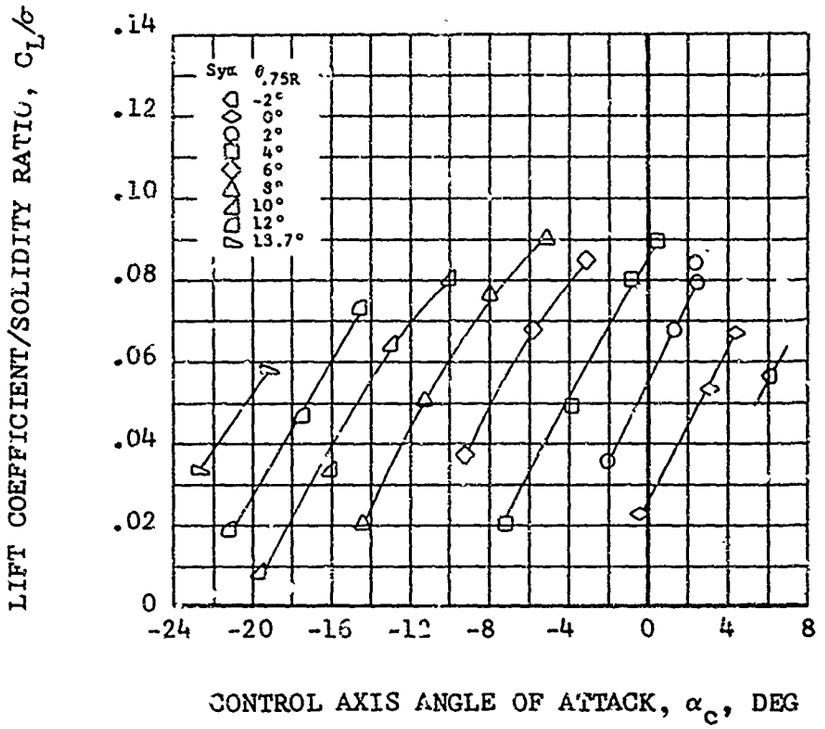

Figure 18. Nondimensional Performance Data for the 44-Foot-Diameter Rotor for Various Blade Collective Pitch Angles, $\mu = 0.41$; $M_{(1.0,\ 90.)} = 0.94$.

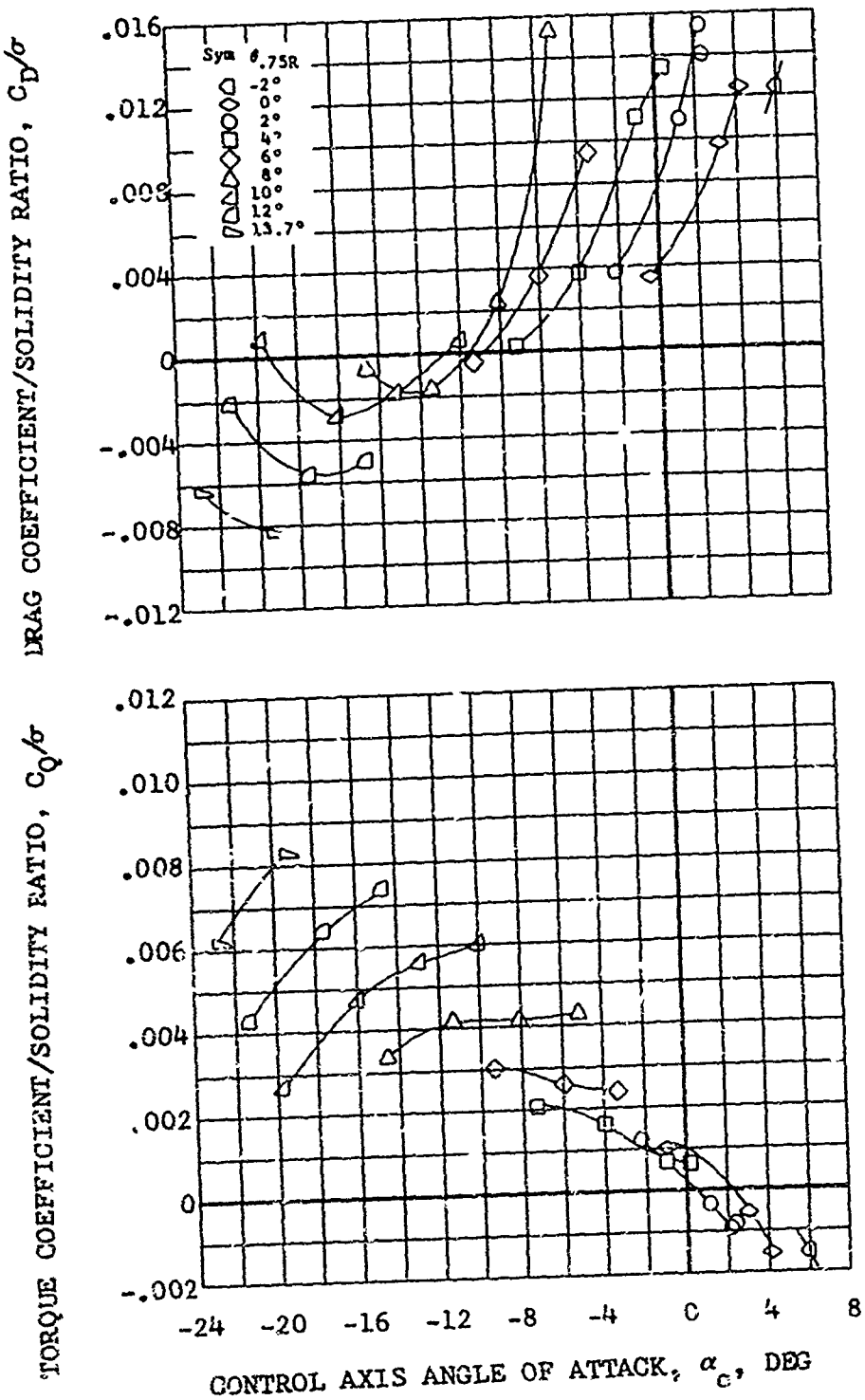

Figure 18. Concluded.

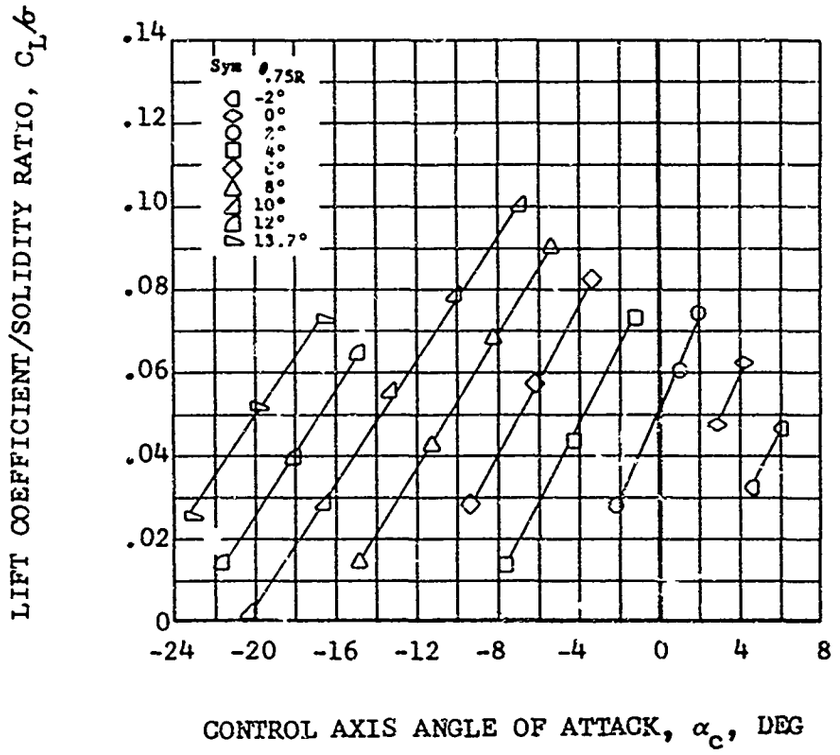

Figure 19. Nondimensional Performance Data for the 44-Foot-Diameter Rotor for Various Blade Collective Pitch Angles, μ = 0.45; $M_{(1.0,\ 90.)}$ = 0.77.

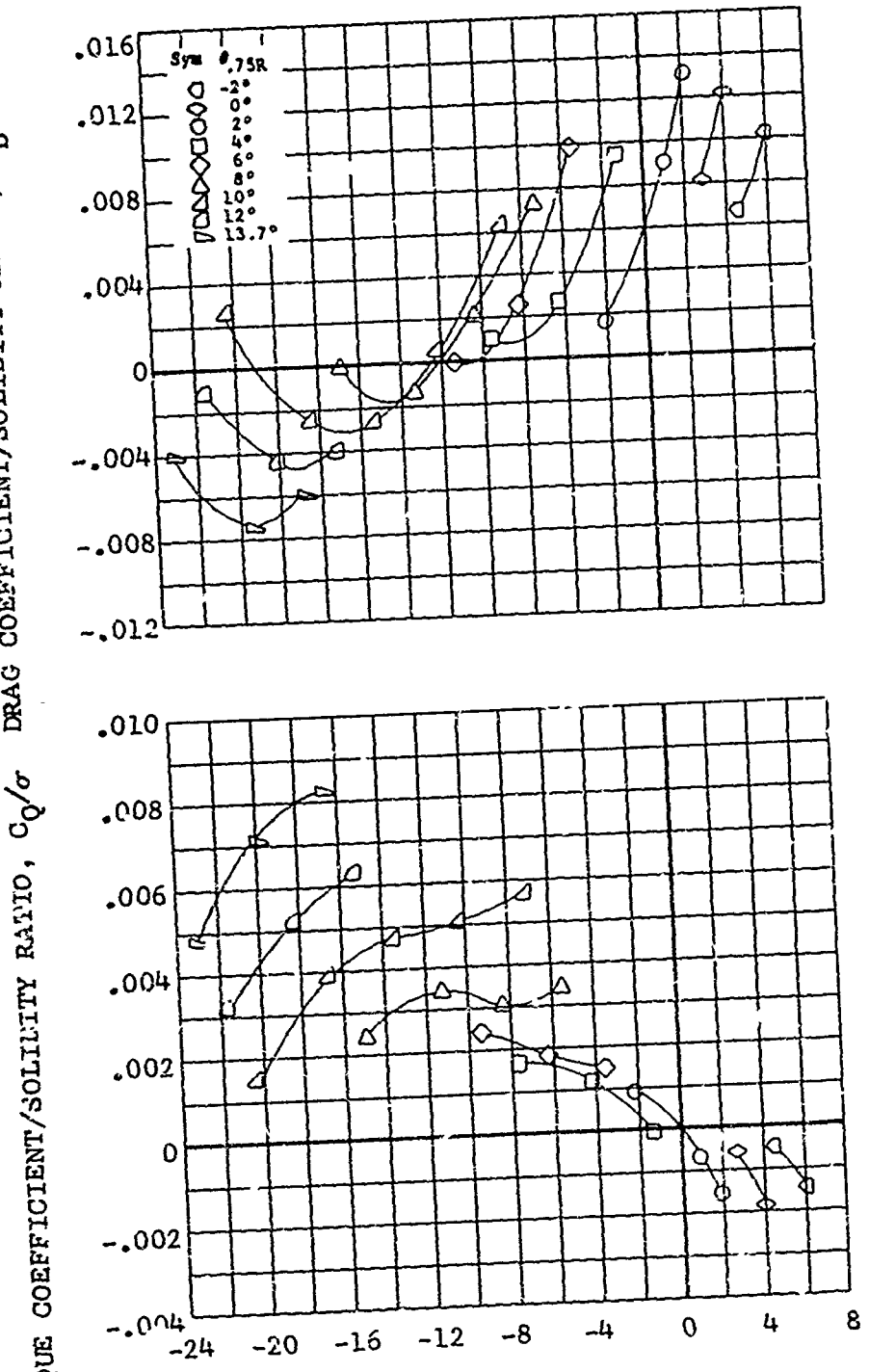

Figure 19. Concluded.

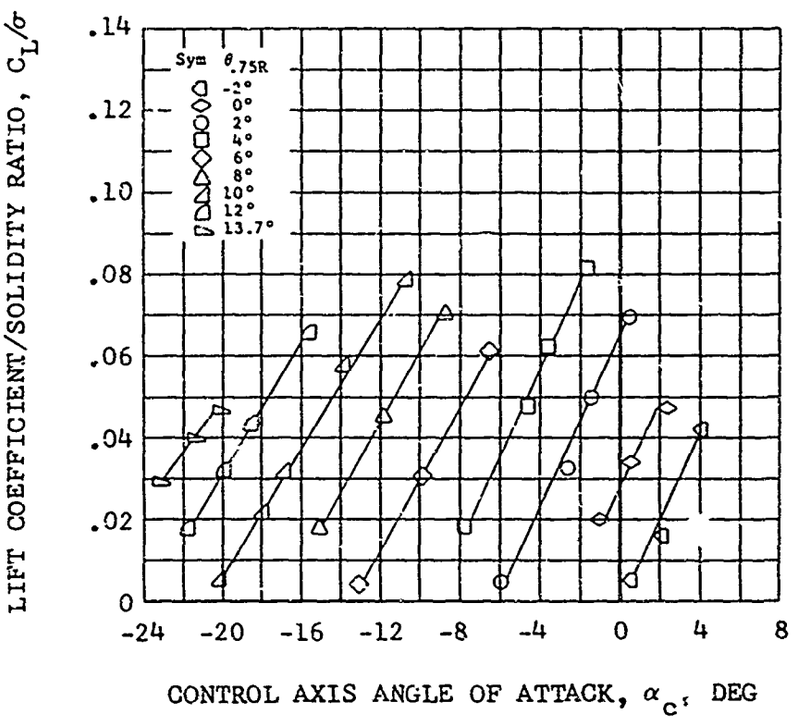

Figure 20. Nondimensional Performance Data for the 44-Foot-Diameter Rotor for Various Blade Collective Pitch Angles, $\mu = 0.45$; $M_{(1.0,\ 90.)} = 0.90$.

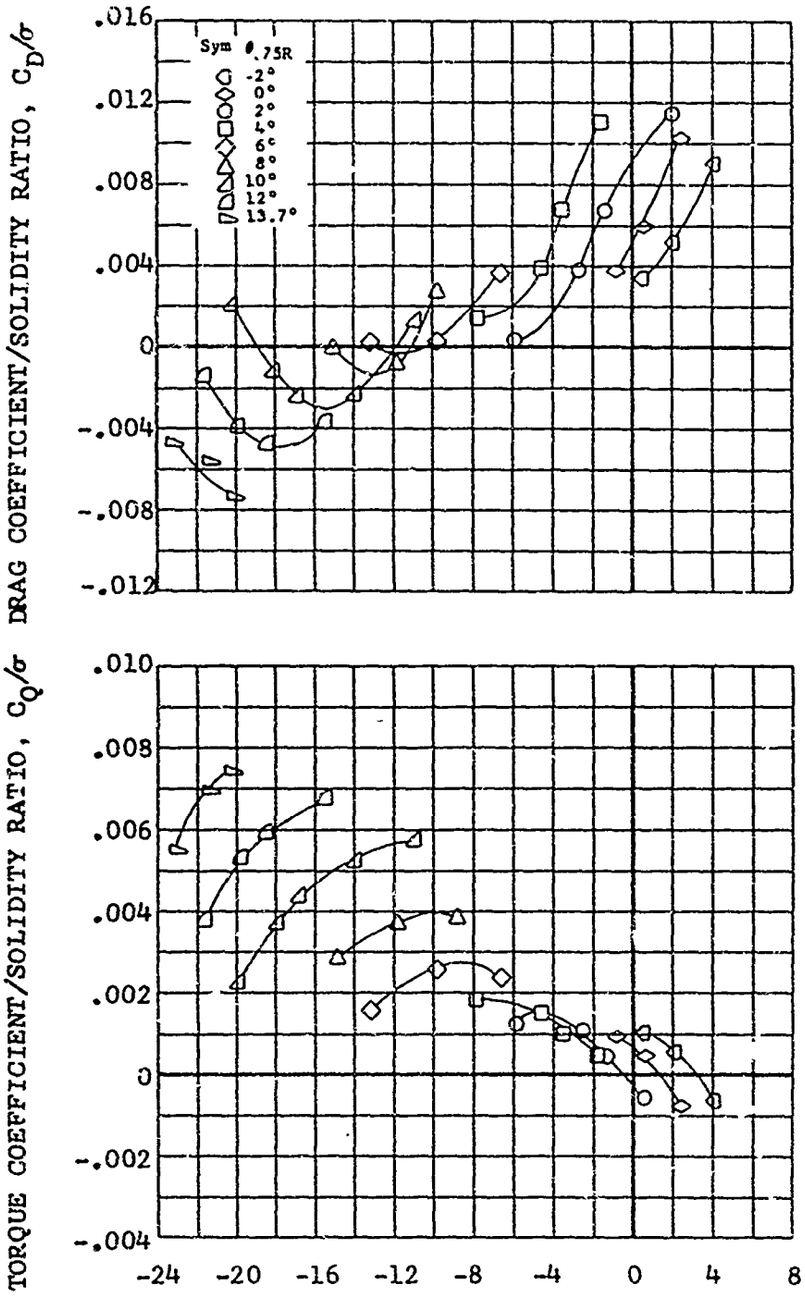

Figure 20. Concluded.

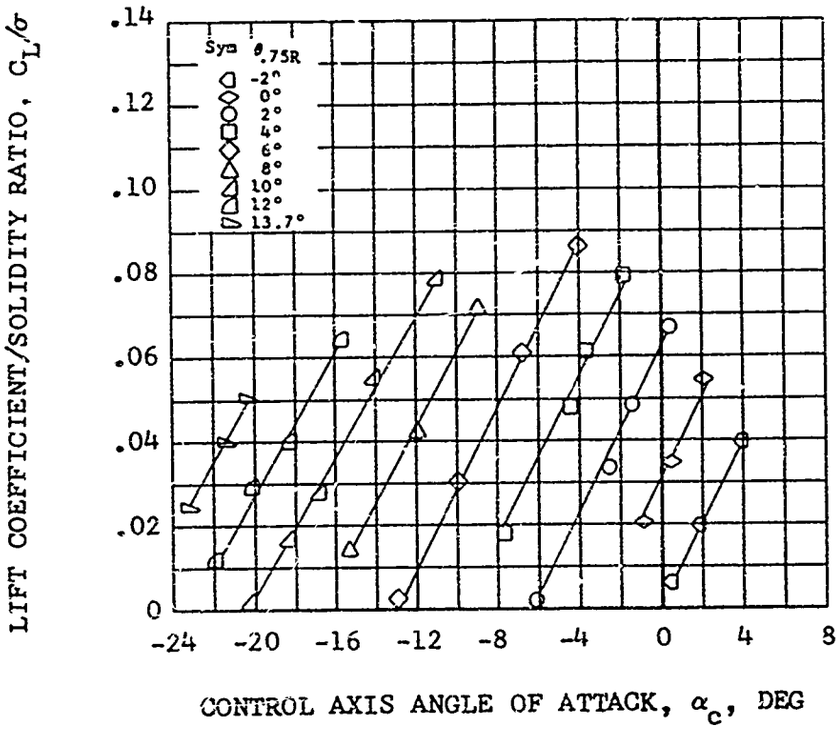

Figure 21. Nondimensional Performance Data for the 44-Foot-Diameter Rotor for Various Blade Collective Pitch Angles, $\mu = 0.46$; $M_{(1.0,\ 90.)} = 0.86$.

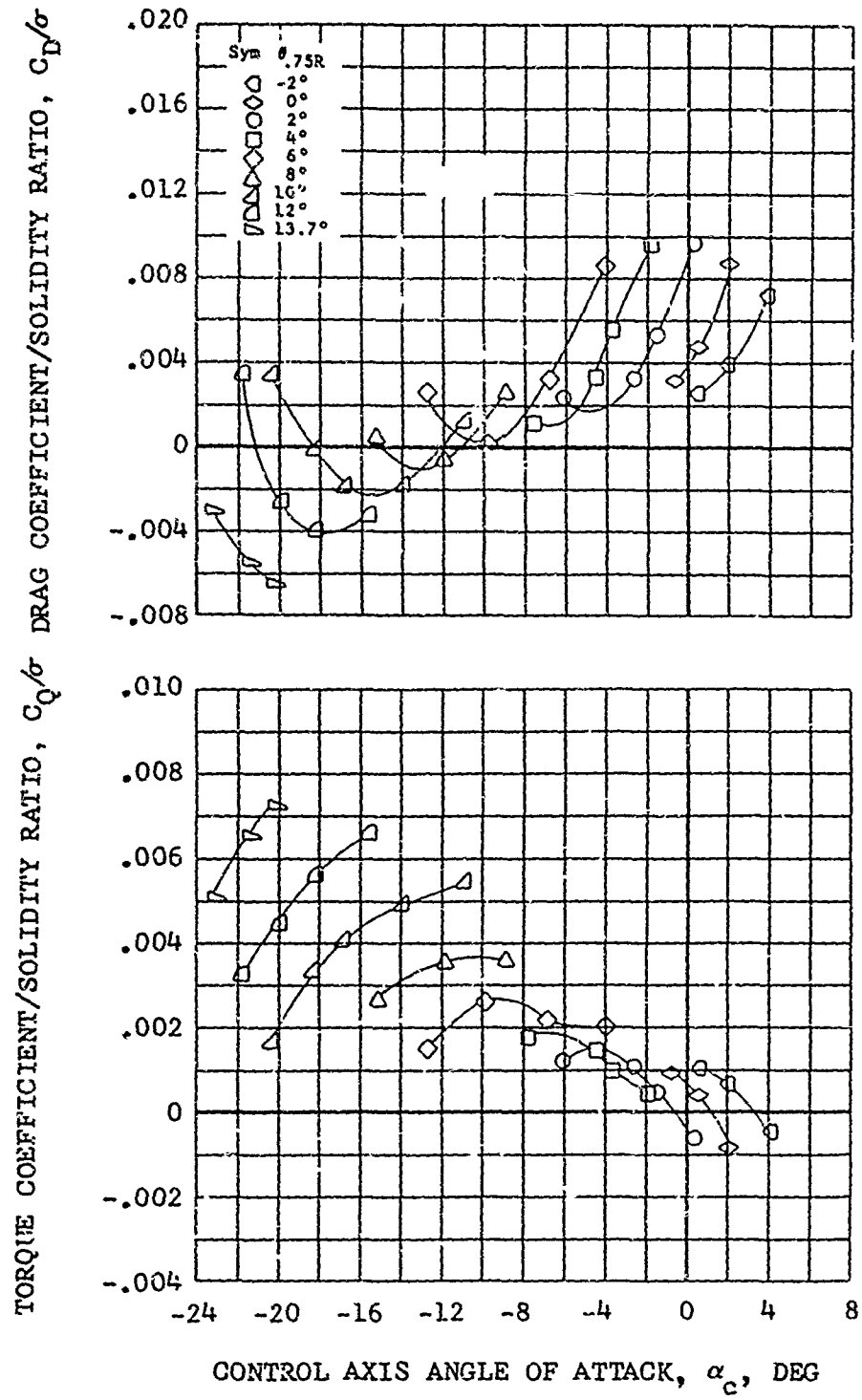

Figure 21. Concluded.

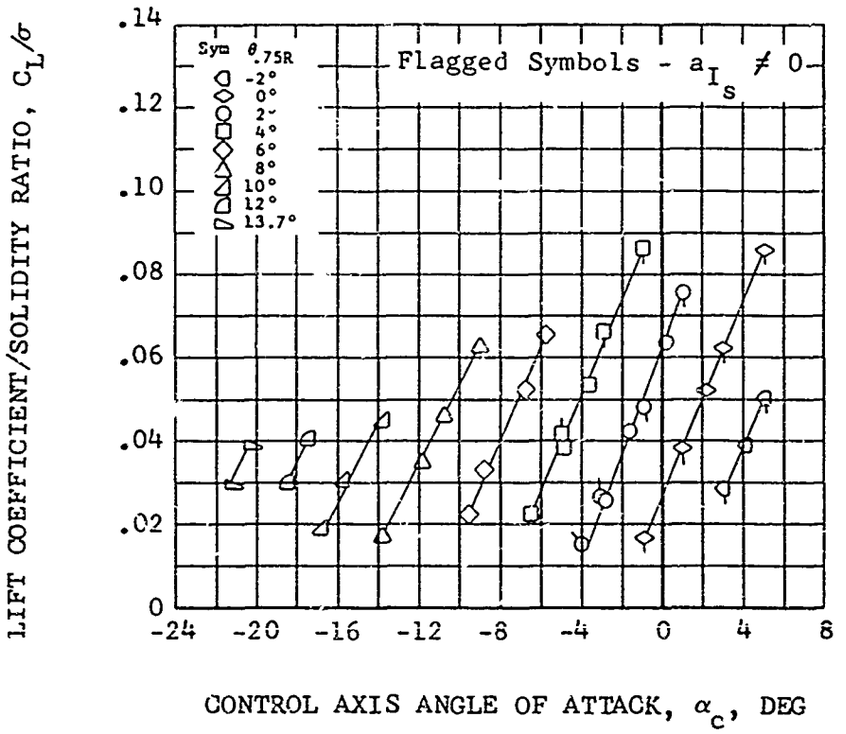

Figure 22. Nondimensional Performance Data for the 44-Foot-Diameter Rotor for Various Blade Collective Pitch Angles, $\mu = 0.51$; $M_{(1.0,\ 90.)} = 0.80$.

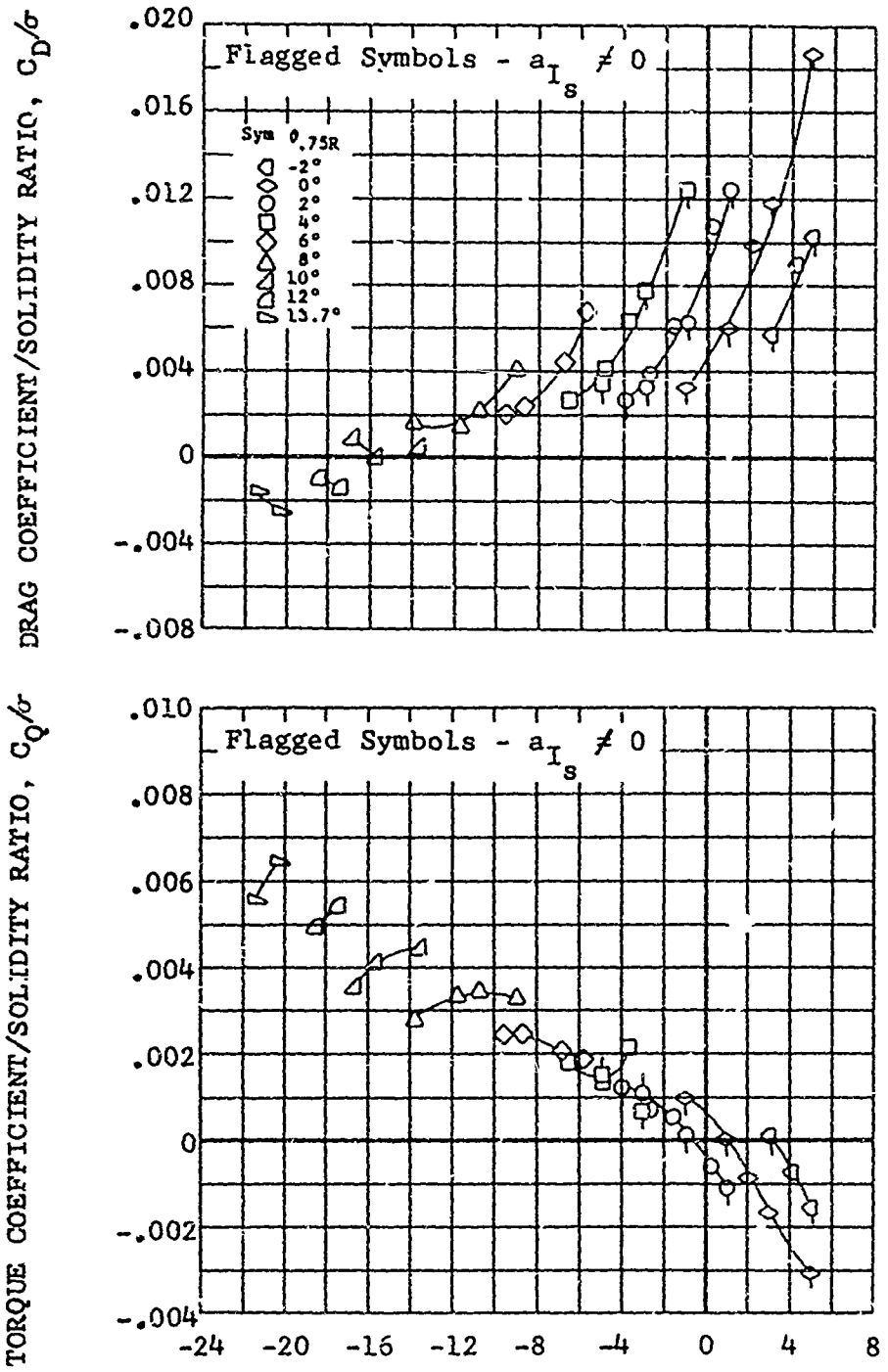

Figure 22. Concluded.

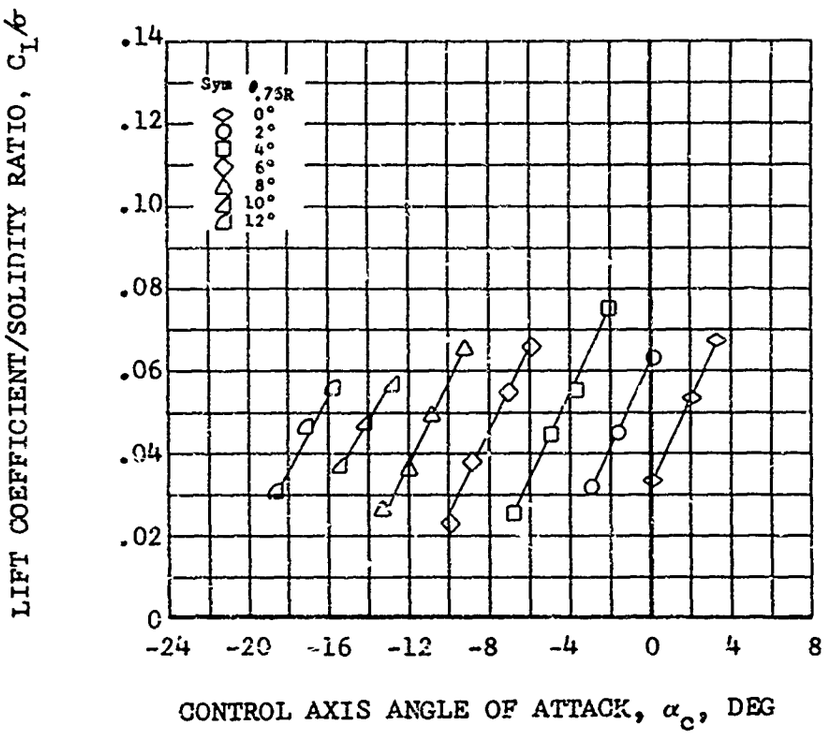

Figure 23. Nondimensional Performance Data for the 44-Foot-Diameter Rotor for Various Blade Collective Pitch Angles, $\mu = 0.52$; $M_{(1.0,\ 90.)} = 0.81$.

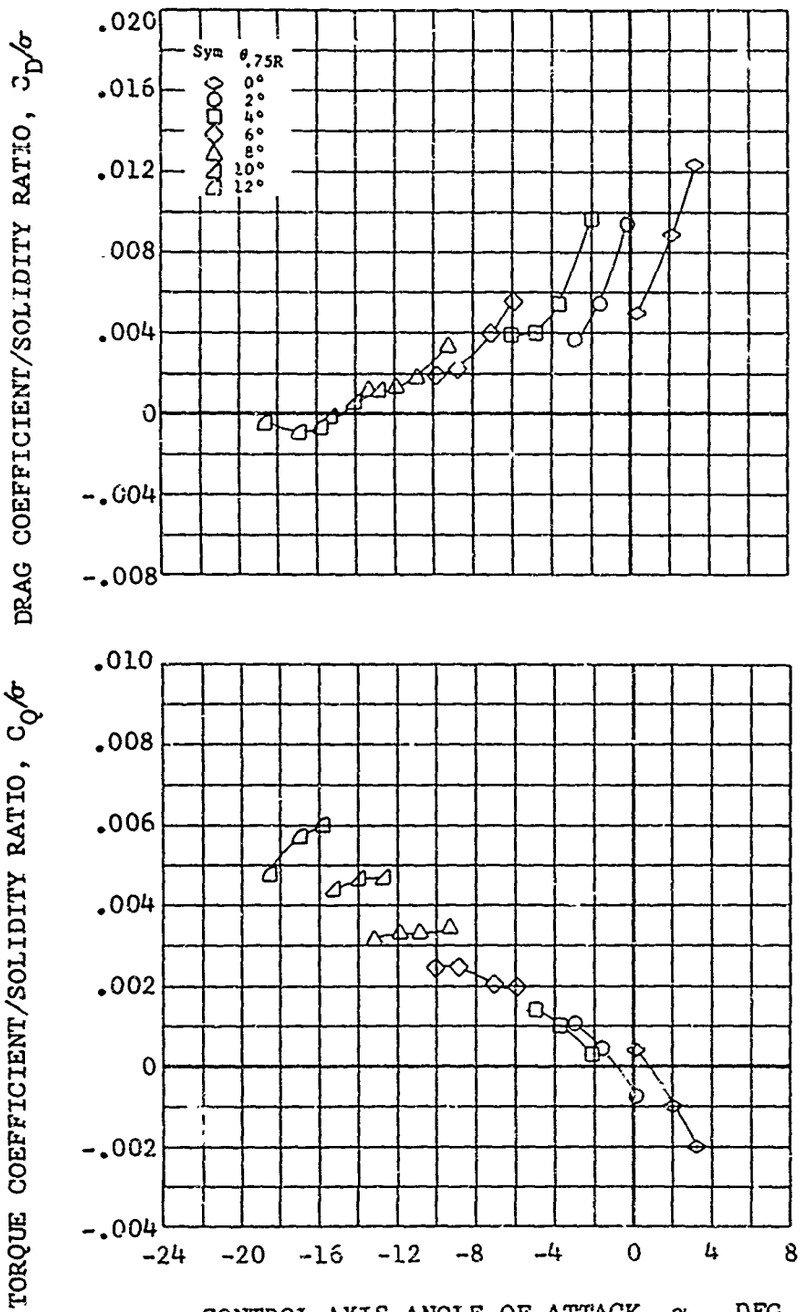

Figure 23. Concluded.

APPENDIX II
TABULAR DATA

The data presented in this appendix were recorded by the Large Scale Aerodynamic Branch of the NASA-Ames Research Center. Table IV relates the test conditions, rotor configuration, and the page number where these data are presented.

Data Reduction

Six-component forces and moments were measured by the wind tunnel balance system. Tare corrections were applied to the balance data to account for forces and moments produced by the exposed model support struts, the faired body, and the rotating hub. The rotating hub tares included all hardware inboard of the 2.66-foot radius station. The tares were applied based on wind tunnel dynamic pressure and shaft angle. Rotor downwash effects on the tares were neglected, and no data adjustments were made for wall effects.

TABLE IV. WIND TUNNEL TABULATED DATA

TABLE IV-1. 44-FOOT ROTOR, $\mu = 0.31$, $M_{(1.0,\ 90.)} = 0.88$

Test 310 Run 3

PT.	$\theta_{.75R}$	α_S	α_C	C_L/σ	C_D/σ	C_Y/σ	C_ℓ/σ	C_m/σ	C_Q/σ	μ	$M_{(1.0,90.)}$
1.	8.0	-10.0	-14.8	0.035508	0.005054	0.000115	-0.000744	-0.000566	0.003618	0.315	0.871
2.	6.0	-10.0	-13.1	0.017023	0.001594	0.000171	-0.000349	-0.000506	0.002133	0.318	0.873
3.	10.0	-10.0	-16.2	0.050949	0.008489	-0.000085	-0.001051	-0.000784	0.005010	0.315	0.878
4.	12.0	-10.0	-17.8	0.065884	0.012123	-0.000311	-0.001553	-0.000639	0.006724	0.316	0.874
5.	13.0	-10.0	-18.5	0.072497	0.013746	-0.000598	-0.001848	-0.000791	0.007807	0.318	0.874
6.	10.0	-15.0	-20.1	0.027827	0.006362	0.000605	-0.001284	-0.000678	0.003806	0.318	0.871
7.	8.0	-15.0	-18.8	0.011840	0.001735	0.000718	-0.000886	-0.000617	0.002024	0.318	0.872
8.	12.0	-15.0	-21.5	0.043130	0.011132	0.000265	-0.001758	-0.000687	0.005455	0.319	0.872
9.	13.7	-15.0	-22.9	0.057129	0.015756	0.000028	-0.002284	-0.000808	0.007670	0.319	0.872
10.	10.0	-5.0	-12.5	0.077466	0.006873	-0.001661	-0.000633	-0.000771	0.005491	0.318	0.873
11.	10.0	-5.0	-12.5	0.066790	0.004110	-0.001837	-0.000646	0.003699	0.005810	0.317	0.870

Test 310 Run 4

1.	10.0	-5.0	-12.5	0.078224	0.006735	-0.001810	-0.000741	-0.000652	0.005757	0.326	0.882
2.	12.0	-5.0	-14.4	0.084345	0.008904	-0.002134	-0.000963	-0.000490	0.007364	0.323	0.882
3.	8.0	-5.0	-10.8	0.061340	0.004494	-0.001314	-0.000509	-0.000552	0.004041	0.323	0.881
4.	6.0	-5.0	-8.7	0.044557	0.002420	-0.000748	-0.000361	-0.000466	0.002819	0.322	0.881
5.	4.0	-5.0	-7.5	0.025168	0.000734	-0.000397	-0.000288	-0.000307	0.001927	0.322	0.880
6.	2.0	-5.0	-5.9	0.008068	-0.000763	-0.000212	-0.000179	-0.000228	0.001314	0.322	0.883
7.	6.0	0.0	-5.3	0.073473	-0.006471	-0.002323	-0.000038	-0.007803	0.002296	0.326	0.880
8.	8.0	0.0	-7.5	0.084615	-0.006439	-0.003430	-0.000030	-0.011950	0.003910	0.327	0.878
9.	10.0	0.0	-9.4	0.090981	0.002170	-0.003830	-0.000954	-0.000926	0.005768	0.324	0.881
10.	4.0	0.0	-3.5	0.054761	-0.001819	-0.001516	-0.000052	-0.000530	0.001475	0.325	0.881
11.	2.0	0.0	-1.7	0.036045	-0.001872	-0.000951	-0.000164	-0.000431	0.001084	0.325	0.880
12.	0.0	0.0	-0.4	0.019807	-0.001802	-0.000552	-0.000122	-0.000299	0.000968	0.327	0.880
13.	-1.0	0.0	0.0	0.011728	-0.001655	-0.000445	-0.000123	-0.000281	0.000998	0.325	0.878
14.	-2.0	0.0	0.7	0.000325	-0.001461	-0.000334	-0.000114	-0.000161	0.001082	0.325	0.878
15.	2.0	5.0	2.0	0.067227	-0.008721	-0.002475	0.000003	-0.000933	-0.000392	0.324	0.879
16.	4.0	5.0	0.1	0.083424	-0.009301	-0.003799	0.000140	-0.000951	0.003266	0.326	0.879
17.	0.0	5.0	3.5	0.048270	-0.007004	-0.001913	0.000028	-0.000610	-0.000350	0.325	0.878
18.	-2.0	5.0	5.0	0.030293	-0.005321	-0.001270	0.000028	-0.000625	-0.000057	0.327	0.881

Test 310 Run 5

1.	4.0	-10.0	-11.6	0.002547	-0.001093	0.000336	-0.000301	-0.000364	0.001209	0.315	0.877

TABLE IV-2. 44-FOOT ROTOR, $\mu = 0.36$, $M_{(1.0,\ 90.)} = 0.80$

Test 310 Run 5

PT	$\theta_{.75R}$	α_S	α_C	C_L/σ	C_D/σ	C_Y/σ	C_ℓ/σ	C_m/σ	C_Q/σ	μ	$M_{(1.0,90.)}$
3.	8.0	-10.0	-14.5	0.029059	0.003464	0.000164	-0.000666	-0.000544	0.003228	0.360	0.797
4.	10.0	-10.0	-16.1	0.044578	0.006685	0.000114	-0.001081	-0.000620	0.004784	0.360	0.798
5.	12.0	-10.0	-17.5	0.058814	0.009745	-0.000162	-0.001384	-0.000787	0.006341	0.359	0.797
6.	13.7	-10.0	-19.7	0.068765	0.013185	-0.000314	-0.001876	-0.000768	0.008220	0.359	0.800
7.	13.7	-15.0	-22.8	0.048058	0.012167	0.000425	-0.002136	-0.000839	0.006869	0.360	0.796
8.	12.0	-15.0	-21.3	0.033850	0.007618	0.000687	-0.001631	-0.000794	0.004826	0.357	0.798
9.	10.0	-15.0	-20.1	0.019238	0.003311	0.000757	-0.001116	-0.000886	0.003076	0.362	0.794
10.	8.0	-15.0	-18.8	0.003249	-0.001286	0.000676	-0.000485	-0.000644	0.001359	0.361	0.796
11.	6.0	-15.0	-17.1	-0.012248	-0.005843	0.000836	-0.000140	-0.001031	-0.000170	0.362	0.794
12.	6.0	-10.0	-13.0	0.011503	0.000215	0.000352	-0.000422	-0.000446	0.001886	0.363	0.795
13.	4.0	-10.0	-11.6	-0.005055	-0.002724	0.000398	-0.000305	-0.000431	0.000771	0.360	0.797
14.	4.0	-5.0	-7.2	0.022682	0.000262	-0.000360	-0.000122	-0.000327	0.001846	0.359	0.797
15.	2.0	-5.0	-6.0	0.003034	-0.001322	-0.000169	-0.000070	-0.000173	0.001213	0.362	0.791
16.	6.0	-5.0	-9.0	0.041630	0.001943	-0.000764	-0.000203	-0.000515	0.002785	0.362	0.792
17.	8.0	-5.0	-10.8	0.059028	0.003714	-0.001075	-0.000420	-0.000494	0.003860	0.357	0.801
18.	12.0	-5.0	-12.5	0.074771	0.005683	-0.001619	-0.000603	-0.000611	0.005471	0.362	0.790
19.	12.0	-5.0	-14.5	0.084792	0.008389	-0.002030	-0.000786	-0.000923	0.007329	0.363	0.790
20.	8.0	0.0	-7.5	0.083250	-0.000380	-0.002836	0.000012	-0.000434	0.003497	0.358	0.799
21.	10.0	0.0	-9.3	0.091238	0.001275	-0.003661	-0.000085	-0.001053	0.005367	0.358	0.799
22.	6.0	0.0	-5.5	0.069596	-0.001577	-0.002170	0.000042	-0.000602	0.002087	0.358	0.798
23.	4.0	0.0	-3.6	0.052280	-0.001977	-0.001330	-0.000026	-0.000458	0.001329	0.358	0.798
24.	2.0	0.0	-2.5	0.032659	-0.001927	-0.000813	-0.000038	-0.000407	0.001018	0.359	0.798
25.	0.0	0.0	-0.5	0.017333	-0.001928	-0.000495	0.000020	-0.000191	0.000955	0.362	0.789
26.	0.0	5.0	3.7	0.047161	-0.006957	-0.001825	0.000033	-0.000452	-0.000532	0.359	0.798
27.	2.0	5.0	2.0	0.064779	-0.008559	-0.002587	0.000084	-0.000631	-0.000593	0.358	0.800
28.	3.0	5.0	0.9	0.073148	-0.008973	-0.002836	0.000111	-0.000717	-0.000463	0.358	0.798
29.	4.0	5.0	-0.1	0.081389	-0.009185	-0.003707	0.000205	-0.000653	-0.000070	0.357	0.800
30.	6.0	5.0	-2.3	0.092988	-0.008483	-0.004618	0.000363	-0.000448	0.001457	0.359	0.798

TABLE IV-2. CONT'D. 44-FOOT ROTOR, $\mu = 0.36$, $M_{(1.0,\ 90.)} = 0.80$

Test 310 Run 13

PT.	$\theta_{.75R}$	α_S	α_C	C_L/σ	C_D/σ	C_Y/σ	C_ℓ/σ	C_m/σ	C_Q/σ	μ	$M_{(1.0,90.)}$
1.	0.0	0.0	-1.0	0.010839	-0.021700	-0.000294	-0.000017	-0.000156	0.000977	0.357	0.801
2.	2.0	2.0	1.0	0.025145	-0.003071	-0.000796	0.000113	-0.000605	0.000652	0.355	0.804
3.	0.0	4.0	3.0	0.039969	-0.005558	-0.001162	0.000014	-0.000450	-0.000006	0.354	0.804
4.	0.0	6.0	5.0	0.056740	-0.010104	-0.001785	-0.000095	-0.000703	-0.001192	0.355	0.803
5.	-2.0	6.0	5.0	0.028082	-0.005137	-0.001210	0.000052	-0.000388	0.000020	0.355	0.803
6.	-2.0	4.0	3.0	0.015648	-0.003010	-0.000822	0.000177	-0.000286	0.000635	0.356	0.803
7.	2.0	4.0	3.0	0.077471	-0.012480	-0.002996	0.000046	-0.000873	-0.001225	0.357	0.803
8.	2.0	6.0	5.0	0.091362	-0.018321	-0.003691	-0.000060	-0.001063	-0.001959	0.357	0.803
9.	2.0	2.0	1.0	0.059997	-0.007083	-0.002311	0.000129	-0.000903	-0.000138	0.356	0.802
10.	2.0	0.0	-1.0	0.043201	-0.003374	-0.001509	-0.000007	-0.000478	0.000722	0.357	0.802
11.	4.0	0.0	-1.0	0.076896	-0.007397	-0.002507	0.000085	-0.000818	0.000446	0.355	0.803
12.	4.0	2.0	1.0	0.091649	-0.012877	-0.003290	0.000221	-0.001310	-0.000005	0.355	0.804

TABLE IV-3. 44-FOOT ROTOR, $= 0.36$, $M_{(1.0,\ 90.)} = 0.90$

Test 310 Run 6

1.	6.0	-5.0	-9.2	0.040090	0.001854	-0.000444	-0.000466	-0.000231	0.002853	0.358	0.903
2.	8.0	-5.0	-11.0	0.056220	0.003478	-0.000953	-0.000505	-0.000329	0.003994	0.356	0.907
3.	10.0	-5.0	-12.9	0.069294	0.005613	-0.001424	-0.000614	-0.000217	0.005591	0.357	0.905
4.	4.0	-5.0	-7.5	0.023180	0.000275	-0.000285	-0.000192	-0.000051	0.001914	0.359	0.900
5.	2.0	-5.0	-6.0	0.002430	-0.001229	-0.000165	-0.000103	0.002576	0.001379	0.363	0.893
6.	2.0	0.0	-1.9	0.035448	-0.002184	-0.000928	0.000041	-0.000266	0.001080	0.356	0.908
7.	0.0	0.0	-0.6	0.018462	-0.001253	-0.000959	0.000721	-0.000012	0.000604	0.357	0.907
8.	4.0	0.0	-3.6	0.053813	-0.002156	-0.001465	-0.000221	-0.000192	0.001453	0.356	0.907
9.	6.0	0.0	-5.7	0.070068	-0.001585	-0.002415	0.000042	-0.000424	0.002315	0.355	0.906
10.	8.0	0.0	-7.7	0.080655	-0.000321	-0.003212	0.000006	-0.000479	0.003806	0.358	0.904
11.	4.0	5.0	-0.5	0.080656	-0.009178	-0.004000	0.000371	-0.000517	0.000444	0.357	0.903
12.	6.0	5.0	-2.6	0.088993	-0.007870	-0.004628	0.000384	-0.000636	0.002146	0.356	0.906
13.	2.0	5.0	1.5	0.067758	-0.009206	-0.002900	0.000133	-0.000581	-0.000497	0.358	0.902
14.	0.0	5.0	3.3	0.051862	-0.007964	-0.002270	0.000055	-0.000411	-0.000459	0.358	0.903
15.	-2.0	5.0	5.0	0.034353	-0.006280	-0.001540	0.000180	-0.000701	-0.000252	0.357	0.905
16.	-2.0	7.0	6.4	0.045904	-0.009233	-0.002117	0.000114	-0.000826	-0.000969	0.357	0.905
17.	0.0	7.0	4.6	0.063938	-0.011611	-0.003206	0.000143	-0.000572	-0.001302	0.358	0.903
18.	2.0	7.0	2.8	0.078687	-0.012933	-0.004211	0.000150	-0.000939	-0.001042	0.357	0.905
19.	4.0	7.0	0.8	0.088014	-0.012375	-0.004916	0.000171	-0.001586	0.000359	0.359	0.905
20.	6.0	-10.0	-13.0	0.015294	0.000922	0.000321	-0.000554	-0.000298	0.002165	0.356	0.908
21.	8.0	-10.0	-14.4	0.030982	0.003882	0.000201	-0.000639	-0.000312	0.003520	0.357	0.903
22.	10.0	-10.0	-16.1	0.044177	0.005851	0.001316	-0.000055	-0.002185	0.004899	0.356	0.907
23.	11.0	-10.0	-17.0	0.052661	0.008413	-0.000245	-0.001152	-0.000717	0.005762	0.358	0.903
24.	11.0	-15.0	-20.6	0.026465	0.005486	0.000660	-0.001311	-0.000632	0.004178	0.358	0.903
25.	12.0	-15.0	-21.3	0.033747	0.007839	0.000440	-0.001545	-0.000546	0.005146	0.356	0.906
26.	10.0	-15.0	-20.0	0.020279	0.003771	0.000718	-0.001228	-0.000515	0.003437	0.358	0.906
27.	8.0	-15.0	-18.4	0.005811	-0.000441	0.000552	-0.000567	-0.000520	0.001716	0.358	0.905

TABLE IV-4. 44-FOOT ROTOR, $\mu = 0.40$, $M_{(1.0,\ 90.)} = 0.83$

Test 310 Run 16

PT.	$\theta_{.75R}$	α_S	α_C	C_L/σ	C_D/σ	C_Y/σ	C_ℓ/σ	C_m/σ	C_Q/σ	μ	$M_{(1.0,90)}$
1.	6.0	-5.0	-9.6	0.033264	0.000886	-0.000562	-0.000270	-0.000112	0.002611	0.403	0.828
2.	6.0	5.0	-3.4	0.085627	-0.007955	-0.004783	0.000416	-0.000415	0.001639	0.400	0.828
3.	4.0	5.0	-1.1	0.071941	-0.009243	-0.004298	0.000289	-0.000651	0.000181	0.401	0.829
4.	2.0	5.0	0.6	0.065253	-0.008990	0.003287	0.000101	0.000716	-0.000538	0.402	0.829
5.	0.0	5.0	2.9	0.050752	-0.007822	-0.002481	0.000152	-0.000432	-0.000617	0.401	0.828
6.	-2.0	5.0	4.4	0.034677	-0.006290	-0.001983	0.000112	-0.000537	-0.000302	0.400	0.829
7.	-2.0	7.0	5.9	0.048515	-0.009527	-0.003722	0.000051	-0.000433	-0.001271	0.401	0.828
8.	0.0	7.0	4.2	0.062026	-0.011335	-0.003502	-0.000030	-0.000528	-0.001575	0.401	0.828
9.	2.0	0.0	-2.5	0.035811	-0.002685	-0.001246	0.000114	-0.000282	0.001021	0.399	0.831
10.	4.0	0.0	-4.1	0.051287	-0.002630	-0.001867	0.000065	-0.000674	0.001428	0.400	0.830
11.	6.0	0.0	-6.3	0.064734	-0.002315	-0.002533	0.000083	-0.000676	0.002136	0.400	0.830
12.	8.0	0.0	-8.4	0.075657	-0.001243	-0.003039	0.000081	-0.000558	0.003502	0.400	0.829
13.	8.0	-3.0	-11.5	0.049971	0.002350	-0.000919	-0.000482	-0.000294	0.003661	0.401	0.830
14.	10.0	-5.0	-13.2	0.062628	0.003936	-0.001376	-0.000705	-0.000621	0.005033	0.400	0.831
15.	10.0	-15.0	-25.2	0.008687	-0.000341	0.000168	-0.000655	-0.000713	0.002348	0.401	0.831
16.	12.0	-15.0	-21.6	0.021635	0.003585	0.000024	-0.001091	-0.000382	0.004031	0.401	0.830
17.	13.7	-15.0	-23.3	0.036263	0.007933	-0.000192	-0.001663	-0.000492	0.006273	0.402	0.830
18.	12.0	-10.0	-18.3	0.048059	0.007967	-0.000307	-0.001163	-0.000443	0.005929	0.402	0.829
19.	10.0	-10.0	-16.6	0.035311	0.004415	-0.000027	-0.000822	-0.000218	0.004347	0.400	0.830
20.	8.0	-10.0	-15.0	0.022223	0.001870	0.000061	-0.000587	-0.000225	0.003032	0.400	0.829
21.	4.0	-5.0	-7.7	0.018541	-0.000366	-0.000299	-0.000149	-0.000012	0.001837	0.402	0.830

TABLE IV-5. 44-FOOT ROTOR, $\mu = 0.41$, $M_{(1.0,\ 90.)} = 0.94$

Test 310 Run 8

PT.	$\theta_{.75R}$	α_S	α_C	C_L/σ	C_D/σ	C_Y/σ	C_ℓ/σ	C_m/σ	C_Q/σ	μ	$M_{(1.0,90.)}$
1.	8.0	-5.2	-11.4	0.051093	0.001603	-0.000920	-0.000599	-0.000659	0.004168	0.417	0.938
2.	10.0	-5.0	-13.1	0.064623	0.003287	-0.001776	-0.000564	-0.000680	0.005612	0.408	0.939
3.	12.0	-5.0	-14.7	0.073438	0.005052	-0.002253	-0.000703	-0.000958	0.007417	0.408	0.938
4.	6.0	-5.0	-9.4	0.037659	0.000400	-0.000715	-0.000307	-0.000792	0.003021	0.407	0.937
5.	4.0	-5.0	-7.4	0.021138	-0.001076	-0.000328	-0.000311	-0.000820	0.002137	0.412	0.938
6.	4.0	0.0	-4.0	0.050326	-0.003739	-0.001797	-0.000004	-0.001070	0.001853	0.411	0.938
7.	6.0	0.0	-6.0	0.068509	-0.003761	-0.002636	-0.000990	-0.001177	0.002650	0.414	0.934
8.	8.0	0.0	-8.1	0.077569	-0.002495	-0.003429	-0.000063	-0.001037	0.004196	0.413	0.934
9.	10.0	0.0	-10.0	0.080281	-0.000643	-0.003860	-0.000136	-0.001282	0.006043	0.410	0.939
10.	2.0	0.0	-2.2	0.036037	-0.003785	-0.001141	-0.000125	-0.001098	0.001239	0.408	0.940
11.	0.0	0.0	-0.5	0.023448	-0.003500	-0.000664	-0.000044	0.002253	0.001059	0.407	0.945
12.	0.0	5.0	3.9	0.054052	-0.009817	-0.002451	-0.000003	-0.001463	-0.000523	0.408	0.946
13.	2.0	5.0	1.1	0.068795	-0.010979	-0.003498	0.000044	-0.001656	-0.000361	0.409	0.944
14.	4.0	5.0	-1.0	0.080036	-0.011121	-0.004386	0.000220	-0.001426	0.000702	0.407	0.946
15.	6.0	5.0	-3.3	0.083701	-0.009609	-0.004714	0.000441	-0.001307	0.002402	0.407	0.948
16.	8.0	5.0	-5.2	0.090312	-0.007788	-0.004256	0.000475	-0.000744	0.004307	0.400	0.947
17.	2.0	7.0	2.2	0.084694	-0.015423	-0.005070	0.000200	-0.001909	-0.000919	0.417	0.930

Test 310 Run 9

1.	0.0	7.0	4.2	0.068213	-0.013504	-0.003580	0.000181	-0.001140	-0.001447	0.413	0.934
2.	-2.0	7.0	6.0	0.056901	-0.012402	-0.002886	0.000325	-0.001121	-0.001462	0.411	0.939
3.	2.0	7.0	2.3	0.080109	-0.014142	-0.004663	0.000571	-0.001594	-0.000834	0.410	0.941
4.	4.0	7.0	0.3	0.089962	-0.013498	-0.005278	0.000865	-0.001258	0.000646	0.411	0.941
5.	8.0	-10.0	-14.6	0.020281	0.009610	0.000468	-0.000697	-0.000739	0.001375	0.410	0.941
6.	10.0	-10.0	-16.1	0.033632	0.008264	0.000336	-0.000814	-0.000707	0.004798	0.411	0.940
7.	12.0	-10.0	-17.6	0.047146	0.005701	0.000222	-0.001391	-0.000609	0.006479	0.411	0.940
8.	13.7	-10.0	-19.4	0.058141	0.008387	-0.000252	-0.001636	-0.000688	0.008367	0.412	0.938
9.	13.7	-15.0	-22.9	0.034101	0.006215	0.000936	-0.001866	-0.000870	0.006239	0.413	0.937
10.	12.0	-15.0	-21.3	0.019040	0.002242	0.001216	-0.001421	-0.000350	0.004311	0.413	0.936
11.	10.0	-15.0	-19.8	0.008292	-0.000812	0.001134	-0.001011	-0.000518	0.002694	0.413	0.936

TABLE IV-6. 44-FOOT ROTOR, $\mu = 0.45$, $M_{(1.0,\ 90.)} = 0.77$

Test 310 Run 7

PT.	$\theta_{.75R}$	α_S	α_C	C_L/σ	C_D/σ	C_Y/σ	C_ℓ/σ	C_m/σ	C_Q/σ	μ	$M_{(1.0,90.)}$
1.	8.0	-5.0	-11.4	0.042977	0.001221	-0.001187	-0.000255	-0.000089	0.003451	0.448	0.769
2.	6.0	-5.0	-9.5	0.028078	0.000020	-0.000731	-0.000125	0.000001	0.002429	0.445	0.772
3.	4.0	-5.0	-7.7	0.013605	-0.001046	-0.000437	-0.000038	0.000015	0.001654	0.444	0.771
4.	10.0	-5.0	-13.4	0.055426	0.002566	-0.001658	-0.000347	-0.000231	0.004702	0.447	0.773
5.	12.0	-5.0	-15.1	0.064586	0.003972	-0.002219	-0.000666	-0.000480	0.006305	0.447	0.772
6.	13.7	-5.0	-16.7	0.073549	0.005947	-0.002296	-0.001626	-0.001323	0.008280	0.447	0.772
7.	12.0	-10.0	-18.2	0.034206	0.004407	-0.000313	-0.000946	-0.000310	0.005281	0.446	0.771
8.	10.0	-10.0	-16.6	0.023748	0.002505	-0.000030	-0.000793	-0.000172	0.003936	0.445	0.771
9.	8.0	-10.0	-15.0	0.014700	-0.000050	-0.000049	-0.000346	-0.000165	0.002500	0.444	0.771
10.	13.7	-10.0	-20.0	0.052335	0.007295	-0.000713	-0.001450	-0.000838	0.007213	0.446	0.770
11.	14.0	-15.0	-23.2	0.025387	0.003815	0.000584	-0.002561	-0.000431	0.004761	0.449	0.772
12.	13.7	-15.0	-21.7	0.014591	0.000863	0.000607	-0.000961	-0.000394	0.003127	0.443	0.771
13.	10.0	-15.0	-20.4	0.002191	-0.002842	0.000703	-0.000596	-0.000844	0.001436	0.447	0.771
14.	6.0	0.0	-6.3	0.057434	-0.002602	-0.002307	0.000140	-0.000322	0.001861	0.448	0.770
15.	8.0	0.0	-8.4	0.068457	-0.002335	-0.002049	0.000045	-0.001264	0.003027	0.448	0.770
16.	10.0	0.0	-10.3	0.078453	-0.000627	-0.003958	0.000119	-0.001461	0.005063	0.447	0.772
17.	4.0	0.0	-4.3	0.043844	-0.002716	-0.001705	0.000167	-0.000104	0.001256	0.446	0.770
18.	2.0	0.0	-2.2	0.028589	-0.002693	-0.001089	0.000075	-0.000268	0.000914	0.446	0.769
19.	11.0	0.0	-11.2	0.082471	0.000190	-0.004363	0.000223	-0.001780	0.006058	0.444	0.768
20.	2.0	5.0	1.0	0.061420	-0.000159	-0.003272	0.000211	-0.000885	-0.000685	0.445	0.770
21.	0.0	5.0	2.8	0.047992	-0.000195	-0.002523	0.000215	-0.000635	-0.000791	0.449	0.770
22.	-2.0	5.0	4.6	0.033195	-0.000723	-0.001993	0.000155	-0.000406	-0.000409	0.449	0.770
23.	4.0	5.0	-1.3	0.073613	-0.000448	-0.004024	0.000261	-0.000808	-0.000090	0.448	0.770
24.	6.0	5.0	-3.5	0.083196	-0.000971	-0.004875	0.000350	-0.001497	0.001462	0.449	0.770
25.	8.0	5.0	-5.5	0.091097	-0.001339	-0.005514	0.000504	-0.001247	0.003479	0.447	0.773
26.	10.0	5.0	-7.0	0.100347	-0.000524	-0.003510	0.000621	-0.001389	0.005673	0.447	0.773
27.	0.0	7.0	4.0	0.062952	-0.002275	-0.003570	-0.000003	-0.001096	-0.001837	0.446	0.772
28.	-2.0	7.0	6.0	0.047245	-0.000323	-0.002706	-0.000151	-0.000777	-0.001480	0.446	0.771
29.	2.0	7.0	2.0	0.075143	-0.003201	-0.004339	-0.000113	-0.001067	-0.001566	0.446	0.771

TABLE IV-7. 44-FOOT ROTOR, μ= 0.45, $M_{(1.0,\ 90.)}$ = 0.90

Test 310 Run 11

PT.	$\theta_{.75R}$	α_s	α_c	C_L/σ	C_D/σ	C_Y/σ	$C_{\mathcal{L}}/\sigma$	$C_{\mathcal{M}}/\sigma$	C_Q/σ	μ	$M_{(1.0,90.)}$
1.	6.0	-5.0	-9.9	0.030915	-0.000277	-0.000785	-0.000140	-0.000622	0.002660	0.445	0.900
2.	8.0	-5.0	-11.9	0.045028	0.000870	-0.001154	-0.000266	-0.000894	0.003698	0.445	0.901
3.	10.0	-5.0	-13.9	0.057773	0.002382	-0.001619	-0.000533	-0.000992	0.005229	0.447	0.897
4.	12.0	-5.0	-15.5	0.066193	0.003740	-0.002060	-0.000575	-0.001229	0.006724	0.446	0.899
5.	13.0	-5.0	-16.4	0.068578	0.005170	-0.002315	-0.000673	-0.001003	0.007508	0.451	0.906
6.	13.0	-3.0	-16.4	0.068780	0.004408	-0.002277	-0.000691	-0.001153	0.007515	0.442	0.900
7.	4.0	-5.0	-7.9	0.017890	-0.001385	-0.000538	-0.000222	-0.000512	0.001837	0.439	0.900
8.	2.0	-5.0	-5.9	0.003947	-0.002349	-0.000392	-0.000041	-0.000435	0.001251	0.439	0.898
9.	2.0	0.0	-2.6	0.033034	-0.003844	-0.001544	0.000090	-0.001046	0.001098	0.443	0.898
10.	4.0	0.0	-4.6	0.048232	-0.003731	-0.002289	0.000234	-0.000822	0.001493	0.444	0.900
11.	6.0	0.0	-6.6	0.061392	-0.003614	-0.002827	0.000073	-0.000961	0.002386	0.446	0.898
12.	8.0	0.0	-8.8	0.070868	-0.002786	-0.003527	0.000142	-0.001227	0.003811	0.445	0.897
13.	10.0	0.0	-10.8	0.078276	-0.001353	-0.003850	0.000028	-0.002037	0.005775	0.446	0.896
14.	9.0	0.0	-9.9	0.019831	-0.003758	-0.001036	0.000120	-0.000854	0.000970	0.445	0.899
15.	-2.0	0.0	0.6	0.005797	-0.003457	-0.000656	0.002029	-0.000729	0.001080	0.447	0.895
16.	2.0	2.0	-1.4	0.049390	-0.006664	-0.002192	0.000121	-0.001323	0.000478	0.445	0.895
17.	4.0	2.0	-3.6	0.062949	-0.006718	-0.003137	0.000224	-0.001308	0.001028	0.445	0.896
18.	6.0	2.0	-5.5	0.034283	-0.005984	-0.001636	0.000042	-0.001262	0.000485	0.447	0.894
19.	-2.0	2.0	2.1	0.015937	-0.005252	-0.001216	-0.000710	-0.004135	0.000634	0.446	0.895
20.	-2.0	5.0	4.1	0.042758	-0.009036	-0.002332	0.000146	-0.001570	-0.000595	0.448	0.895
21.	0.0	5.0	2.4	0.047327	-0.010316	-0.003152	0.000071	-0.003754	-0.000770	0.448	0.894
22.	2.0	5.0	0.5	0.069948	-0.011536	-0.003867	0.000096	-0.001839	-0.000577	0.447	0.893
23.	5.0	5.0	-1.7	0.081038	-0.011081	-0.004826	0.000378	-0.001671	0.000510	0.447	0.894
24.	8.0	-10.0	-15.1	0.017404	0.000041	0.000140	-0.000506	-0.000259	0.002874	0.450	0.893
25.	6.0	-10.0	-13.2	0.004177	-0.002296	0.000035	-0.000257	-0.000510	0.001631	0.449	0.892
26.	10.0	-10.0	-16.8	0.031380	0.002419	-0.000009	-0.000837	-0.000594	0.004374	0.447	0.895
27.	12.0	-10.0	-18.5	0.043406	0.004764	-0.000195	-0.001011	-0.000768	0.005873	0.446	0.899
28.	13.7	-10.0	-20.3	0.047177	0.007281	-0.000478	-0.002452	-0.002625	0.007614	0.449	0.896
29.	13.7	-12.0	-21.4	0.040569	0.005532	-0.000340	-0.001357	0.000287	0.007029	0.445	0.897
30.	12.0	-12.0	-19.8	0.032481	0.003865	-0.000079	-0.001247	-0.000466	0.005262	0.450	0.887
31.	10.0	-12.0	-18.0	0.021134	0.001315	0.000222	-0.000802	-0.000745	0.003684	0.451	0.888
32.	13.7	-15.0	-23.2	0.029179	0.004589	0.000588	-0.001734	-0.001043	0.005508	0.445	0.897
33.	12.0	-15.0	-21.7	0.017472	0.001315	0.000666	-0.001368	-0.000756	0.003760	0.452	0.887
34.	10.0	-15.0	-20.1	0.004897	-0.002100	0.000561	-0.001582	-0.000729	0.002008	0.451	0.886

TABLE IV-8. 44-FOOT ROTOR, $\mu = 0.46$, $M_{(1.0,\ 90.)} = 0.86$

Test 310 Run 12

PT	$\theta_{.75R}$	α_s	α_c	C_L/σ	C_D/σ	C_Y/σ	C_ℓ/σ	C_m/σ	C_Q/σ	μ	$M_{(1.0,90.)}$
1.	8.0	-5.0	-12.0	0.042112	0.000632	-0.000775	-0.000409	-0.000512	0.000547	0.462	0.865
2.	10.0	-5.0	-14.0	0.055047	0.001821	-0.001248	-0.000510	-0.001084	0.000943	0.464	0.862
3.	12.0	-5.0	-15.6	0.064233	0.003308	-0.001719	-0.000655	-0.001216	0.000596	0.463	0.864
4.	6.0	-5.0	-10.0	0.030752	-0.000370	-0.000552	-0.000325	-0.000427	0.000606	0.462	0.865
5.	4.0	-5.0	-7.7	0.017345	-0.001358	-0.000264	-0.000241	-0.000429	0.000827	0.465	0.863
6.	2.0	-5.0	-6.2	0.001750	-0.002306	-0.000004	-0.000168	-0.000092	0.001216	0.462	0.866
7.	4.0	0.0	-4.5	0.048240	-0.003354	-0.001811	-0.000318	-0.000487	0.001433	0.462	0.865
8.	6.0	0.0	-6.8	0.060819	-0.003221	-0.002618	0.000078	-0.000973	0.002186	0.465	0.861
9.	8.0	0.0	-8.9	0.071453	-0.002525	-0.003268	0.000078	-0.000856	0.003611	0.464	0.862
10.	10.0	0.0	-10.9	0.078060	-0.001221	-0.003679	0.000024	-0.001342	0.005454	0.465	0.864
11.	2.0	0.0	-2.6	0.033921	-0.003243	-0.001368	0.000040	-0.000737	0.001049	0.466	0.864
12.	0.0	0.0	-0.8	0.020528	-0.003110	-0.000742	-0.000055	-0.000643	0.000901	0.466	0.863
13.	-2.0	0.0	0.5	0.006242	-0.002703	-0.000535	0.000070	-0.000366	0.001048	0.465	0.862
14.	4.0	2.0	0.3	0.034769	-0.004748	-0.001552	0.000054	-0.000597	0.000400	0.466	0.861
15.	-2.0	2.0	2.0	0.019580	-0.003850	-0.000923	0.000125	-0.000586	0.000637	0.464	0.864
16.	2.0	2.0	-1.5	0.048690	-0.005373	-0.002278	0.000144	-0.000717	0.000470	0.468	0.858
17.	4.0	2.0	-3.7	0.061234	-0.005628	-0.002973	0.000234	-0.000992	0.000918	0.464	0.864
18.	4.0	5.0	-1.8	0.079080	-0.009620	-0.004112	0.000315	-0.000831	0.000423	0.468	0.857
19.	6.0	5.0	-4.0	0.086294	-0.008614	-0.005320	0.000550	-0.000985	0.002002	0.468	0.857
20.	2.0	5.0	0.3	0.066916	-0.009691	-0.003912	0.000179	-0.000900	-0.000588	0.468	0.856
21.	0.0	5.0	2.1	0.054723	-0.008751	-0.003071	0.000283	-0.000622	-0.000806	0.468	0.856
22.	-2.0	5.0	4.0	0.039578	-0.007233	-0.002374	0.000106	-0.000559	-0.000519	0.467	0.862
23.	10.0	-10.0	-16.8	0.027762	0.001798	-0.000005	-0.000738	-0.000466	0.004120	0.464	0.864
24.	8.0	-10.0	-15.3	0.014579	-0.000450	0.000120	-0.000599	-0.000362	0.004723	0.463	0.863
25.	6.0	-10.0	-12.9	0.002109	-0.002465	0.000143	-0.000310	-0.000239	0.001524	0.462	0.864
26.	12.0	-10.0	-18.3	0.039514	0.003995	-0.000296	-0.000731	-0.000583	0.005620	0.464	0.863
27.	13.7	-10.0	-20.3	0.050493	0.006411	-0.000692	-0.001307	-0.000705	0.007347	0.464	0.863
28.	13.7	-12.0	-21.6	0.039784	0.005450	-0.000384	-0.001353	-0.000580	0.006617	0.464	0.863
29.	12.0	-12.0	-20.0	0.028883	0.002723	-0.000203	-0.000930	-0.000897	0.004998	0.463	0.864
30.	10.0	-12.0	-18.3	0.016342	0.000193	-0.000020	-0.000687	-0.000260	0.003369	0.463	0.863
31.	13.7	-15.0	-23.3	0.024399	0.002445	0.000090	-0.001421	-0.000722	0.005133	0.464	0.864
32.	12.0	-15.0	-21.9	0.012386	-0.000433	0.000139	-0.000870	-0.000472	0.003232	0.464	0.862
33.	10.0	-15.0	-20.4	0.000799	-0.003389	-0.000034	-0.000384	-0.000530	0.001681	0.462	0.868

TABLE IV-9. 44-FOOT ROTOR, μ= 0.51, $M_{(1.0,\ 90.)}$ = 0.80

Test 310 Run 10

PT.	$\theta_{.75R}$	α_s	α_c	C_L/σ	C_D/σ	C_Y/σ	C_ℓ/σ	C_m/σ	C_Q/σ	μ	$M_{(1.0,90.)}$
1.	6.0	-5.0	-9.6	0.022667	-0.002019	-0.001046	-0.000015	-0.000537	0.002409	0.514	0.805
2.	6.0	0.0	-6.8	0.052420	-0.004565	-0.002712	0.000218	-0.001374	0.002079	0.518	0.802
3.	8.0	0.0	-9.0	0.062578	-0.004079	-0.003698	0.000253	-0.001068	0.003304	0.519	0.802
4.	4.0	0.0	-4.9	0.036421	-0.004191	-0.001809	-0.000078	-0.001078	0.001393	0.511	0.809
5.	2.0	0.0	-2.8	0.025717	-0.003992	-0.002232	0.001218	-0.001040	0.000698	0.512	0.808
6.	2.0	5.0	0.2	0.063394	-0.010822	-0.003824	0.000203	-0.002681	-0.000572	0.521	0.799
7.	0.0	5.0	2.1	0.051865	-0.009857	-0.002415	-0.000901	-0.001806	-0.000868	0.521	0.799
8.	-2.0	5.0	4.1	0.039291	-0.008956	-0.001981	-0.000074	-0.002073	-0.000721	0.512	0.809
9.	8.0	-3.0	-11.8	0.034465	-0.001424	-0.001367	-0.000033	-0.001366	0.003326	0.512	0.806
10.	10.0	-5.0	-13.7	0.045155	-0.000521	-0.001683	-0.000322	-0.001601	0.004409	0.508	0.811
11.	10.0	-10.0	-16.8	0.018796	-0.001034	-0.000526	-0.000347	-0.000688	0.003547	0.509	0.810
12.	12.0	-10.0	-18.5	0.029770	0.000892	-0.000625	-0.001044	-0.000750	0.004935	0.509	0.812
13.	13.7	-10.0	-20.4	0.039634	0.002499	-0.000828	-0.000695	-0.001959	0.006449	0.510	0.809
14.	13.7	-12.0	-21.5	0.029564	0.001409	-0.000208	-0.001360	-0.000734	0.005536	0.512	0.810
15.	12.0	-8.0	-17.4	0.040251	0.001331	-0.001075	-0.001078	-0.001123	0.005371	0.512	0.809
16.	10.0	-8.0	-15.7	0.030722	-0.000031	-0.000931	-0.000248	-0.000745	0.004061	0.510	0.808
17.	8.0	-8.0	-13.9	0.017003	-0.001686	-0.000720	-0.000056	-0.000711	0.002808	0.510	0.808
18.	8.0	-3.0	-10.8	0.045438	-0.002271	-0.002260	-0.000130	-0.001549	0.003418	0.512	0.809
19.	6.0	-3.0	-8.8	0.033009	-0.002384	-0.001793	0.000227	-0.001625	0.002457	0.510	0.810
20.	4.0	-3.0	-6.6	0.022859	-0.002774	-0.001762	0.000433	-0.000729	0.001865	0.510	0.810
21.	4.0	2.0	-3.7	0.053653	-0.006409	-0.001368	-0.001943	-0.001497	0.002150	0.516	0.811
22.	2.0	2.0	-1.6	0.043028	-0.006145	-0.002170	0.000027	-0.001007	0.000549	0.512	0.808
23.	6.0	2.0	-5.8	0.065472	-0.006759	-0.003538	0.000305	-0.001869	0.001848	0.511	0.810

Test 310 Run 14

1.	2.0	-2.0	-4.0	0.015670	-0.002709	-0.000687	-0.000078	-0.000283	0.001275	0.514	0.805
2.	2.0	-2.0	-3.0	0.026319	-0.003368	-0.000901	-0.000069	-0.000609	0.001129	0.517	0.803
3.	2.0	0.0	-1.0	0.048181	-0.006329	-0.001738	-0.000017	-0.001039	0.000157	0.514	0.805
4.	2.0	2.0	1.0	0.076086	-0.012457	-0.002878	0.000059	-0.001250	-0.001070	0.518	0.799
5.	0.0	0.0	-1.0	0.016944	-0.003288	-0.000729	-0.000041	-0.000148	0.000999	0.511	0.806
6.	0.0	2.0	1.0	0.038727	-0.006967	-0.001637	-0.000120	-0.000629	0.000078	0.513	0.805
7.	0.0	4.0	3.0	0.062579	-0.011672	-0.002527	-0.000223	-0.001235	-0.001653	0.513	0.805
8.	0.0	6.0	5.0	0.085738	-0.018666	-0.003391	-0.000281	-0.001471	-0.003029	0.515	0.805
9.	-2.0	6.0	5.0	0.050832	-0.010246	-0.002825	-0.000192	-0.000564	-0.001529	0.514	0.804
10.	-2.0	4.0	3.0	0.028585	-0.005644	-0.001678	-0.000077	-0.000571	0.000122	0.510	0.809
11.	4.0	0.0	-1.0	0.087023	-0.012557	-0.003416	0.000492	-0.001468	0.000251	0.510	0.808
12.	4.0	-2.0	-3.0	0.066455	-0.009678	-0.002664	0.000053	-0.001630	0.000649	0.513	0.804
13.	4.0	-4.0	-5.0	0.041972	-0.006379	-0.001503	-0.000091	-0.000751	0.001491	0.510	0.808

TABLE IV-10. 44-FOOT ROTOR, $\mu = 0.52$, $M_{(1.0,\ 90.)} = 0.81$

Test 310 Run 15

PT.	$\theta_{.75R}$	α_S	α_C	C_L/σ	C_D/σ	C_Y/σ	$C_{\mathcal{L}}/\sigma$	$C_{\mathcal{M}}/\sigma$	C_Q/σ	μ	$M_{(1.0,90.)}$
1.	6.0	-5.0	-10.1	0.023890	-0.001968	-0.000595	-0.000408	-0.000715	0.002443	0.526	0.811
2.	8.0	-5.0	-12.0	0.036611	-0.001253	-0.001154	-0.000312	-0.001052	0.003290	0.522	0.814
3.	10.0	-5.0	-14.1	0.047761	-0.000502	-0.001646	-0.000465	-0.001049	0.004600	0.523	0.812
4.	12.0	-5.0	-15.8	0.055655	0.000587	-0.002035	-0.000669	-0.001370	0.005998	0.522	0.812
5.	12.0	-7.0	-17.0	0.046380	0.000987	-0.001258	-0.000707	-0.000993	0.005675	0.524	0.810
6.	12.0	-10.0	-18.6	0.030306	0.000467	-0.000419	-0.000933	-0.000729	0.004777	0.522	0.811
7.	10.0	-7.0	-15.3	0.037174	0.000083	-0.000904	-0.000544	-0.000655	0.004331	0.521	0.811
8.	8.0	-7.0	-13.3	0.026670	-0.001163	-0.000735	-0.000757	-0.000810	0.003183	0.521	0.810
9.	8.0	0.0	-9.3	0.004825	-0.003386	-0.002196	-0.000070	-0.001430	0.003407	0.521	0.809
10.	6.0	0.0	-7.1	0.005322	-0.004117	-0.002799	-0.000056	-0.001243	0.002016	0.521	0.814
11.	4.0	0.0	-4.9	0.044657	-0.004084	-0.002104	-0.000051	-0.000709	0.001354	0.524	0.809
12.	2.0	0.0	-2.9	0.032504	-0.003744	-0.001441	-0.000026	-0.000600	0.001047	0.524	0.809
13.	2.0	2.0	-1.6	0.046001	-0.005610	-0.002286	0.000028	-0.000686	0.000484	0.522	0.812
14.	0.0	2.0	0.2	0.033584	-0.005249	-0.001713	0.000075	-0.000594	0.0 [illegible] 0	0.521	0.811
15.	0.0	5.0	2.0	0.053466	-0.008962	-0.003315	-0.000010	-0.000626	-0.0 [illegible] +8	0.518	0.814
16.	0.0	7.0	3.2	0.067547	-0.012421	-0.004557	-0.000104	-0.000851	-0.0 [illegible] 932	0.520	0.810
17.	2.0	5.0	0.2	0.063885	-0.009539	-0.004078	-0.000032	-0.000820	-0.000716	0.516	0.814
18.	4.0	5.0	-2.1	0.075076	-0.009764	-0.005293	0.000311	-0.001079	0.000336	0.524	0.807
19.	4.0	2.0	-3.7	0.055160	-0.005478	-0.003134	-0.000091	-0.000802	0.001007	0.527	0.805
20.	6.0	2.0	-5.9	0.065907	-0.005580	-0.003937	0.000256	-0.001247	0.001926	0.522	0.810
21.	6.0	-3.0	-8.8	0.038569	-0.002215	-0.001499	-0.000058	-0.000776	0.002470	0.521	0.809
22.	4.0	-3.0	-6.8	0.025216	-0.004019	-0.134523	0.189577	-0.002980	0.051591	0.526	0.804
23.	8.0	-3.0	-10.9	0.049530	-0.001816	-0.002005	-0.000143	-0.001167	0.003233	0.519	0.813
24.	10.0	-3.0	-12.8	0.056892	-0.001078	-0.002609	-0.000176	-0.001559	0.004672	0.519	0.812

TABLE IV-11. 34-FOOT ROTOR, μ= 0.51, $M_{(1.0,\ 90.)}$ = 0.64

Test 310 Run 19

PT.	$\theta_{.75R}$	α_S	α_C	C_L/σ	C_D/σ	C_Y/σ	$C_{\mathcal{L}}/\sigma$	$C_{\mathcal{M}}/\sigma$	C_Q/σ	μ	$M_{(1.0,90.)}$
1.	8.0	-2.0	-9.6	0.046126	-0.002715	-0.002206	-0.000310	0.006463	0.003015	0.511	0.646
2.	10.0	-2.0	-11.6	0.056642	-0.002633	-0.002827	-0.000117	0.006402	0.003963	0.512	0.647
3.	6.0	2.0	-7.8	0.037260	-0.002936	-0.002568	0.001134	0.006751	0.002702	0.514	0.644
4.	4.0	-2.0	-5.8	0.023677	-0.002850	-0.001259	-0.000291	0.006514	0.001788	0.508	0.643
5.	2.0	-2.0	-3.7	0.012665	-0.003122	-0.000668	0.000766	0.007035	0.001333	0.512	0.644
6.	0.0	-2.0	-2.0	0.000790	-0.003366	-0.000252	-0.000120	0.006589	0.001133	0.511	0.644
7.	0.0	2.0	0.7	0.023335	-0.004668	-0.002350	0.001438	0.006673	0.001103	0.512	0.641
8.	2.0	2.0	-1.2	0.036099	-0.005268	-0.002182	-0.000029	0.006361	0.000790	0.508	0.642
9.	4.0	2.0	-3.3	0.048393	-0.005751	-0.003036	0.000347	0.006589	0.001220	0.512	0.641
10.	6.0	2.0	-5.5	0.058285	-0.006354	-0.003638	0.000243	0.005049	0.001762	0.511	0.640
11.	8.0	2.0	-7.2	0.068211	-0.006441	-0.004321	0.000155	0.005222	0.002674	0.511	0.640
12.	10.0	2.0	-8.8	0.078962	-0.006637	-0.005276	0.000468	0.004484	0.004177	0.511	0.639
13.	10.0	0.0	-10.2	0.068045	-0.004457	-0.003828	-0.000121	0.005080	0.004008	0.509	0.641
14.	12.0	-2.0	-15.7	0.068407	-0.002004	-0.003666	-0.000338	0.005353	0.005772	0.509	0.641
15.	12.0	-4.0	-14.6	0.056992	-0.000886	-0.002757	-0.000394	0.005471	0.005433	0.507	0.643
16.	10.0	-4.0	-12.7	0.044839	-0.001340	-0.002082	-0.000301	0.005905	0.004233	0.512	0.639
17.	8.0	-4.0	-11.1	0.034428	-0.001771	-0.001515	-0.000294	0.005875	0.003276	0.510	0.641
18.	6.0	-4.0	-9.1	0.025109	-0.002136	-0.001145	0.000013	0.006067	0.002545	0.509	0.638
19.	4.0	-4.0	-7.2	0.012107	-0.002654	-0.000585	-0.000395	0.006091	0.001744	0.507	0.638
20.	6.0	-6.0	-10.9	0.012714	-0.002425	-0.000451	-0.000327	0.005962	0.002109	0.507	0.639
21.	8.0	-6.0	-12.1	0.023259	-0.001573	-0.000874	-0.000402	0.005629	0.003075	0.508	0.639
22.	10.0	-6.0	-13.8	0.034121	-0.000881	-0.001108	-0.000448	0.005533	0.004067	0.511	0.638
23.	12.0	-6.0	-15.6	0.047435	0.000117	-0.001865	-0.000652	0.005280	0.005531	0.510	0.637
24.	14.0	-6.0	-17.8	0.061678	0.001358	-0.001935	-0.001060	0.005154	0.007227	0.511	0.637
25.	8.0	0.0	-8.5	0.056982	-0.004081	-0.003142	0.000168	0.005772	0.002922	0.511	0.637
26.	6.0	0.	-6.7	0.046701	-0.003978	-0.002521	0.000051	0.006070	0.002210	0.510	0.637
27.	4.0	0.	-4.7	0.035182	-0.003859	-0.001962	-0.000195	0.005902	0.001623	0.510	0.637
28.	2.0	0.0	-2.5	0.025141	-0.003805	-0.001369	-0.000088	0.006094	0.001162	0.510	0.637
29.	0.0	0.0	-0.5	0.012107	-0.003608	-0.000774	-0.000070	0.006164	0.001023	0.508	0.638
30.	0.0	4.0	2.0	0.036319	-0.007106	-0.002292	0.000098	0.005563	0.000024	0.508	0.638
31.	0.0	6.0	3.1	0.046460	-0.009814	-0.003002	-0.000195	0.005651	-0.000824	0.513	0.637
32.	2.0	6.0	1.5	0.058647	-0.010736	-0.003858	0.000105	0.006239	-0.000800	0.513	0.637
33.	2.0	4.0	0.1	0.047105	-0.007965	-0.002766	-0.000107	0.005517	0.000187	0.511	0.639
34.	4.0	4.0	-2.1	0.059128	-0.008394	-0.003687	-0.000014	0.006040	0.000628	0.512	0.639
35.	4.0	6.0	-0.9	0.068953	-0.010935	-0.004547	0.000299	0.005817	0.000035	0.510	0.641
36.	6.0	6.0	-3.9	0.080700	0.011746	-0.005350	0.000193	0.005714	0.000999	0.514	0.637
37.	6.0	4.0	-4.2	0.070018	-0.008894	-0.004576	0.000119	0.005874	0.001524	0.514	0.637
38.	6.0	8.0	-1.7	0.092874	-0.015077	-0.006294	0.000569	0.005636	0.000548	0.513	0.637
39.	4.0	8.0	0.2	0.083006	-0.014777	-0.005358	0.000177	0.005779	-0.000692	0.510	0.635
40.	4.0	10.0	1.5	0.095287	-0.018664	-0.006016	0.000059	0.005776	-0.001515	0.510	0.635

TABLE IV-11. CONT'D. 34-FOOT ROTOR, $\mu = 0.51$, $M_{(1.0,\ 90.)} = 0.64$

Test 310 Run 24

PT.	$\theta_{.75R}$	α_s	α_c	C_L/σ	C_D/σ	C_Y/σ	C_ℓ/σ	C_m/σ	C_Q/σ	μ	$M_{(1.0,90.)}$
36.	2.0	-4.0	-5.2	0.002667	-0.003105	-0.000724	-0.000249	0.004948	0.001406	0.505	0.623
37.	4.0	-6.0	-8.6	0.003011	-0.003077	-0.000607	-0.000283	0.004956	0.001504	0.505	0.623
38.	6.0	10.0	-0.5	0.101994	-0.019034	-0.005766	0.000315	0.003558	0.000092	0.503	0.623
39.	8.0	8.0	-3.6	0.097067	-0.014866	-0.004902	0.000519	0.004210	0.002034	0.505	0.623
40.	8.0	6.0	-4.8	0.087236	-0.011658	-0.004095	0.000543	0.004307	0.002198	0.505	0.623
41.	8.0	4.0	-6.1	0.080157	-0.009377	-0.004952	0.000186	0.004033	0.002365	0.506	0.624
42.	10.0	4.0	-7.5	0.087047	-0.008878	-0.004439	0.000586	0.004201	0.003950	0.507	0.624
43.	12.0	0.0	-12.1	0.078739	-0.003202	-0.003746	0.000694	0.003920	0.005844	0.504	0.623

TABLE IV-12. 34-FOOT ROTOR, $\mu = 0.65$, $M_{(1.0,\ 90.)} = 0.54$

Test 310 Run 23

PT.	$\theta_{.75R}$	α_s	α_c	C_L/σ	C_D/σ	C_Y/σ	C_ℓ/σ	C_m/σ	C_Q/σ	μ	$M_{(1.0,90.)}$
1.	0.0	0.0	-0.9	0.010147	-0.004985	-0.001162	-0.000035	0.009654	0.001320	0.650	0.541
2.	0.0	2.0	-0.0	0.022483	-0.006042	-0.001985	-0.000114	0.010279	0.000875	0.652	0.541
3.	0.0	4.0	0.9	0.037459	-0.008408	-0.002577	-0.000581	0.010399	0.000057	0.653	0.542
4.	0.0	6.0	2.0	0.047077	-0.010030	-0.003570	-0.000573	0.010700	-0.000684	0.654	0.542
5.	0.0	7.0	2.4	0.051923	-0.012493	-0.004197	-0.000075	0.007905	-0.001327	0.650	0.540
6.	0.0	8.0	3.0	0.060443	-0.014462	-0.004864	-0.000333	0.007609	-0.002008	0.649	0.540
7.	0.0	5.0	1.6	0.040322	-0.009311	-0.003115	-0.000557	0.008926	-0.000149	0.650	0.541
8.	2.0	5.0	-0.6	0.046860	-0.010144	-0.003810	-0.000834	0.008776	0.000049	0.653	0.539
9.	2.0	6.0	-0.2	0.050666	-0.010776	-0.004735	-0.000355	0.008947	-0.000367	0.650	0.540
10.	2.0	7.0	0.1	0.056556	-0.012295	-0.005338	-0.000522	0.008260	-0.000937	0.650	0.540
11.	2.0	8.0	0.6	0.065347	-0.014536	-0.005516	-0.000472	0.007830	-0.001668	0.649	0.540
12.	2.0	4.0	-1.4	0.042469	-0.009225	-0.003465	-0.000315	0.008659	0.000429	0.650	0.541
13.	2.0	2.0	-2.3	0.029816	-0.007067	-0.002813	0.000059	0.008281	0.001001	0.650	0.541
14.	2.0	0.0	-3.2	0.017574	-0.005761	-0.001695	-0.000500	0.008892	0.001333	0.651	0.541
15.	2.0	-2.0	-4.2	0.008193	-0.005309	-0.001097	-0.000141	0.008906	0.001407	0.649	0.540
16.	4.0	-2.0	-6.5	0.014088	-.005532	-0.001745	-0.000140	0.008630	0.001794	0.650	0.541
17.	4.0	-4.0	-7.5	0.004061	-.005402	-0.000847	-0.000604	0.009830	0.001679	0.655	0.539
18.	4.0	0.0	-4.7	0.024088	-.006170	-0.002373	-0.000230	0.008961	0.001728	0.654	0.539
19.	4.0	2.0	-4.5	0.037528	-0.007674	-0.003885	0.000226	0.008861	0.001397	0.654	0.539
20.	4.0	3.0	-4.1	0.044141	-0.008722	-0.004132	0.000203	0.009377	0.001148	0.654	0.539
21.	4.0	4.0	-3.6	0.050881	-0.009872	-0.004709	0.000015	0.008952	0.000797	0.654	0.539
22.	4.0	5.0	-3.1	0.053976	-0.010619	-0.005235	0.000309	0.009715	0.000575	0.653	0.539
23.	4.0	6.0	-2.5	0.058981	-0.011881	-0.005619	-0.000188	0.009287	0.000207	0.654	0.538
24.	4.0	7.0	-2.0	0.066281	-0.014205	-0.006063	-0.000246	0.008313	-0.000446	0.654	0.538
25.	4.0	8.0	-1.5	0.071390	-0.015049	-0.006685	0.000326	0.007480	-0.000695	0.653	0.538
26.	6.0	7.0	-3.9	0.072951	-0.014447	-0.006615	-0.000036	0.008697	0.000567	0.654	0.538
27.	6.0	8.0	-3.5	0.077654	-0.015319	-0.006134	0.000156	0.009455	0.000344	0.654	0.538
28.	6.0	6.0	-4.5	0.064735	-0.012742	-0.006552	0.000043	0.007916	0.000752	0.654	0.538
29.	6.0	4.0	-5.6	0.055625	-0.010494	-0.005583	0.000277	0.008272	0.001413	0.657	0.539
30.	6.0	2.0	-6.6	0.042896	-0.008218	-0.004556	0.000773	0.008431	0.001929	0.654	0.538
31.	6.0	0.0	-7.6	0.032187	-0.006727	-0.003426	0.000350	0.009060	0.001974	0.654	0.538
32.	6.0	-2.0	-8.7	0.021724	-0.006038	-0.002268	-0.000267	0.009245	0.002103	0.654	0.538
33.	6.0	-4.0	-9.5	0.008660	-0.005405	-0.001188	-0.000118	0.009395	0.001923	0.654	0.538
34.	8.0	-4.0	-11.6	0.016060	-0.005794	-0.001297	-0.000852	0.009294	0.002450	0.654	0.538
35.	8.0	-6.0	-12.6	0.007338	-0.006192	-0.001012	0.549288	0.009290	0.002172	0.655	0.538
36.	8.0	-2.0	-10.7	0.027809	-0.006252	-0.002432	-0.000117	0.009607	0.002527	0.655	0.538
37.	8.0	0.0	-9.7	0.037534	-0.006920	-0.003765	0.000290	0.009177	0.002524	0.654	0.538
38.	8.0	2.0	-8.7	0.049291	-0.008325	-0.004949	0.000818	0.008972	0.002420	0.655	0.538
39.	8.0	4.0	-7.5	0.061954	-0.010735	-0.005614	0.000437	0.008481	0.002046	0.654	0.538
40.	8.0	6.0	-6.0	0.074285	-0.013998	-0.005741	0.000472	0.007690	0.001984	0.654	0.538
41.	8.0	8.0	-4.0	0.099529	-0.021385	-0.006365	0.000627	0.005711	0.002073	0.655	0.538
42.	10.0	6.0	-6.0	0.102562	-0.021474	-0.006745	0.001195	0.004153	0.004141	0.653	0.538
43.	10.0	4.0	-8.0	0.080400	-0.014919	-0.006284	0.000475	0.006463	0.003596	0.657	0.538
44.	10.0	2.0	-10.0	0.059472	-0.010149	-0.005109	0.000601	0.008090	0.003286	0.657	0.539
45.	10.0	0.0	-11.5	0.044512	-0.008054	-0.004379	0.000743	0.008438	0.003279	0.655	0.538
46.	10.0	-2.0	-12.5	0.035409	-0.007286	-0.003269	-0.000080	0.008604	0.003237	0.654	0.539
47.	10.0	-4.0	-13.5	0.022676	-0.006194	-0.001869	-0.000369	0.009311	0.003040	0.655	0.538
48.	10.0	-6.0	-14.5	0.013116	-0.006206	-0.001178	0.000687	0.009518	0.002735	0.655	0.538
49.	10.0	-8.0	-15.4	0.003851	-0.007262	-0.000367	-0.000465	0.008758	0.002048	0.655	0.538

TABLE IV-13. 34-FOOT ROTOR, $\mu = 0.76$, $M_{(1.0,\ 90.)} = 0.50$

Test 310 Run 20

PT.	$\theta_{.75R}$	α_S	α_C	C_L/σ	C_D/σ	C_Y/σ	C_ℓ/σ	C_m/σ	C_Q/σ	μ	$M_{(1.0,90)}$
1.	8.0	0.0	-9.5	0.042433	-0.007378	-0.003689	0.000086	0.011269	0.002507	0.675	0.538
2.	6.0	0.0	-7.6	0.034035	-0.006486	-0.003241	-0.000209	0.011667	0.002138	0.674	0.537
3.	6.0	0.0	-7.8	0.025665	-0.007874	-0.003312	0.000025	0.012568	0.001803	0.747	0.502
4.	8.0	0.0	-9.8	0.034513	-0.008471	-0.004429	0.000067	0.016331	0.002015	0.754	0.500
5.	8.0	-2.0	-11.1	0.021555	-0.008527	-0.002841	0.000155	0.015036	0.001978	0.754	0.500
6.	10.0	-2.0	-12.9	0.024571	-0.009255	-0.003354	-0.000160	0.016476	0.002424	0.754	0.500
7.	6.0	-2.0	-9.1	0.013461	-0.007842	-0.001913	-0.000159	0.013371	0.001749	0.756	0.500
8.	6.0	-4.0	-9.8	0.004121	-0.007621	-0.001079	-0.000449	0.013045	0.001538	0.756	0.500
9.	8.0	-4.0	-11.9	0.006192	-0.008782	-0.001291	-0.000584	0.013948	0.001641	0.757	0.500
10.	10.0	-4.0	-13.8	0.012330	-0.009237	-0.001868	-0.000401	0.015318	0.002232	0.757	0.500
11.	10.0	-4.0	-8.0	-0.004284	-0.006792	-0.000497	-0.000283	0.013878	0.001260	0.757	0.500
12.	4.0	-2.0	-6.6	0.007763	-0.006507	-0.001258	-0.000476	0.013830	0.001446	0.757	0.500
13.	2.0	-2.0	-4.1	0.004178	-0.005738	-0.000898	-0.000254	0.014519	0.001277	0.757	0.500
14.	2.0	0.0	-3.3	0.014783	-0.006337	-0.001688	0.000161	0.014335	0.001389	0.758	0.500
15.	0.0	0.0	-1.1	0.006686	-0.005992	-0.001049	-0.000159	0.014338	0.001091	0.757	0.500
16.	0.0	2.0	-0.1	0.022658	-0.006735	-0.002303	0.000005	0.014860	0.001090	0.758	0.500
17.	0.0	4.0	0.7	0.024302	-0.008075	-0.003314	-0.000090	0.000545	0.000105	0.758	0.500
18.	0.0	6.0	1.9	0.043995	-0.008164	-0.004136	-0.000266	0.017446	-0.000462	0.758	0.500
19.	0.0	8.0	2.4	0.069857	-0.013652	-0.005547	-0.000627	0.017723	-0.002218	0.757	0.500
20.	2.0	8.0	3.5	0.077460	-0.012668	-0.006270	-0.000714	0.020643	-0.002131	0.757	0.500
21.	2.0	6.0	-0.6	0.059174	-0.011942	-0.005508	-0.000033	0.015205	-0.000728	0.758	0.500
22.	2.0	4.0	-1.8	0.044084	-0.007786	-0.004394	-0.000014	0.017847	0.000470	0.758	0.500
23.	4.0	4.0	-3.9	0.049453	-0.010625	-0.005402	0.000424	0.013595	0.000691	0.758	0.500
24.	4.0	2.0	-4.8	0.034527	-0.008925	-0.004611	0.000879	0.012571	0.001287	0.758	0.500
25.	4.0	0.0	-5.8	0.022084	-0.007645	-0.003365	0.000553	0.012943	0.001502	0.758	0.500
26.	6.0	2.0	-7.0	0.040999	-0.009735	-0.004883	0.000485	0.012802	0.001598	0.769	0.496
27.	2.0	2.0	-2.6	0.029972	-0.008096	-0.003177	-0.000174	0.012784	0.001164	0.759	0.500
28.	4.0	6.0	-3.0	0.061068	-0.012662	-0.006819	0.000566	0.012702	0.000019	0.759	0.500

TABLE IV-14. 34-FOOT ROTOR, $\mu = 0.86$, $M_{(1.0,\ 90.)} = 0.47$

Test 310 Run 21

PT.	$\theta_{.75R}$	α_S	α_C	C_L/σ	C_D/σ	C_Y/σ	C_ℓ/σ	C_m/σ	C_Q/σ	μ	$M_{(1.0,90.)}$
1.	0.0	0.0	-1.1	0.009157	-0.007066	-0.000928	-0.000609	0.019990	0.001227	0.869	0.462
2.	0.0	2.0	-3.4	0.025285	-0.007946	-0.002131	-0.001057	0.018328	0.000885	0.850	0.467
3.	0.0	4.0	0.3	0.044369	-0.010758	-0.003270	-0.000794	0.018133	0.000358	0.856	0.465
4.	0.0	6.0	1.3	0.054647	-0.013275	-0.004359	-0.000654	0.016965	-0.000846	0.850	0.467
5.	0.0	8.0	3.0	0.077753	-0.015555	-0.006229	-0.000520	0.020132	-0.002[illegible]4	0.850	0.467
6.	2.0	6.0	-1.0	0.059741	-0.013436	-0.005632	-0.000740	0.018068	-0.000793	0.855	0.465
7.	2.0	4.0	-2.1	0.045267	-0.012326	-0.004386	-0.000361	0.016314	0.000170	0.857	0.465
8.	2.0	2.0	-2.9	0.027029	-0.009406	-0.002906	-0.000627	0.016881	0.001093	0.857	0.465
9.	2.0	0.0	-3.4	0.013687	-0.007142	-0.001837	-0.000715	0.019224	0.001087	0.856	0.465
10.	2.0	-2.0	-4.2	-0.002154	-0.007212	-0.000710	-0.000968	0.018179	0.001157	0.857	0.466
11.	4.0	-2.0	-6.6	0.002573	-0.008071	-0.002013	-0.000178	0.018512	0.001372	0.856	0.465
12.	4.0	-4.0	-7.5	-0.013518	-0.008901	0.000086	-0.001055	0.017211	0.000723	0.857	0.466
13.	4.0	0.0	-6.0	0.014034	-0.008878	-0.003038	-0.000111	0.017350	0.001504	0.857	0.466
14.	4.0	2.0	-5.1	0.030507	-0.009361	-0.004190	-0.000304	0.019339	0.001134	0.857	0.466
15.	4.0	4.0	-4.3	0.044482	-0.010418	-0.005873	0.000292	0.019743	0.000550	0.855	0.465
16.	4.0	6.0	-3.4	0.059869	-0.013269	-0.007381	-0.000040	0.019467	-0.000016	0.857	0.466
17.	4.0	8.0	-2.4	0.087129	-0.016728	-0.008449	-0.000737	0.020044	-0.000731	0.856	0.465
18.	6.0	6.0	-5.0	0.074493	-0.016773	-0.009339	0.000586	0.016632	0.000787	0.855	0.465
19.	6.0	4.0	-6.6	0.049443	-0.014345	-0.006794	0.000166	0.015839	0.001338	0.856	[illegible]
20.	6.0	2.0	-7.5	0.036642	-0.012173	-0.005773	0.000310	0.016996	0.001303	0.856	0.466
21.	6.0	0.0	-8.4	0.016861	-0.010392	-0.003967	0.000220	0.017821	0.001262	0.857	0.466
22.	6.0	-2.0	-9.2	0.001999	-0.010986	-0.002194	-0.000301	0.016006	0.001053	0.857	0.466
23.	6.0	-4.0	-10.0	-0.012105	-0.011411	-0.000839	-0.000730	0.016735	0.000505	0.857	0.466
24.	6.0	-6.0	-10.8	-0.042337	-0.012749	0.000001	-0.000694	0.003029	0.000095	0.856	0.465
25.	8.0	-6.0	-12.7	-0.020181	-0.013683	-0.000182	-0.000842	0.017438	-0.000478	0.856	0.466
26.	8.0	-4.0	-12.0	-0.010774	-0.012739	-0.000748	-0.000896	0.017636	0.000588	0.857	0.466
27.	8.0	-2.0	-11.2	0.005842	-0.012090	-0.002571	-0.000297	0.017488	0.001092	0.856	0.465
28.	8.0	0.0	-10.3	0.017837	-0.011751	-0.003784	-0.000809	0.018193	0.001039	0.856	0.465
29.	8.0	2.0	-9.7	0.032029	-0.012296	-0.005867	0.000005	0.018325	0.001610	0.856	0.465
30.	10.0	0.0	-12.1	0.032562	-0.013828	-0.006097	0.000271	0.018403	0.001969	0.857	0.466
31.	10.0	-2.0	-13.3	0.010328	-0.013647	-0.003584	-0.000254	0.018052	0.001573	0.857	0.466
32.	10.0	-4.0	-14.1	-0.003352	-0.014224	-0.002418	-0.000110	0.017204	0.001268	0.857	0.466
33.	10.0	-6.0	-15.0	-0.013660	-0.014925	-0.001386	0.000239	0.018022	-0.000007	0.857	0.466
34.	10.0	-8.0	-15.8	-0.024691	-0.016487	-0.000103	-0.000591	0.017118	-0.001364	0.851	0.467

TABLE IV-15. 34-FOOT ROTOR, $\mu = 0.94$, $M_{(1.0,\ 90.)} = 0.49$

Test 310 Run 22

PT.	$\theta_{.75R}$	α_S	α_C	C_L/σ	C_D/σ	C_Y/σ	C_ℓ/σ	C_m/σ	C_Q/σ	μ	$M_{(1.0,90.)}$
1.	0.0	0.0	-1.4	0.016292	-0.009670	-0.001045	0.004606	0.035292	0.001309	0.945	0.500
2.	0.0	2.0	-0.6	0.032574	-0.010043	-0.002956	0.005006	0.036825	0.000949	0.947	0.499
3.	0.0	4.0	0.2	0.048434	-0.010786	-0.003729	0.004376	0.039295	0.000276	0.947	0.499
4.	0.0	6.0	1.1	0.065219	-0.014055	-0.005639	0.005099	0.034839	-0.001133	0.938	0.496
5.	2.0	4.0	-2.5	0.046688	-0.010841	-0.005357	0.005623	0.035258	0.000439	0.934	0.496
6.	2.0	6.0	-1.4	0.061049	-0.012904	-0.006331	0.005703	0.035255	-0.000439	0.934	0.496
7.	2.0	8.0	-0.7	0.090781	-0.017473	-0.007170	0.005149	0.035502	-0.002595	0.933	0.496
8.	2.0	2.0	-3.0	0.031664	-0.010052	-0.004002	0.005371	0.034674	0.001117	0.936	0.496
9.	2.0	0.0	-3.9	0.011960	-0.008421	-0.002032	0.004230	0.035754	0.001381	0.944	0.493
10.	2.0	5.0	-1.9	0.051355	-0.011579	-0.005627	0.005474	0.036380	0.000020	0.943	0.492
11.	2.0	7.0	-1.2	0.076214	-0.016296	-0.007694	0.006277	0.035118	-0.000947	0.950	0.493
12.	4.0	7.0	-3.4	0.076074	-0.017715	-0.009071	0.005690	0.031610	-0.000283	0.944	0.491
13.	4.0	8.	-3.0	0.086372	-0.017158	-0.007570	0.005431	0.037296	-0.000624	0.950	0.492
14.	4.0	6.0	-4.0	0.064593	-0.015600	-0.008583	0.005736	0.034049	-0.000275	0.950	0.492
15.	4.0	5.0	-4.5	0.050625	-0.012742	-0.007456	0.005772	0.036362	0.000430	0.944	0.494
16.	4.0	4.0	-5.0	0.046599	-0.013040	-0.006599	0.005947	0.033738	0.000999	0.942	0.489
17.	4.0	2.0	-5.8	0.028182	-0.011534	-0.004876	0.005831	0.032874	0.001186	0.943	0.489
18.	4.0	0.0	-6.4	0.011544	-0.010247	-0.003813	0.005781	0.032772	0.001215	0.944	0.489
19.	6.0	0.0	-8.6	0.008460	-0.013235	-0.004009	0.005886	0.031466	0.000893	0.943	0.489
20.	6.0	2.0	-7.9	0.030758	-0.014543	-0.006393	0.006517	0.031249	0.001047	0.944	0.489
21.	6.0	4.0	-7.0	0.039885	-0.014293	-0.007371	0.006391	0.033900	0.001454	0.943	0.489
22.	6.0	5.0	-6.5	0.052430	-0.015486	-0.008258	0.006240	0.033543	0.001081	0.945	0.489
23.	6.0	6.0	-6.0	0.060495	-0.016417	-0.008561	0.006366	0.033640	0.000989	0.944	0.489
24.	8.0	2.0	-9.9	0.027558	-0.016400	-0.006503	0.006469	0.032069	0.001354	0.946	0.488
25.	8.0	1.0	-10.4	0.017816	-0.016220	-0.005715	0.006583	0.031191	0.001334	0.946	0.488
26.	8.0	0.0	-10.8	0.009641	-0.016463	-0.004516	0.005866	0.030658	0.000839	0.946	0.488

TABLE IV-16. 34-FOOT ROTOR, $\mu = 1.10$, $M_{(1.0,\ 90.)} = 0.51$

Test 310 Run 24

PT	$\theta_{.75R}$	α_S	α_C	C_L/σ	C_D/σ	C_Y/σ	C_ℓ/σ	C_m/σ	C_Q/σ	μ	$M_{(1.0,90.)}$
1.	0.0	0.0	-1.0	0.011358	-0.007943	-0.001043	-0.000773	0.032879	0.001505	0.933	0.489
2.	0.0	0.0	-1.2	0.012140	-0.009380	-0.001286	-0.000491	0.046411	0.001561	0.994	0.505
3.	0.0	0.0	-1.2	0.014520	-0.010062	-0.001343	-0.000403	0.057483	0.001554	1.034	0.514
4.	0.0	0.0	-1.3	0.018777	-0.011240	-0.001123	-0.001098	0.076990	0.001568	1.093	0.526
5.	0.0	0.0	-1.4	0.018883	-0.011155	-0.000991	-0.001193	0.076622	0.001378	1.096	0.524
6.	0.0	2.0	-0.6	0.047906	-0.012696	-0.003014	-0.000209	0.075720	0.001512	1.099	0.521
7.	0.0	4.0	-0.2	0.069374	-0.015749	-0.004502	-0.001548	0.079923	0.000512	1.103	0.525
8.	0.0	6.0	0.5	0.087370	-0.019777	-0.006727	-0.001764	0.077742	-0.000835	1.111	0.522
9.	0.0	6.0	0.6	0.089867	-0.018441	-0.006787	-0.001161	0.074320	-0.001243	1.096	0.517
10.	2.0	6.0	-1.7	0.084591	-0.018434	-0.007993	-0.000847	0.070420	-0.000611	1.090	0.516
11.	2.0	7.0	-1.4	0.099758	-0.022567	-0.008670	-0.000755	0.069761	-0.001661	1.095	0.517
12.	2.0	5.0	-2.3	0.070154	-0.017612	-0.007001	-0.000438	0.070148	0.000462	1.092	0.516
13.	2.0	4.0	-2.6	0.059979	-0.015556	-0.006349	0.000226	0.071808	0.000975	1.094	0.516
14.	2.0	3.0	-3.1	0.047212	-0.012895	-0.005277	0.000343	0.072380	0.001444	1.093	0.515
15.	2.0	2.0	-3.5	0.035843	-0.012671	-0.004838	-0.000072	0.070665	0.001605	1.094	0.515
16.	2.0	1.0	-3.7	0.024251	-0.013024	-0.003789	-0.000270	0.068807	0.001760	1.095	0.515
17.	2.0	0.0	-4.1	0.013370	-0.012627	-0.003006	-0.000077	0.068954	0.001739	1.094	0.514
18.	2.0	-1.0	-4.3	0.004248	-0.012316	-0.002103	-0.001297	0.069510	0.001656	1.094	0.514
19.	1.0	0.0	-3.0	0.013696	-0.011292	-0.002549	-0.000720	0.068814	0.001671	1.093	0.514
20.	1.0	2.0	-2.0	0.042760	-0.012857	-0.004154	0.000015	0.070340	0.001572	1.091	0.513
21.	1.0	4.0	-1.4	0.069081	-0.015253	-0.005233	-0.000571	0.071078	0.000756	1.091	0.513
22.	1.0	6.0	-0.8	0.088362	-0.018668	-0.007899	-0.000615	0.070838	-0.000851	1.092	0.513
23.	3.0	6.0	-3.2	0.076078	-0.018667	-0.008400	-0.000724	0.069008	-0.000217	1.092	0.512
24.	3.0	7.0	-2.7	0.085803	-0.019579	-0.008884	-0.000912	0.069324	-0.000373	1.093	0.512
25.	4.0	7.0	-3.5	0.092317	-0.022889	-0.009389	-0.000479	0.067476	-0.000467	1.095	0.512
26.	4.0	6.0	-4.3	0.069039	-0.018768	-0.008729	-0.000701	0.069936	0.000730	1.096	0.512
27.	4.0	4.0	-5.1	0.050287	-0.016977	-0.007666	0.000291	0.069084	0.000791	1.096	0.512
28.	4.0	2.0	-6.0	0.033820	-0.014827	-0.005848	-0.001510	0.069234	0.000743	1.094	0.511
29.	4.0	0.0	-6.7	0.009104	-0.015327	-0.004345	-0.000060	0.067295	0.000912	1.094	0.511
30.	5.0	0.0	-7.9	0.000770	-0.016904	-0.005155	-0.000346	0.067701	0.000565	1.093	0.511
31.	6.0	0.0	-8.9	0.001113	-0.018485	-0.005240	-0.000418	0.068165	0.000315	1.094	0.511
32.	6.0	2.0	-8.3	0.020529	-0.017801	-0.007167	-0.000402	0.066896	0.000746	1.094	0.511
33.	6.0	1.0	-8.8	0.007938	-0.017515	-0.005828	0.000100	0.067005	0.000648	1.093	0.510
34.	7.0	0.0	-10.1	-0.000393	-0.019516	-0.005506	-0.000029	0.068122	0.000422	1.093	0.510
35.	3.0	0.0	-5.8	0.006914	-0.013469	-0.003994	0.000207	0.066448	0.001605	1.095	0.510

Unclassified
Security Classification

DOCUMENT CONTROL DATA - R & D

(Security classification of title, body of abstract and indexing annotation must be entered when the overall report is classified)

1. ORIGINATING ACTIVITY (Corporate author) Bell Helicopter Company Fort Worth, Texas	2a. REPORT SECURITY CLASSIFICATION Unclassified 2b. GROUP

3. REPORT TITLE

WIND TUNNEL INVESTIGATION OF SEMIRIGID FULL-SCALE ROTORS OPERATING AT HIGH ADVANCE RATIOS

4. DESCRIPTIVE NOTES (Type of report and inclusive dates)

Final

5. AUTHOR(S) (First name, middle initial, last name)

Bruce D. Charles
Watson H. Tanner

6. REPORT DATE	7a. TOTAL NO. OF PAGES	7b. NO. OF REFS
January 1969	94	10

8a. CONTRACT OR GRANT NO.	9a. ORIGINATOR'S REPORT NUMBER(S)
DAAJ02-67-C-0061	USAAVLABS Technical Report 69-2
b. PROJECT NO. 1F162204A13903	
c.	9b. OTHER REPORT NO(S) (Any other numbers that may be assigned this report)
d.	BHC Report 576-099-010

10. DISTRIBUTION STATEMENT

This document has been approved for public release and sale; its distribution is unlimited.

11. SUPPLEMENTARY NOTES	12. SPONSORING MILITARY ACTIVITY
	U.S. Army Aviation Materiel Laboratories, Fort Eustis, Va.

13. ABSTRACT

A joint U.S. Army Aviation Materiel Laboratories/NASA-Ames/Bell Helicopter Company experimental investigation of full-scale rotor blades was conducted in the NASA-Ames Large Scale Wind Tunnel. Specifically, a UH-1B 44-foot-diameter rotor having reduced-thickness tips was evaluated in a range of Mach numbers up to 0.94 and advance ratios of up to 0.52. Additionally, UH-1D rotor blades reduced in diameter to 34 feet were tested at advance ratios of up to 1.1. Calculated performance is compared with the experimental results obtained to establish the validity of the theoretical technique at high advance ratios. In general, it was found that quasi-static, two-dimensional techniques were adequate up to an advance ratio of about 0.5. Above this advance ratio, theoretical techniques break down, especially with respect to calculating rotor propulsive force or drag. Theory-experiment comparison with the 44-foot-diameter rotor, operated at high Mach numbers, showed that Mach number effects are predictable to an advance ratio of at least 0.45. The 34-foot-diameter rotor became increasingly sensitive to control input with advance ratio. At an advance ratio of 1.1, this rotor system displayed a long transient response to a control input before obtaining its steady-state orientation, and at the largest values of collective pitch, the flapping would not completely stabilize.

DD FORM 1 NOV 68 1473 REPLACES DD FORM 1473, 1 JAN 64, WHICH IS OBSOLETE FOR ARMY USE.

Unclassified
Security Classification

Unclassified
Security Classification

14. KEY WORDS	LINK A		LINK B		LINK C	
	ROLE	WT	ROLE	WT	ROLE	WT
Rotor performance Thin-tipped main rotor blades High advance ratio High advancing tip Mach number						

Unclassified
Security Classification

434-69